การแยกลูทีนอิสระและกรดไขมันในดีเอสเทอริไฟด์โอริโอเรซินของดาวเรืองด้วยโครมาโตรกราฟี และการสร้างแบบจำลองทางคณิตศาสตร์

นายวีระวัฒน์ คลอวุฒิมันตร์

วิทยานิพนธ์นี้เป็นส่วนหนึ่งของการศึกษาตามหลักสูตรปริญญาวิศวกรรมศาสตรดุษฎีบัณฑิต
สาขาวิชาวิศวกรรมเคมี ภาควิชาวิศวกรรมเคมี
คณะวิศวกรรมศาสตร์ จุฬาลงกรณ์มหาวิทยาลัย
ปีการศึกษา 2560

CHROMATOGRAPHIC SEPARATION OF FREE LUTEIN AND FATTY ACIDS IN DE-ESTERIFIED MARIGOLD OLEORESIN AND ITS MATHEMATICAL MODELLING

Mr. Weerawat Clowutimon

A Dissertation Submitted in Partial Fulfillment of the Requirements
for the Degree of Doctor of Engineering Program in Chemical Engineering
Department of Chemical Engineering
Faculty of Engineering
Chulalongkorn University
Academic Year 2017

Thesis Title	CHROMATOGRAPHIC SEPARATION OF FREE LUTEIN AND FATTY ACIDS IN DE-ESTERIFIED MARIGOLD OLEORESIN AND ITS MATHEMATICAL MODELLING
By	Mr. Weerawat Clowutimon
Field of Study	Chemical Engineering
Thesis Advisor	ProfessorArtiwan Shotipruk, Ph.D.

Accepted by the Faculty of Engineering, Chulalongkorn University in Partial Fulfillment of the Requirements for the Doctoral Degree

.....Dean of the Faculty of Engineering
(Associate Professor Supot Teachavorasinskun, D.Eng.)

THESIS COMMITTEE

.....Chairman
(Associate ProfessorSeeroong Prichanont, Ph.D.)

.....Thesis Advisor
(ProfessorArtiwan Shotipruk, Ph.D.)

.....Examiner
(Pimporn Ponpesh, Ph.D.)

.....Examiner
(ProfessorSuttichai Assabumrungrat, Ph.D.)

.....External Examiner
(Phatthanon Prasitchoke, Ph.D.)

วีระวัฒน์ คลอวุฒิมันตร์ : การแยกลูทีนอิสระและกรดไขมันในดีเอสเทอริไฟด์โอริโอเรซินของดาวเรืองด้วยโครมาโตรกราฟีและการสร้างแบบจำลองทางคณิตศาสตร์ (CHROMATOGRAPHIC SEPARATION OF FREE LUTEIN AND FATTY ACIDS IN DE-ESTERIFIED MARIGOLD OLEORESIN AND ITS MATHEMATICAL MODELLING) อ.ที่ปรึกษาวิทยานิพนธ์หลัก: ศ. ดร.อาทิวรรณ โชติพฤกษ์, 144 หน้า.

กลีบของดอกดาวเรืองเป็นแหล่งที่อุดมไปด้วยสารแซนโทฟิลล์ คือ ลูทีนซึ่งเป็นสารที่มีความสามารถต้านอนุมูลอิสระและมะเร็ง แม้ว่าดอกดาวเรืองจะมีลูทีนในปริมาณมาก แต่ทว่าลูทีนส่วนใหญ่อยู่ในรูปกรดไขมันของลูทีนซึ่งเป็นสารที่ไม่มีค่าชีวประสิทธิผล ดังนั้นกระบวนการแยกและการทำบริสุทธิ์ของลูทีนหลังการสกัดดอกดาวเรืองด้วยตัวทำละลายอินทรีย์จึงมีความจำเป็น ขั้นตอนที่สำคัญขั้นตอนหนึ่ง คือ ปฏิกิริยาดีเอสเทอริฟิเคชันของกรดไขมันของลูทีนในสารสกัดโอริโอเรซินของดาวเรืองโดยการทำปฏิกิริยากับสารละลายเบส เช่น สารละลายโพแทสเซียมไฮดรอกไซด์ เพื่อให้ได้ลูทีนอิสระ ผลิตภัณฑ์ที่ได้ยังมีสิ่งปนเปื้อนเจือปนโดยเฉพาะอย่างยิ่งกรดไขมัน ซึ่งต้องนำไปผ่านกระบวนการทำบริสุทธิ์อีกขั้นตอนหนึ่ง เช่น กระบวนการโครมาโตรกราฟี ในงานวิจัยนี้มีวัตถุประสงค์เพื่อศึกษาการแยกลูทีนอิสระและกรดไขมันในคอลัมน์โครมาโตรกราฟีวัฏภาคธรรมดาขนาดกึ่งอุตสาหกรรม โดยใช้ซิลิกาเจลเป็นเฟสนิ่งและสารละลายผสมเอกเซนและเอทิลอะซิเตตเป็นเฟสเคลื่อนที่ จากการวิเคราะห์วัฏภาคของตัวทำละลายอินทรีย์ของผลิตภัณฑ์จากกระบวนการดีเอสเทอริฟิเคชั่นด้วย HPLC, MS, NMR และ FT-IR พบว่า กรดไขมันเป็นสิ่งเจือปนหลัก มีปริมาณเท่ากับ 49.12 มิลลิกรัมต่อกรัมโอริโอเรซิน และส่วนใหญ่เป็นกรดปาล์มิติก ความเร็วที่เหมาะสมของเฟสเคลื่อนที่ซึ่งประเมินจาก HETP คือ 0.16 เซนติเมตรต่อวินาที ซึ่งที่สภาวะนี้ความบริสุทธิ์ของลูทีนอิสระที่ได้เมื่อชะด้วยเฟสเคลื่อนที่แบบไอโซเครติกเท่ากับ 93.3% และเมื่อชะด้วยเฟสเคลื่อนที่แบบเกรเดียนท์เท่ากับ 99.2% จากนั้นผู้วิจัยได้พัฒนาแบบจำลองทางคณิตศาสตร์ที่เหมาะสมเพื่ออธิบายการถ่ายโอนมวลของการแยกสารประกอบ 2 ชนิด ได้แก่ ลูทีนอิสระและกรดไขมัน พารามิเตอร์ของแบบจำลองที่จำเป็น คือ สมดุลดูดซับ สัมประสิทธิ์การถ่ายเทมวลรวม และ สัมประสิทธิ์การแพร่ตามแนวแกน โดยสมดุลดูดซับคำนวณจากการทดลองแบบกะ ซึ่งพบว่า เป็นเส้นตรงในช่วงความเข้มข้นที่สมดุลต่ำ (<100 ไมโครกรัมต่อมิลลิลิตร) ในขณะที่สัมประสิทธ์การถ่ายเทมวลรวมและสัมประสิทธิ์การแพร่ตามแนวแกนคำนวณจากความสัมพันธ์ในงานวิจัยที่มีการตีพิมพ์ก่อนหน้าหรือความสัมพันธ์ที่พัฒนามาจากการทดลองในงานวิจัยนี้ จากนั้นนำสมดุลดูดซับและพารามิเตอร์ของแบบจำลองไปประยุกต์กับแบบจำลอง ผลการทดลองพบว่า transport model ทำนายผลการทดลองของสารทั้ง 2 ชนิดในคอลัมน์ขนาดกึ่งอุตสาหกรรมและขนาดอุตสาหกรรมได้แม่นยำที่สุด ค่าสัมประสิทธิ์สหสัมพันธ์ซึ่งมีค่ามากกว่า 0.70 แสดงให้เห็นว่าแบบจำลองและผลการทดลองมีความสอดคล้องกันสูง

ภาควิชา วิศวกรรมเคมี ลายมือชื่อนิสิต .....

สาขาวิชา วิศวกรรมเคมี ลายมือชื่อ อ.ที่ปรึกษาหลัก .....

ปีการศึกษา 2560

5471449621 : MAJOR CHEMICAL ENGINEERING
KEYWORDS: MARIGOLD, LUTEIN, CHROMATOGRAPHY, MASS TRANSFER MODEL

WEERAWAT CLOWUTIMON: CHROMATOGRAPHIC SEPARATION OF FREE LUTEIN AND FATTY ACIDS IN DE-ESTERIFIED MARIGOLD OLEORESIN AND ITS MATHEMATICAL MODELLING. ADVISOR: PROF.ARTIWAN SHOTIPRUK, Ph.D., 144 pp.

The petal of marigold flowers has been reported to be the richest source of a xanthophyll, namely lutein which exhibits strong antioxidant and anticancer properties. Although large amount of lutein can be obtained, the compound in the flowers exists as esterified lutein, which is not readily bio-available. As a result, a number of separation and purification steps are required after solvent extraction of marigold flowers. One of the key steps is de-esterification of lutein fatty acid esters in the extract, or namely marigold oleoresin, by the reaction of the oleoresin with alkali solution, e.g., KOH, to obtain free lutein. The impurities remained in the reaction product, particularly fatty acids, were separated in the further purification process, e.g., chromatography. In this study, we aimed to study chromatographic separation of free lutein and fatty acids in a normal-phase semi-preparative scale with silica gel as a stationary phase and hexane and ethyl acetate mixture as a mobile phase. Based on HPLC, MS, NMR and FT-IR analyses of organic phase of the de-esterification reaction product, fatty acids were found to be the main impurity. The amount of fatty acids was determined to be 49.12 g/g of oleoresin and it was mostly palmitic acid. At the most suitable mobile phase velocity (0.16 cm/s), determined based on HETP evaluation, free lutein of 93.3% purity could be achieved with an isocratic mode of operation, and as high as 99.2% purified lutein was resulted when a single step gradient mode was employed. Further investigation then involved the development of a suitable mathematical model to describe the mass transfer of the two compounds to be separated: free lutein and fatty acids. Required model parameters: adsorption isotherms, overall mass transfer and axial dispersion coefficients, were determined. The adsorption isotherms were determined from a batch isotherm experiment and were to be linear for the lower range of equilibrium concentrations (<100 µg/ml), while other model parameters were determined from empirical correlation from literature or from correlations developed experimentally in this study. The isotherms and model parameters were then applied to the mass transfer model. The transport model was found to best predict the experimental data of both compounds in both semi-preparative and preparative columns. The correlation factor, higher than 0.70, indicated that the model prediction and experimental results were highly consistent.

Department:	Chemical Engineering	Student's Signature	.....
Field of Study:	Chemical Engineering	Advisor's Signature	.....
Academic Year:	2017		

ACKNOWLEDGEMENTS

This project would not have been possible without direct and indirect assistance from many people. Foremost, I would like to express his gratitude to the thesis advisor, Aj. Pim, Prof. Artiwan Shotipruk, Ph.D., for all technical support, invaluable guidance and encouragement. In addition, appreciation is also extended to all the committee members, Assoc. Prof. Seeroong Prichanont, Ph.D., Prof. Sutthichai Assabumrungrat, Ph.D., Pimporn Ponpesh, Ph.D., and Phatthanon Prasitchoke, Ph.D., for their support and helpful recommendations.

I gratefully acknowledge Thailand Research Fund through The Royal Golden Jubilee Ph.D. Program (RGJ-TRF) in collaboration with Chulalongkorn University for the financial support. Also, my sincere thanks are also given to PPT Global Chemical, Co. Ltd. for supporting dried marigold powder used in this project.

I also thank Panatpong Boonnoun, Ph.D., for helping me many times correcting my papers and for providing recommendations on my thesis work.

I wish to thank Khun Sunan Rangseekarnsong from the Scientific and Technological Research Equipment Center, Chulalongkorn University, for her assistance in sample analyses with HPLC.

Lastly, this project would not have been completed without lots of support from my family and friends (Bo, Tang, Sai, On, Toon, View, Preaw, Aim, Nu Phee and Arm).

CONTENTS

Page

LIST OF FIGURES

LIST OF TABLES

CHAPTER I
INTRODUCTION

1.1 Motivation

Marigold is an ordinary ornamental plant and has become increasingly important as a source of several bioactive compounds, e.g., carotenoids, terpenoids, flavonoids (Vasudevan et al., 1997, Gong et al., 2012, Siriamornpun et al., 2012), used in pharmaceutical and nutraceutical applications. In Thailand and several other eastern countries, the plant is cultivated for cut flowers to make garlands for religious purposes. Owing to high amount of carotenoids, marigold flowers are employed as natural food colorants, particularly in poultry industry to enhance the yellow pigment of egg yolks (Vasudevan et al., 1997, Piccaglia et al., 1998, Zorn et al., 2003, Jiang et al., 2005). The main carotenoid in marigold flower is lutein ($C_{40}H_{56}O_2$), a carotenoid having two dihydroxyl groups attached to the two ionone rings at the end of the molecule. Lutein possesses antioxidant and anticancer properties and is also known for its ability to protect human eyes by filtering out the damaging blue light and prevent age-related macular degeneration (AMD) (Landrum and Bone, 2001, Zorn et al., 2003, Molnar et al., 2004, Shibata et al., 2004, Jiang et al., 2005). The worldwide market for extracted lutein is indeed expected to grow to US$308 million by 2018 (Lin et al., 2015). For these reasons, there has been growing interest on extraction of marigold lutein for use in pharmaceutical and cosmetic industries.

In general, to obtain marigold lutein, dried marigold flowers are first extracted by organic solvent (i.e., hexane). The organic solvent is generally removed by evaporation during which essential oil and volatile terpenes vaporize and may be

recovered (Muley et al., 2009, May and Quirin, 2014). The remaining solid, namely marigold oleoresin, contains high content of lutein esters (approximately 5-30%) (Xu et al., 2007), which is mostly present in a di-esterified form of fatty acids, particularly palmitic acid and stearic acid, occupying at the sites of hydroxyl groups (Piccaglia et al., 1998, Jiang et al., 2005, Abdel-Aal and Rabalski, 2015). Compared with free lutein, lutein esters are more stable against heat and UV-light. However, their bio-availability is considerably lower. Although the more bio-available free lutein may be attained via the in vivo hydrolysis of lutein esters by human enzymes, the efficacy is generally less than 5% (Breithaupt et al., 2002, Granado et al., 2002). Consequently, a process of de-esterification of lutein esters into free lutein is crucial, and is generally carried out by reacting the oleoresin with alkali solution (e.g., KOH or NaOH), typically in water or a relatively low molecular weight alcohol (ethanol or propanol) (Breithaupt et al., 2002, Alves-Rodrigues and Shao, 2004). As a result of de-esterification, fatty acids, a by-product, is a major impurity of concern, since they are present mostly as saturated fat, which can cause high level of low-density lipoprotein (LDL), resulting in risks of heart attack and stroke (Muley et al., 2009). Further purification steps are often needed to remove fatty acids from de-esterified marigold oleoresin to achieve the recommended purity level for human consumption (>95%) (Khachik, 1995).

In early purification works, crystallization was most frequently employed to purify free lutein in the de-esterified product (Madhavi and Kagan, 2002, Khachik, 1995, 2001). By adding a polar solvent (e.g., water) into the solution of de-esterified marigold lutein (originally dissolved in a relatively low polarity organic solvent such as low molecular weight alcohol), free lutein crystallizes out of the solution, However, due to the low solubility of fatty acids in the polar solvent, they can also be co-

precipitated. Higher free lutein purity could be achieved by further adding warm water and alcohol to the crystals to remove fatty acids (Xu et al., 2007). As an alternative, fatty acids could also be removed prior to the crystallization by adding excess alkali of approximately 1-3 times of oleoresin weight (Xu et al., 2007) during the de-esterification process to convert fatty acids into fatty acids salts, which becomes soluble in polar solvents, eliminating the problem of co-precipitation (Pena, 2009, Ausich and Sanders, 1997). However, by either technique, the high temperature or the excess alkali provokes the degeneration of free lutein, resulting in low product recovery, often less than 70% (Sarkar et al., 2012).

In more recent studies, liquid chromatography has been applied either as a stand-alone process or together with crystallization, for purification of free lutein in the de-esterified marigold oleoresin. With appropriate use of a stationary phase and a mobile phase, as well as an operating mode (gradient versus isocratic) and operating conditions (e.g., mobile phase flow rate), the process can be optimized such that high purity and recovery of the final product can be attained. For example, a purification process of free lutein in de-esterified marigold oleoresin reported by Khachik (2001) comprises crystallization and subsequent normal-phase column chromatography using silica gel as a stationary phase and tetrahydrofuran (THF) as a mobile phase. It was found that as high as 83.1% recovery of high purity free lutein (97% purity based on percentage of peak area) could be obtained. Yingyeun (2013), in the following study, reported a 79% recovery of purified free lutein (95% purity based on the percentage of peak area) was resulted from a normal-phase column chromatography of de-esterified marigold sample using silica gel as the stationary phase and a 70:30 v/v mixture of hexane and ethyl acetate as the mobile phase. Although chromatography has shown

high potential for the purification of de-esterified marigold oleoresin, the purity of the resulted free lutein reported in the previous studies was based on the percentage of peak areas of analytical chromatography, typically connected to a UV-detector which cannot detect fatty acid. Without careful analysis of the fatty acids with appropriate analytical tools (e.g., HPLC with ELSD-detector), the fatty acids might not have been taken into account, and thus the percentage of free lutein purity might be overestimated. In addition, in the previous studies, the chromatographic processes had been studied only in the laboratory scale, which is much smaller than that of for the industrial scale production. To reduce a number of costly experiments in up-scaling the process, mathematical models based on material and energy balances simulated in a computer program have played a key role. Choopakdee (2012) applied a mathematical model to describe the transport behavior of free lutein in a preparative chromatography column. The results showed that the model could well predict transport behavior of free lutein in the column with deviation less than 13%. However, other components in de-esterified marigold oleoresin, particularly fatty acids, have not been considered in this work.

In this study, we therefore aimed to quantify and identify fatty acids in marigold oleoresin and de-esterified marigold lutein samples. The quantification was carried out using HPLC connected to an ESLD detector while the identification was carried out NMR, FT-IR and MS analyses. Then, the most suitable chromatographic condition for separating the fatty acids and free lutein was determined in a normal-phase semi-preparative column. Silica gel and mixtures of hexane and ethyl acetate were used as the stationary phase and mobile phase, respectively. Furthermore, a mathematical model for describing transport behavior of the compounds was developed using free

lutein as a test compound. The most suitable mass transfer model for describing the chromatographic process was first determined. Required model parameters: adsorption isotherm, axial dispersion and mass transfer coefficients, were determined. The adsorption isotherm was studied using batch adsorption experiments, while the axial dispersion and mass transfer coefficients were determined from appropriate correlations. Finally, the model was used to predict the transport behavior of the compounds in both semi-preparative and preparative columns. In addition, the comparison between the model prediction and experimental results was performed to evaluate the model abilities for predicting the experimental transport behavior of the compounds and their separation.

1.2 Objectives

1.2.1 To identify and quantify fatty acids in marigold oleoresin and de-esterified marigold lutein.

1.2.2 To determine a suitable condition for chromatographic separation of free lutein and fatty acids in de-esterified marigold lutein.

1.2.3 To develop a suitable mathematical model for describing transfer behavior of free lutein and fatty acids in chromatography columns.

1.3 Working scopes

The overall working scope of is shown in Figure 1.1. Firstly, the amount of free lutein and fatty acids in marigold oleoresin and de-esterified marigold lutein were quantified. The most suitable chromatographic condition for free lutein and fatty acid

separation was then evaluated. Finally, modelling of chromatographic separation of free lutein and fatty acid was investigated. The details of each step are described as follow:

1.3.1 Characterize marigold oleoresin by spectrophotometer to measure total xanthophyll content. Quantify the total amount of free lutein and fatty acids in marigold oleoresin and de-esterified marigold lutein using HPLC analysis. Identify types of fatty acids in de-esterified marigold lutein using NMR, FT-IR and MS analyses.

1.3.2 Determine a suitable condition for the separation of free lutein and fatty acids in a semi-preparative column. The parameters studied were mobile phase velocity (0.12-0.23 cm/s) and elution mode, i.e., isocratic and gradient mode. In the isocratic elution, the mobile phase was a mixture of hexane and ethyl acetate at a ratio of 70:30 v/v, while, in the gradient elution, the mobile phase was a mixture of hexane and ethyl acetate at a ratio of 85:15 v/v during the first elution step (12 or 20 min), followed by a ratio 70:30 v/v.

1.3.3. Investigate mathematical model for chromatographic separation of free lutein and fatty acid. The details are described as follows:

1.3.3.1 Determine adsorption isotherms of free lutein and fatty acids at 30 ^{o}C using batch experiment. The ratio of adsorbent to working solution was fixed at 0.5g: 10 ml. The initial concentration of free lutein and fatty acid were 5 – 300 and 100 – 1000 µg/ml, respectively.

1.3.3.2 Determine the most suitable mass transfer model by comparing the experimental data and the prediction from 3 different models, i.e., ideal model, equilibrium-dispersive model, and transport model, at the mobile phase velocity of 0.12, 0.16, and 0.21 cm/s.

1.3.3.3 Use the suitable mass transfer model to predict experimental transfer behavior of free lutein and fatty acids in both semi-preparative and preparative columns and validate the prediction with the experimental data. The conditions used in the semi-preparative and preparative columns are shown in Figure 1.1.

The results of 1.3.1 and 1.3.2 are provided in chapter 4 while the results of 1.3.3 are provided in chapter 5.

1.4 Expected benefits

1.4.1 To be able to identify and quantify fatty acids in de-esterified marigold oleoresin.

1.4.2 To obtain a suitable condition for separation of free lutein and fatty acids by preparative column chromatography.

1.4.3 To obtain a suitable mathematical model for describing the phenomena of free lutein and fatty acids in chromatography columns which is useful for the future process development in a pilot and industrial scale system.

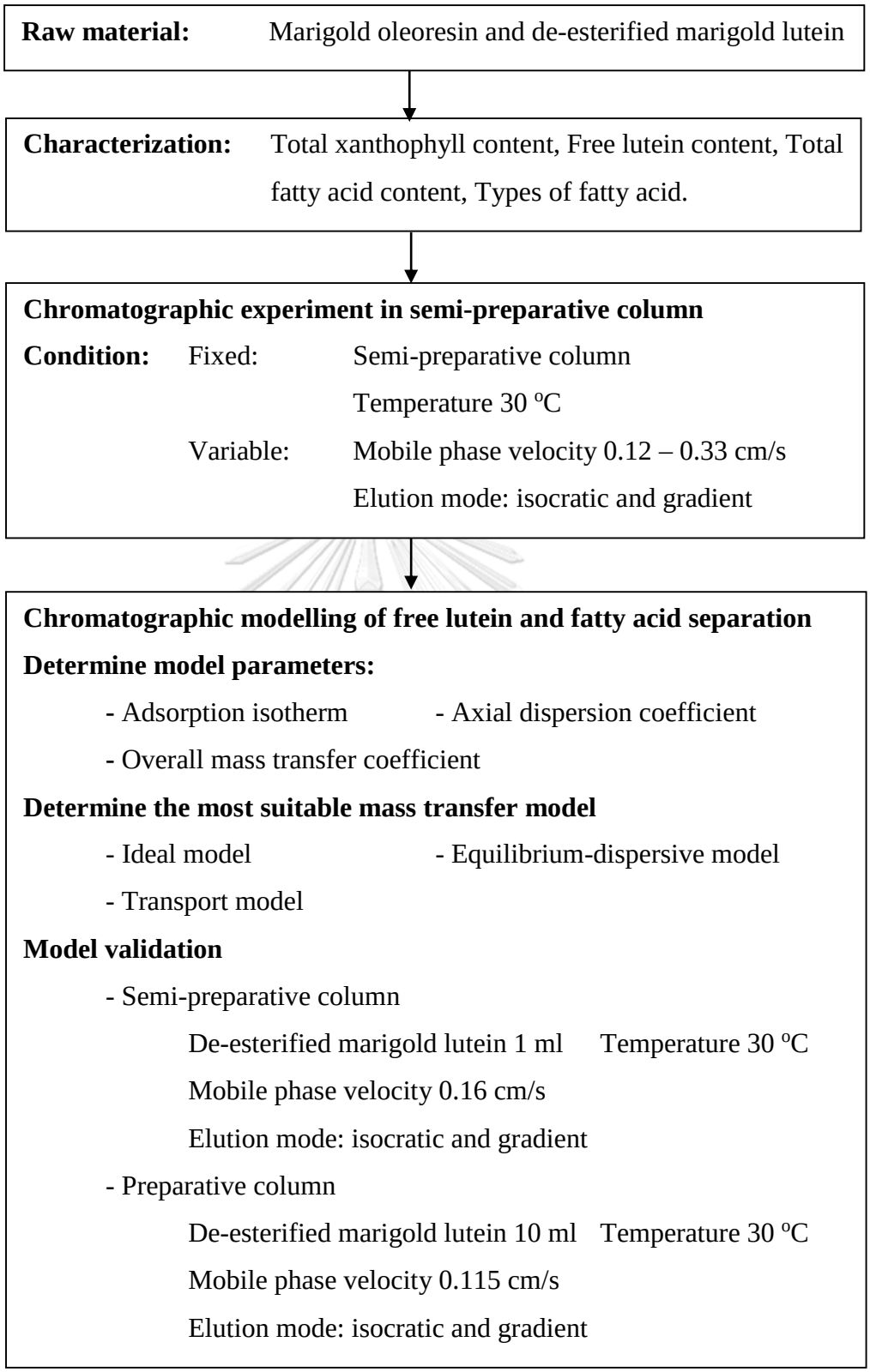

Figure 1. 1 Diagram of experiments for chromatographic separation of free lutein and fatty acids in de-esterified marigold lutein

CHAPTER II
BACKGROUND AND LITERATURE REVIEWS

2.1 Marigold flowers

Marigold, an herbaceous plant in the sunflower family, is normally about 10 to 220 cm tall and has pinnate green leaves. Its floral heads are 4-6 cm diameter with color gold, orange, red and yellow (Figure 2.1). The plant is widely cultivated in temperate climate in tropical parts around the world including Thailand, particularly the species *Tagetes erecta* (*T. erecta*). The vast quantities of marigold flowers are used in ornaments and garlands for several purposes such as religious ceremonies.

Figure 2. 1 Marigold flower (*T. erecta*)

(http://www.mullerseeds.com/tagetes-taishan-orange.html)

Marigold flower heads are the only part which is used in pharmaceutical applications since they have high content of carotenoids which can protect people from the environmental damage. The carotenoids present in marigold flowers can filter out

the visible blue light damaging human cataracts and can protect the age-related macular degeneration (AMD) (Vasudevan et al., 1997, Landrum and Bone, 2001, Zorn et al., 2003, Jiang et al., 2005).

2.2 Carotenoids in marigold

Carotenoids, one of the most widespread natural compound pigments, generally present in all photosynthetic organisms and are compounds in fruits, vegetables, and flowers, having yellow to red colors. They are isoprenoids consisting of eight isoprene units, containing 40 atoms of carbon, joined together with covalent bonds. The carotenoid structure can be presented in the form of straight chain such as lycopene, or contain the ring(s) at the end of the chain such as β-carotene, as shown in Figure 2.2. In general, carotenoids can be classified into 2 groups; hydrogenated and oxygenated carotenoids. The hydrogenated carotenoids are the compounds composing of only hydrocarbon chain, for instance, lycopene and β-carotene. The compounds in this group can be characterized as non-polar compounds which are generally dissolved in non-polar solvents such as oil. The other group, oxygenated carotenoids or xanthophylls, is the group of carotenoids composing of oxygen atom(s), for instance, lutein and zeaxanthin, as shown in Figure 2.3. Although oxygenated carotenoids are more polar than hydrogenated carotenoids, they consist of a long chain of carbon atoms, making them non-polar compounds and dissoluble in non-polar organic solvents.

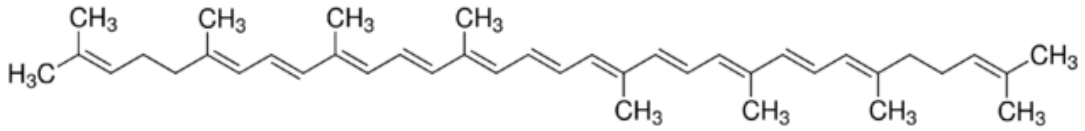

(a)

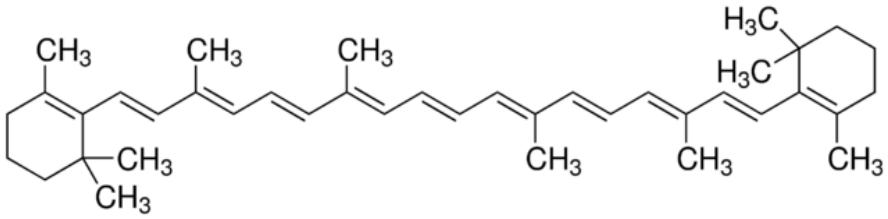

(b)

Figure 2. 2 Chemical structure of hydrogenated carotenoids (a) lycopene (b) β-carotene

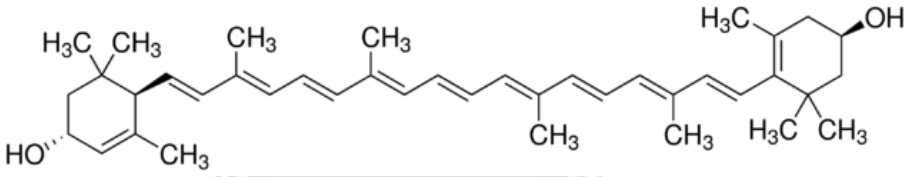

(a)

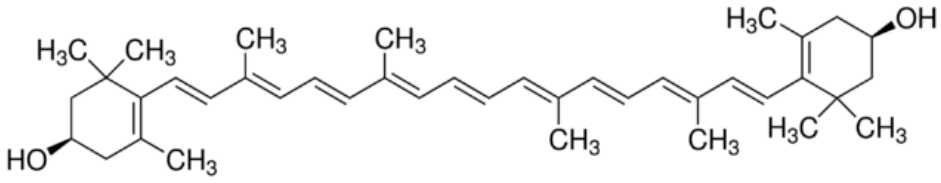

(b)

Figure 2. 3 Chemical structure of oxygenated carotenoids (a) lutein (b) zeaxanthin

The amount of carotenoids presenting in marigold flowers is around 5-15 wt.% and most of them are in the form of xanthophylls, particularly lutein and zeaxanthin. The percentage of each carotenoid in marigold flowers is summarized in Table 2.1.

Table 2. 1 Carotenoids in marigold flower (Sowbhagya et al., 2004)

Hydrogenated carotenoids	Distribution (%)	Oxygenated carotenoids	Distribution (%)
Phytoene	2.4	α-Cryptoxanthin	0.8
Phytofluene	2.6	β-Cryptoxanthin	0.5
α-Carotene	0.1	Lutein	72.3
β-Carotene	0.5	Antheraxanthin	0.1
Zeacarotene	0.5	Zeaxanthin	16.4
		Neoxanthin	0.8

2.3 Lutein

Lutein ($C_{40}H_{56}O_2$), whose physical properties are summarized in Table 2.2, is one of the major constituents of egg yolks, green vegetables, and orange fruits and is the main antioxidant identified within the eye retina. Due to strong antioxidant properties, lutein plays an important role in the maintenance of eye health and the prevention of cataracts by filtering out the visible blue light damaging the eye retina. In addition, the antioxidant qualities of the compound also help promote healthy skin during sun exposure and can prevent various diseases such as heart attack and stroke. (Vasudevan et al., 1997, Landrum and Bone, 2001, Zorn et al., 2003, Molnar et al., 2004, Jiang et al., 2005). For this reason, lutein is therefore widely consumed as in the diet or as food supplement or is applied to pharmaceutical and cosmetic industries. The worldwide market of lutein is expected to grow to US$308 million by 2018 (Lin et al., 2015).

Table 2. 2 Physical properties of lutein

Molecular weight	568.87 g/mol
Melting point	190 ^{o}C
Solubility in water	Insoluble
Solubility in fats	Soluble
Appearance	Red-orange crystallize solid

In marigold flowers, lutein generally exists in the esterified form of fatty acids such as di-palmitate, di-stearate, and palmitate-stearate lutein esters, as shown in Table 2.3. The amount and type of lutein esters varies depending on soil, weather and cultivation method (Vasudevan et al., 1997, Abdel-Aal and Rabalski, 2015).

Although lutein esters are stable against heat and UV-light, bio-availability of the compounds is very low, as they cannot be directly absorbed by human body. Consequently, lutein esters must be first converted to free lutein before it can be absorbed by human, typically by alkaline hydrolysis (Xu et al., 2007, Pena, 2009). To obtain lutein in free form, the compound readily adsorbed by human, processes for isolation of lutein esters and conversion of these esters to free lutein have been proposed (Zorn et al., 2003, Sarkar et al., 2012).

Table 2. 3 Type of lutein ester in marigold flowers

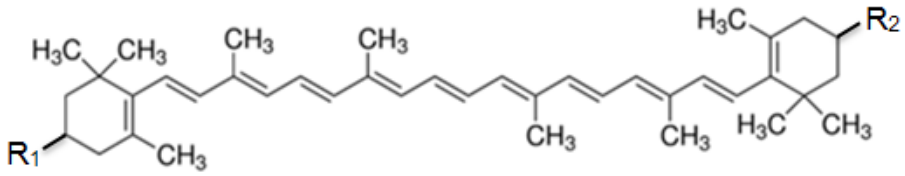

Lutein fatty acid ester	Structure of lutein fatty acid ester	
	R_1	R_2
Free lutein	OH	OH
Monopalmitate	OH	$OCO(CH_2)_{14}CH_3$
	$OCO(CH_2)_{14}CH_3$	OH
Monostearate	OH	$OCO(CH_2)_{16}CH_3$
	$OCO(CH_2)_{16}CH_3$	OH
Di-palmitate	$OCO(CH_2)_{14}CH_3$	$OCO(CH_2)_{14}CH_3$
Di-stearate	$OCO(CH_2)_{16}CH_3$	$OCO(CH_2)_{16}CH_3$
Palmitate-Stearate	$OCO(CH_2)_{16}CH_3$	$OCO(CH_2)_{14}CH_3$
Stearate-Palmitate	$OCO(CH_2)_{14}CH_3$	$OCO(CH_2)_{16}CH_3$

2.4 Isolation of lutein from marigold flowers

A process for isolation and purification of lutein from marigold flowers includes extraction lutein esters from the marigold flowers, de-esterification of the extracted lutein (marigold oleoresin) with an alkali solution, and purification of the de-esterified lutein by crystallization or chromatography. Detail of each step is described as followings.

2.4.1 Extraction of lutein esters from marigold flowers

In extraction, the selection of suitable solvent is one of the key factors determining the extraction efficiency. The concept of the solvent selection is related to the solubility of solute in the solvent. The most suitable solvent should have the polarity close to that of the solutes. Although lutein contains oxygenated polar groups at the end of the molecule, the overall polarity of the molecule is still low due to long chain of carbon atoms in the molecules. Hence, in most studies, lutein is generally extracted by non-polar solvents such as hexane (Piccaglia et al., 1998, Tsao et al., 2004) and petroleum ether (Philip, 1977).

After extraction, the extract was concentrated by evaporating the solvent, during which essential oil and volatile terpenes may be recovered. The remaining solid or marigold oleoresin containing high lutein content is obtained. However, lutein present in the oleoresin is mostly in the form of esterified lutein which is not readily taken up by human. A process to convert lutein esters to free lutein, more active form, is further required.

2.4.2 De-esterification of marigold oleoresin

To convert lutein esters to free lutein, de-esterification can be carried out using enzyme hydrolysis (Zorn et al., 2003). Alternative to enzyme hydrolysis, de-esterification can also be carried out using a more economically feasible process shown in Figure 2.4, by reacting the oleoresin with alkali solution, preferably strong alkali such as NaOH or KOH, typically in low molecular weight alcohol (Vechpanich, 2008, Pena, 2009, Xu et al., 2007).

The yield of free lutein was found to be function of alkali concentration, reaction temperature and reaction time. Specifically, the process operated at high temperature and high alkali concentration for a long time resulted in the degeneration of free lutein (Sarkar et al., 2012). On the other hand, low temperature and alkali concentration could not completely de-esterify the lutein fatty acid esters. Relatively consistent among various studies, the most efficient condition was found to be 0.5 M KOH at 50 ^{o}C for 30 min (Vechpanich and Shotipruk, 2011).

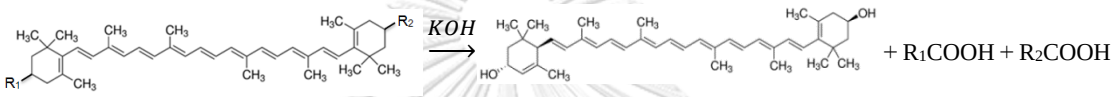

Figure 2. 4 De-esterification reaction of lutein esters

Based on the reaction shown in Figure 2.4, other than the desired product, free lutein, fatty acids (R-COOH) would be expected in the resulted reaction mixture. Since the fatty acids in marigold sample are mostly saturated fatty acids which could be a leading cause high level of LDL, resulting in risks of several diseases such as stroke and heart attack (Muley et al., 2009), further purification steps are required to separate them from free lutein. Generally, the free lutein purity of more than 90% has been reported to be suitable for human consumption (Khachik, 1995).

2.4.3 Purification of de-esterified lutein

Crystallization

The most commercially employed process for the purification of active compounds of interest is crystallization, a process involving the formation of solid

crystals from a solution whereby mass transfer of a solute from the liquid to the pure solid crystals takes place. In general, crystallization consists of two major steps: nucleation and crystal growth. Nucleation is the step in which the solute molecules dispersed in the solution start to gather into clusters that become stable under the current operating conditions. These stable clusters constitute the nuclei. The clusters therefore need to reach a critical size in order to become stable nuclei. Such critical size is dictated by many different factors (i.e., temperature and supersaturation). It is at the stage of nucleation that the atoms arrange in a defined and periodic manner that defines the crystal structure. The crystal growth is the subsequent size increase of the nuclei that succeed in achieving the critical cluster size. Crystal growth is a dynamic process occurring in equilibrium where solute molecules precipitate out of the solution and dissolve back into the solution. Supersaturation is one of the driving forces of crystallization as the solubility of a species is an equilibrium process. Depending on the conditions, either nucleation or growth may be predominant over the other, and this could be a factor dictating the crystal size.

Reviews of several studies conducting on extraction and purification of marigold lutein by crystallization (Madhavi and Kagan, 2002, Xu et al., 2007, Khachik, 1995, Ausich and Sanders, 1997) are summarized in Figure 2.5. Generally, a polar solvent such as water is added to the de-esterified sample, previously dissolved in a non-polar solvent to crystallize free lutein out of the solution. The crystals were then filtered out from the supernatant containing water-soluble impurities such as soap, wax, chlorophyll, flavonoids, anthocyanin and the remaining alkali. Finally, the crystals are washed by a polar solvent (e.g., water) and/or a non-polar solvent (e.g., hexane) to remove the remaining impurities.

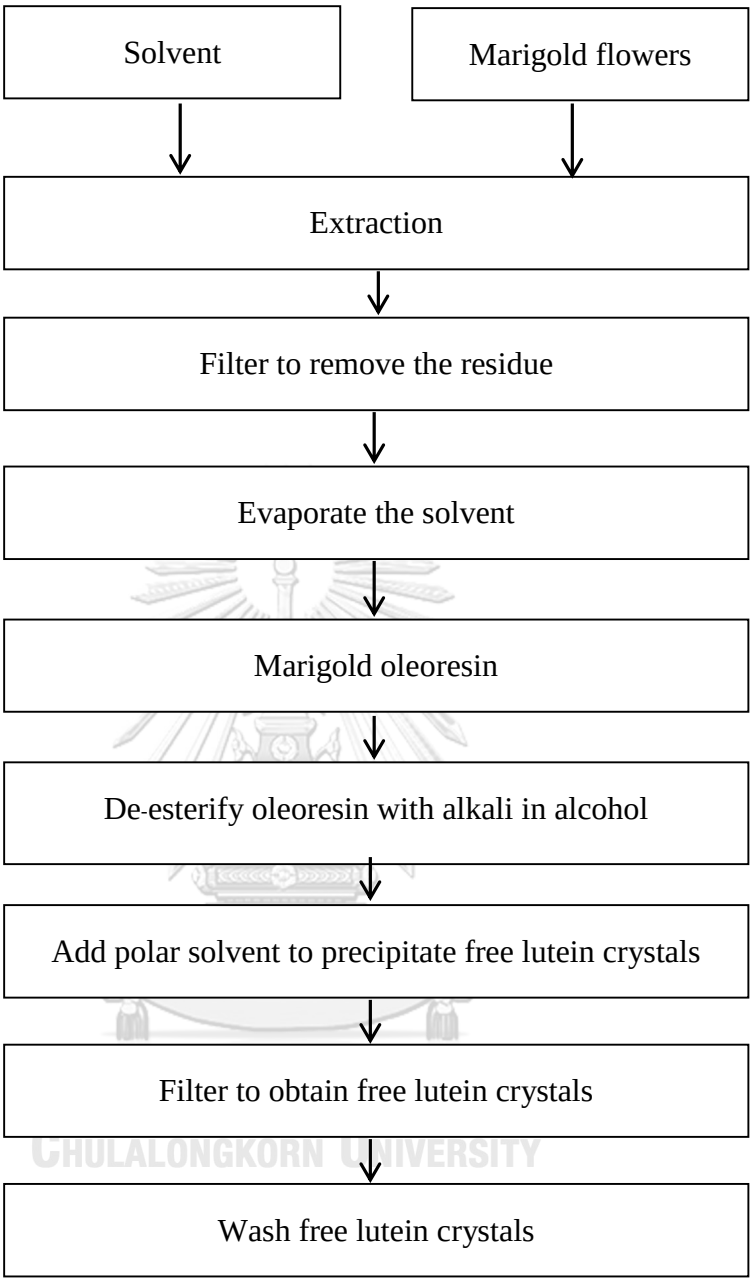

Figure 2. 5 Process for extraction and crystallization of marigold lutein

During the crystallization process however, non-polar impurities, particularly fatty acids, a by-product of the de-esterification process, may also co-precipitate. Higher free lutein purity might be achieved by further washing the crystals with warm mixture of water and alcohol (Xu et al., 2007) or adding excess alkali during the prior de-esterification to convert the fatty acids to fatty acid salts, which would then be

soluble in polar solvents (Pena, 2009, Ausich and Sanders, 1997). However, the high temperature and the excess alkali provoke the degeneration of free lutein, resulting in low recovery (Sarkar et al., 2012).

Chromatography

Chromatography is a technique whereby two or more compounds in a mixture within can be separated a single device. This technique can be either analytical or preparative. Analytical chromatography is employed to identify and quantify each component in a mixture while preparative chromatography is used to purify a large amount of a compound or compounds from a multi-component mixture. The principle of this technique lies upon to the affinity of each compound on stationary phase and mobile phase. As shown in Figure 2.6, as the mobile phase carry the injected homogeneous mixture of two compounds (represented by • and ♦) though the column packed with the stationary phase, the component ♦, which has lower affinity to the stationary phase compared with the component •, would move faster and would be eluted earlier from the column. Because of their considerable effects on the performance of the chromatography column, the selection of appropriate mobile phase and stationary phase is a very first and foremost task for a particular application.

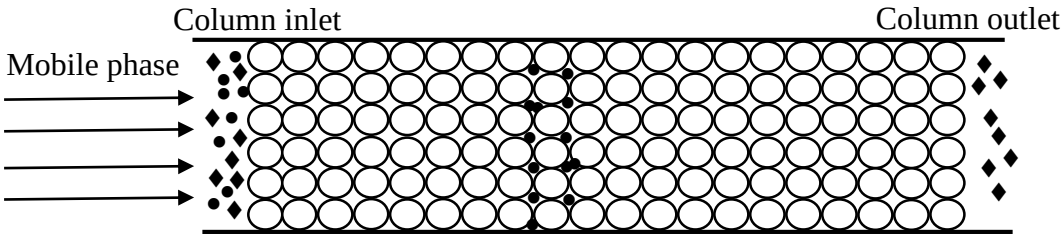

Figure 2. 6 Separation of compounds by chromatography

Key parameters to be considered for the selection of suitable system of mobile phase and stationary phase are distribution coefficient (K) of each compound and the selectivity or separation factor (α) of adjacent components, defined by equation (2.1) – (2.2), and depicted in Figure 2.7.

$$K = \frac{C_s}{C_m} = \frac{t_R - t_0}{t_o} \tag{2.1}$$

$$\alpha = \frac{K_i}{K_j} = \frac{t_{R,i} - t_0}{t_{R,j} - t_0} \tag{2.2}$$

where C_s and C_m are the concentrations in the stationary phase and the mobile phase, respectively. t_0 is the dead time of column. $t_{R,i}$ and $t_{R,j}$ are the retention times of the more retained component and the less retained component, respectively.

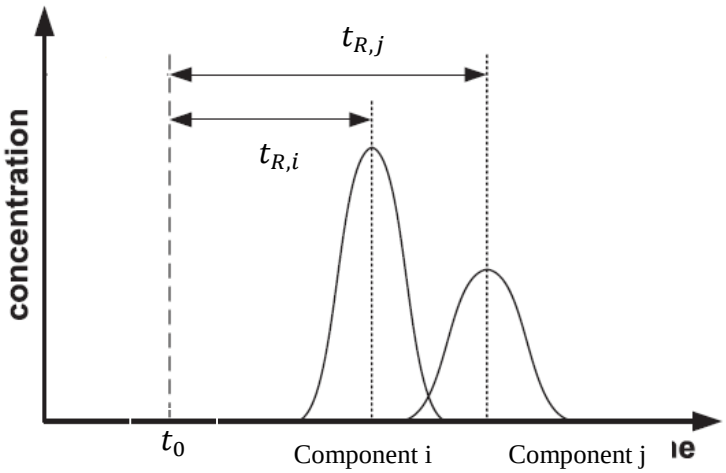

Figure 2. 7 Chromatogram of sample containing 2 components

(Schmidt-Traub, 2005)

By definition, the selectivity is always greater than one, as when α is equal to one, the two peaks are co-eluting (i.e., distribution coefficient are identical). Hence, higher selectivity leads to the further apart the two peaks of adjacent apices. However, the α value is not directly indicative of the peaks separation, and hence a new parameter, resolution value (R_s), is introduced. The R_s, on the other hand, is a quantitative measure

of how well two elution peaks can be separated. From Figure 2.7, the resolution is defined as the difference in retention time between two components, divided by the combined widths of the elution peaks as described by equation (2.3).

$$R_S = \frac{2(t_{R,j} - t_{R,i})}{w_i + w_j} \tag{2.3}$$

where w_i and w_j are the peak widths, at the baseline ($w = 4\sigma$, where σ is the standard deviation of retention time), of the components i and j, respectively. The suitable value of R_s for chromatographic separation is suggested to be around 1.5. This value is called *the baseline resolution*. When the value of R_s is smaller than 1.5, the separation of two adjacent compounds is considered imcomplete. Nevertheless, chromatography process operating at the R_s value much higher than 1.5 would be uneconomical (Schmidt-Traub, 2005).

To obtain the baseline resolution, the selection of suitable stationary phase and mobile phase is the key factor. In preparative scale, generic adsorbents (e.g., silica gel and activated carbon) are generally used as the stationary phase. In biotechnology applications, such as purification of free lutein from natural sources (Boonnoun et al., 2012, Shibata et al., 2004), the commonly used stationary phase is silica gel due to its high stability and reusability. For the mobile phase selection, thin layer chromatography (TLC) is an economic mean used to screen the suitable mobile phase. Samples are spotted on TLC plates which are then placed in the chamber containing a mobile phase. When the mobile phase is adsorbed and travels up the TLC plate, the components dissolve in the solvent and move up along the TLC plate at different rates, depending on the intermolecular forces between the component and the stationary phase and the component and the mobile phase. The selection of the suitable mobile phase using TLC

is related to the retention factor (R_f); the ratio of the distance of components spots to distance of the eluent. The R_f of the interested component on TLC plate should be different from other components and the suggested value would be between 0.2-0.8 (Anjinta, 2013).

For purification from natural sources, including marigold flowers, chromatography has been applied in both analytical and preparative scales. For analytical scale, Jiang et al. (2005) used a reverse phase chromatography column to separate free lutein and lutein esters in de-esterified marigold oleoresin. The stationary phase was C-18 silica gel while the mobile phase was a mixture of acetonitrile, methanol and ethyl acetate (55:1:44 v/v). The results showed that retention time of the compounds varied depending on their polarity, molecular weight and structures (cis- and trans-). These results are in good agreement with other studies (Molnar et al., 2004, Shibata et al., 2004, Tsao et al., 2004, Tsao and Yang, 2011).

For preparative scale, Boonnoun et al. (2012) studied the purification of de-esterified marigold lutein using a normal phase chromatography column with an isocratic elution mode. The de-esterified sample was first analyzed to identify all components in the solution by liquid chromatography mass spectroscopy (LC-MS). A mixture of hexane and ethyl acetate at various ratios (50:50 – 100:0 v/v) was then applied to determine the suitable mobile phase of the system using TLC study. The best mobile phase ratio was used to purify de-esterified lutein in the column packed with silica gel. From the LC-MS analysis, free lutein and anhydrolutein, free lutein which has one fewer hydroxyl group, were main components of the de-esterified sample. The TLC results show that the best ratio of hexane and ethyl acetate mixture for the separation was 70:30 v/v. At such condition, purity of free lutein could achieve up to

95% (based on chromatogram peak area). Yingyeun (2013), in the following study, studied the effect of operating conditions (eluent flow rate, particle size of stationary phase and column length) on the purity of free lutein purified in a normal phase chromatography column. The results show that yield of high purity free lutein (>95% based on chromatogram peak area) could achieve 79% when the volumetric flow rate of the mobile phase (hexane: ethyl acetate 70:30 v/v) was 15 ml/min, with 20 cm column (I.D. 35 mm) packed with silica gel of 25-40 μm particle size. Although high yield and purity of free lutein extracted from marigold could be achieved by chromatography columns, the optimum condition to achieve the highest column performance and the content of fatty acids in de-esterified marigold lutein have not been investigated. In addition, the experiments were carried out in only laboratory scales which are not suitable for industrial production. An up-scaling process is therefore required.

2.5 Efficiency of preparative chromatographic column

In the previous part, the emphasis was place on the selection of the mobile phase and the stationary phase which determines how the equilibrium behavior affect the overall performance of the chromatographic processes. Other factors involve the behavior of fluid flow and the mass transfer of the components in the chromatography column. These factors the key determinants of the column efficiency, which is generally link to the broadening of the chromatographic bands of species undergoing the chromatographic process. Two theories, the plate theory and the rate theory, have been developed to describe this phenomenaon of band-broadening of a solute when it moves along the column. The plate theory describes the mechanism of retention and gives an

equation that allows the calculation of the column efficiency. On the other hand, the rate theory is based on the mechanism of peak dispersion (or band-broadening) and provides an equation (Van Deemter equation) that allows the calculation of the column efficiency in terms of the mobile phase velocity and other physical and chemical properties of the solute and distribution system.

2.5.1 The plate theory

By this theory, the column is presumably divided into many small zones called theoretical plates. In each zone, the solute is assumed to be in equilibrium distribution between the mobile phase and the stationary phase. The height of each zone is referred to as the height of an equivalent theoretical plate (HETP). The relation between number of plates (N) and HETP is according to equation (2.4).

$$HETP = \frac{L_c}{N} \tag{2.4}$$

where L_C is the column length.

Large N could imply high separation performance of the column. For Gaussian peak profile, the column efficiency can be described by equation (2.5), in term of standard deviation (σ) or variance (σ^2) of the Gaussian distribution.

$$HETP = \frac{\sigma^2}{L_c} \tag{2.5}$$

In general, the plot of the outlet concentration and time, called elution chromatogram, can be classified as symmetric and asymmetric peak as illustrated in Figure 2.8.

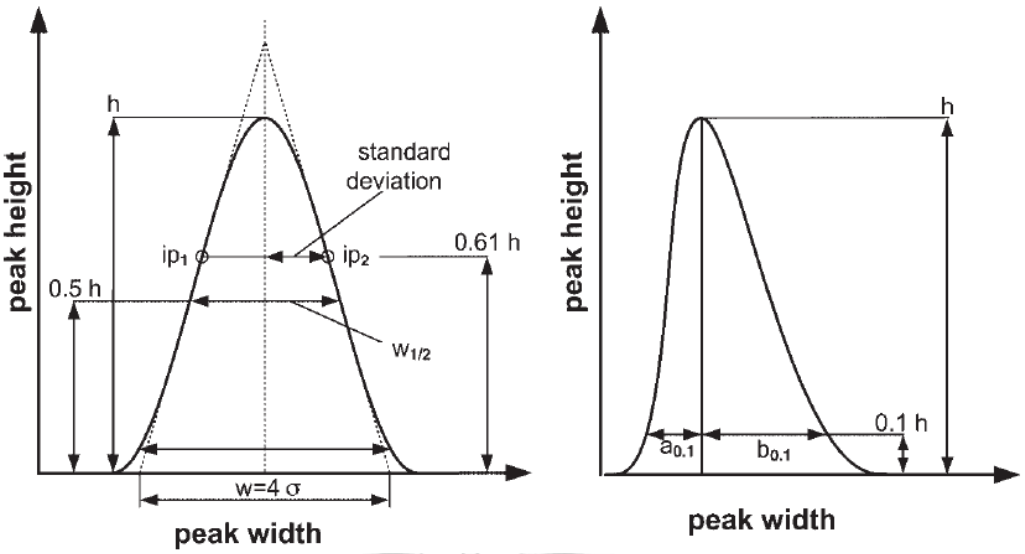

Figure 2. 8 Chromatogram peak type (a) symmetric peak (b) asymmetric peak (Schmidt-Traub, 2005)

The degree of peak asymmetry (T_p) is calculated from the difference between peak halves at 1/10th of the peak height (Figure 2.8b), equation (2.6).

$$T_p = \frac{b_{0.1}}{a_{0.1}} \tag{2.6}$$

If T_p is in the range of 0.9-1.1, the peak is Gaussian or symmetric peak. However, if T_p is more than 1.1, the peak is tailing. If T_p is less than 0.9, the peak is fronting. For the Gaussian peak, the efficiency in term of plate number can be calculated using peak width at half-height ($w_{1/2}$), according to equation (2.7).

$$N = 5.54\left(\frac{t_R}{w_{1/2}}\right)^2 \tag{2.7}$$

where t_R is mean retention time of the compound in the column.

On a contrary, for an asymmetric peak, the mean retention time of the chromatogram is calculated by the first absolute moment, μ_t (equation (2.8)). The variance (σ_t^2) is determined by the second absolute moment according to equation (2.9).

$$\mu_t = \frac{\int_0^\infty tc(t)dt}{\int_0^\infty c(t)dt} \quad (2.8)$$

$$\sigma_t^2 = \frac{\int_0^\infty (t-\mu_t)^2 c(t)dt}{\int_0^\infty c(t)dt} \quad (2.9)$$

The plate number of asymmetric peaks can be calculated by equation (2.10).

$$N = 41.7\left[\frac{\left(\frac{t_R}{w_{1/2}}\right)^2}{1.25+\frac{b_{0.1}}{a_{0.1}}}\right] \quad (2.10)$$

2.5.2 The rate theory

While the plate model assumes that the equilibrium is infinitely fast, the rate theory is a quantitative analysis that describes the processes at work inside the column, and takes into account of the time taken for the solute to equilibrate between the stationary phase and the mobile phase. The band-broadening of a chromatography peak is therefore affected by the rate of elution. It is also affected by the different paths available to solute molecules as they travel between particles of the stationary phase. As a summary, there are 4 main causes of band-broadening: eddy diffusion, flow distribution, axial diffusion (longitudinal diffusion) and mass transfer resistance between the mobile phase and the stationary phase.

2.5.2.1 Eddy diffusion

When the mobile phase and the solute move through a column, packed with fine particles, the solute in the mobile phase will move through the void between particles in different paths due to the inconstancy of the sizes of particles. Solute molecules that move through the column directly; path 3 in Figure 2.8, will be eluted out of the column

first, while other molecules that travel through the voids at random will be eluted out of the column later. This will cause band-broadening due to different path lengths.

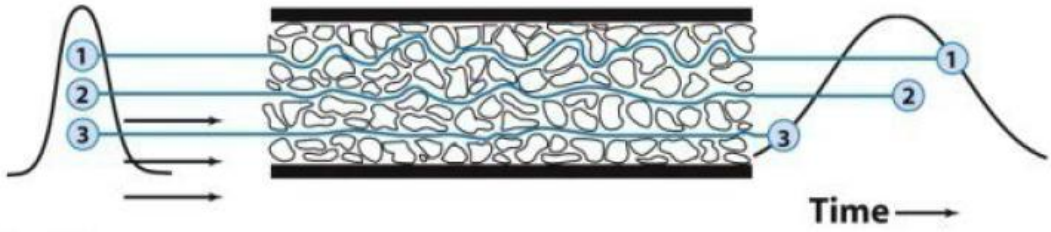

Figure 2. 9 Eddy diffusion between particles in a packed bed

(Skoog and Leary, 1992)

2.5.2.2 Flow distribution

In general, velocity of mobile phase in a chromatographic column is very low and can be assumed to be laminar flow between particle channels. The fluid velocity at the center of a channel is faster than that near the wall or particle surface (the longer arrow represents the greater local eluent velocity). Thus, the solute will also move faster at the center than other regions as illustrated in Figure 2.9. To reduce the effect of flow distribution on the band-broadening which will impact column efficiency, the particles packed in the column should be a uniform size. The ratio of the largest and smallest particle should not be greater than 2 (Meyer, 2010).

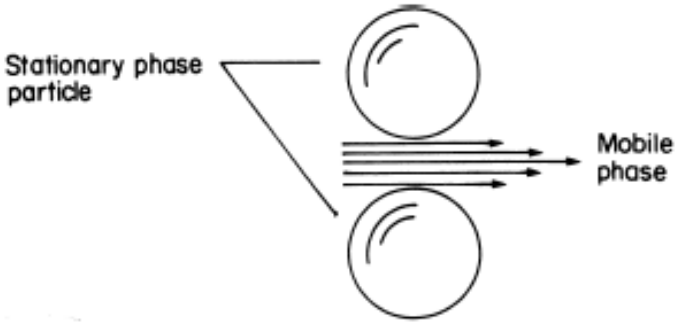

Figure 2. 10 Flow distribution in chromatographic bed (Meyer, 2010)

The band-broadening due to eddy diffusion and flow distribution is mainly affected by the particle size of stationary phase as described by equation (2.11).

$$HETP = 2\lambda d_p \tag{2.11}$$

where λ is the particle shape constant and d_p is the particle diameter.

According to equation (2.11), the band-broadening can be reduced by decreasing the particle size of stationary phase.

2.5.2.3 Axial diffusion of solute in mobile phase

When solute molecules were injected into a chromatography column, it will spread out across the column length by axial diffusion (longitudinal diffusion) as expressed in Figure 2.10. The diffusion causes by the concentration gradient of solute in the column without any external force. The value of HETP resulted from this effect is inversely proportional to the velocity of mobile phase as described by equation (2.12). This is because the retention time of solute decreases as the mobile phase velocity is increased.

$$HETP = \frac{2k_D D_m}{u} \tag{2.12}$$

where k_D is the obstruction factor. D_m is molecular diffusivity of the compound in mobile phase and u is the mobile phase interstitial velocity.

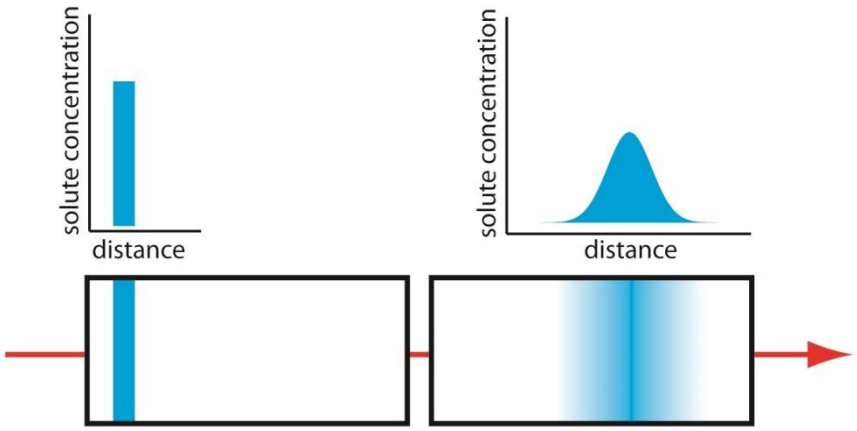

Figure 2. 11 Axial diffusion in a chromatography column

2.5.2.4 Mass transfer resistance between mobile phase and stationary phase

In general, the particles of chromatography column are porous and uniform size as shown in Figure 2.12.

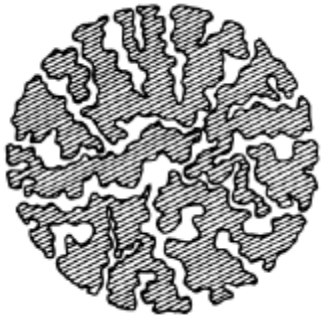

Figure 2. 12 Porous material for chromatographic process (Meyer, 2010)

Within the structure of a particle, the mobile phase fills in the pores and the fluid within these pores can be assumed to be stagnant. The solute molecules, then, transfer into the pore by diffusion process due to the concentration gradient. Two mechanisms proposed by Meyer (2010) have been used to describe the process.

1) The solute does not retain inside the particle pores. They diffuse back to the mobile phase. Time required for transferring depends on the depth of the pores. This

results in the band-broadening. Moreover, the diffusion rate also depends on the viscosity of mobile phase. The solute can diffuse faster and move quickly out of the pore when the viscosity is low.

2) The solute might interact with the stationary phase at the active sites (point C in Figure 2.13), possibly by solute adsorption. Thus, the solute will retain on the surface or inside the pore of the particle. The solute molecules outside the particle can be adsorbed and desorbed more easily than the solute molecules inside the pore.

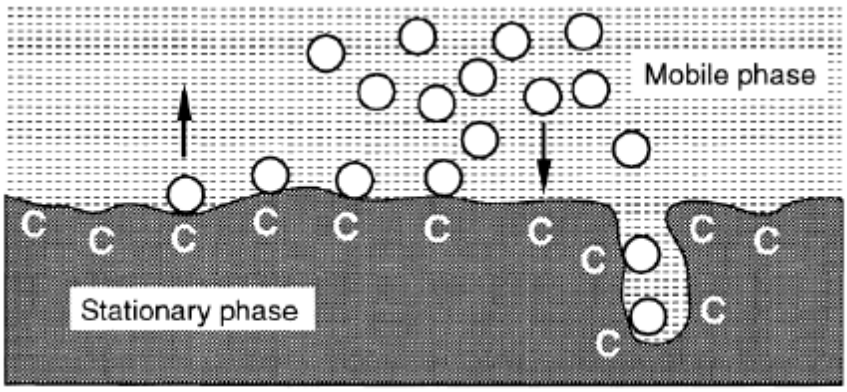

Figure 2. 13 Mass transfer between stationary phase and mobile phase in a chromatography column (Meyer, 2010)

In both cases, the band-broadening increases with increasing mobile phase velocity since the molecules remaining in the mobile phase move faster and are eluted out of the column before the molecules adsorbed inside pores of the stationary phase. Hence, the band-broadening relates to diffusion rate in the stagnant fluid and diffusion rate on the stationary phase surface described in equation (2.13) and (2.14), respectively.

$$HETP = \left(\frac{d_p^2 d_c^2}{D_m}\right) u \tag{2.13}$$

$$HETP = \left(\frac{k_s d_f^2}{D_s}\right) u \tag{2.14}$$

where d_c is the column diameter. d_f is the film thickness and D_s is the diffusion coefficient of the compound on the stationary phase.

By summing up all above contributions to the band-broadening, the Van Deemter equation, which describe the oveall column efficiency is obtained as follows:

$$HETP = 2\lambda d_p + \left(\frac{d_p^2 d_c^2}{D_m}\right) u + \left(\frac{k_s d_f^2}{D_s}\right) u + \frac{2k_D D_m}{u} \quad (2.15)$$

Equation (2.15) can be rewritten as simple as equation (2.16).

$$HETP = A + Bu + \frac{C}{u} \quad (2.16)$$

The first term, A , is related to eddy diffusion effect which is independent of mobile phase velocity. The second term, the Bu term, is linearly proportional to the fluid velocity and summarizes the effect of mass transfer resistance, which dominates the process at high mobile phase velocity. The last term, the $\frac{C}{u}$ term, represents the effect of axial dispersion of solute molecules in the fluid phase. This term dominates the process at low mobile phase velocity.

Figure 2.14 shows the plot of the relationship between HETP and the mobile phase velocity, according to equation (2.16). The upturned part of the curve is found at the lowest HETP (at the optimum velocity). At such condition, the column can be operated at the maximum theoretical plate number, resulting in the highest column efficiency.

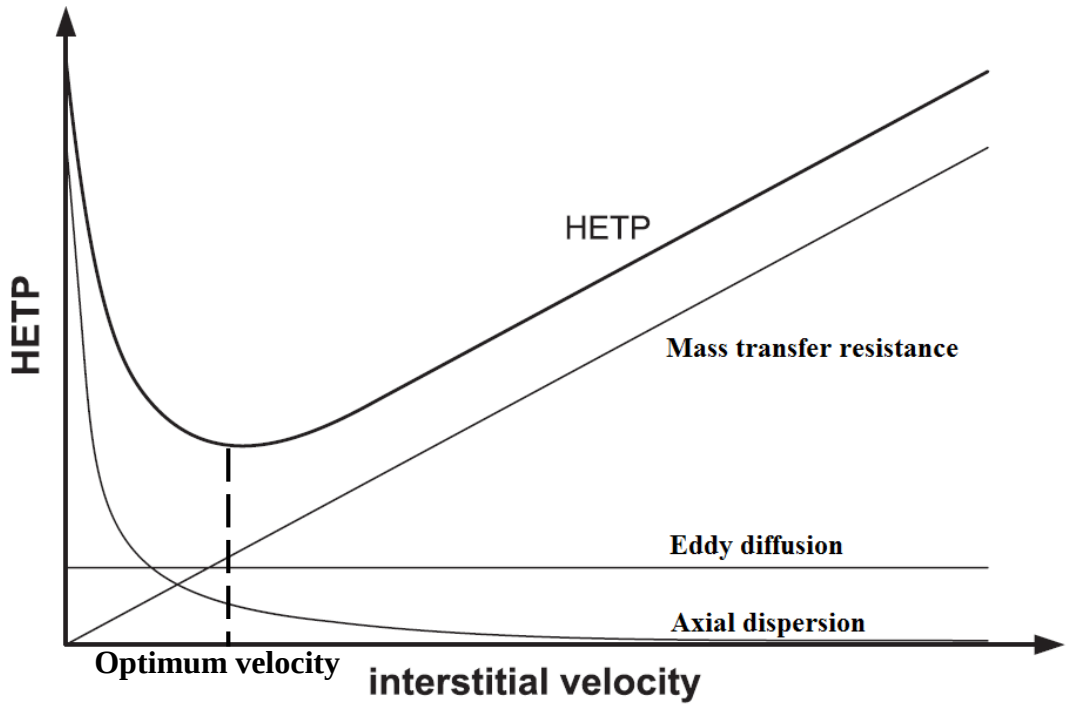

Figure 2. 14 The relationship between HETP and mobile phase velocity (Schmidt-Traub, 2005)

2.6 Mass transfer model

The next after determining selection of the suitable systems (i.e., mobile phase and stationary phase) and the mobile phase velocity (section 2.4 and 2.5) is to experimentally test the process in a laboratory scale column chromatography. More importantly, the process scale-up from small-scale experiments to an economically optimal plant scale would be an ultimate goal. However, determination of the optimal operating conditions combining with complex systems by sole experiments is difficult and time consuming. Virtual experiments by numerical modeling can considerably reduce time and resources used in the up-scale process. To achieve this, a suitable mass transfer model and accurate model parameters for the chromatography column are needed. If the models are validated, they can be used to provide accurate prediction in

large scales or describe the transport behavior of compounds in chromatography column. In this part, therefore, modelling of chromatographic separation process is introduced. The derivation of mathematical models for a preparative chromatography column is explained and reviews of literatures in which these models were applied are summarized. Finally, the procedures in which the model parameters (adsorption isotherm and transport parameters, i.e., axial dispersion and mass transfer coefficients) to achieve accurate simulation results are explained.

In general, a mathematical modl for mass transfer of a slute in chromatography column can be developed base on the 4-step mechanism of mass transfer in a column packed with porous particles (Crittenden et al., 1986), which are:

1) Molecular diffusion (dispersion) and convective mass transfer of solute from bulk fluid to the boundary layer (external mass transfer)

2) Mass transfer of solute across the boundary layer toward the particle pores (film mass transfer)

3) Molecular diffusion of solute along the pore surface (surface diffusion) and inside the pores of the particles (pore diffusion)

4) Adsorption equilibrium or adsorption kinetics

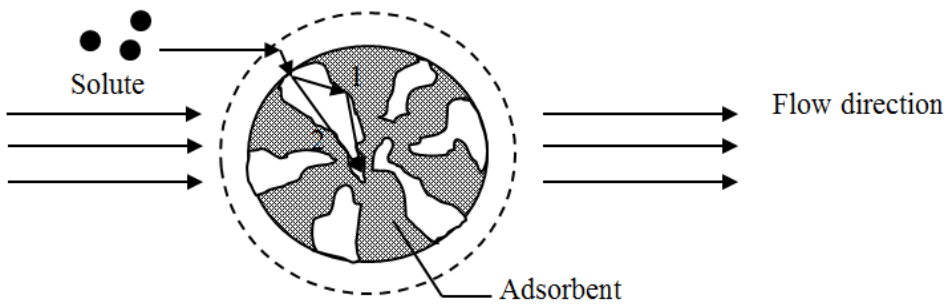

Figure 2. 15 Mass transfer mechanism in a packed bed column

(Schulte and Epping, 2005)

Figure 2.15 illustrates the mass transfer mechanism occurred in a packed bed column. In the first step, the solute molecules move from bulk fluid to boundary layer by molecular diffusion and convective transport. Then, the molecules move through the boundary layer and toward the particle pores. Inside the pores, the molecules move toward the center of the particle by surface diffusion (path no. 1) or pore diffusion (path no.2). The molecules move by surface diffusion when the attractive force between solute molecule and pore surface is strong. For pore diffusion, the molecules have weak attractive force to the pore surface and move to the center of particle by Fick's Law. In chromatographic process, the attractive force is generally weak; therefore, surface diffusion can be negligible. When the solute molecules approach to the pore bottom, the adsorption kinetics or adsorption equilibrium occurs. Generally, external mass transfer and adsorption process are very fast; therefore, the limiting step of the process is either film mass transfer or pore diffusion.

2.6.1 Derivation of mathematical models

Mathematical modeling of mass transfer is generally based on material, energy and momentum balances in addition to equations of the thermodynamic equilibrium of solute, between the solid phase and fluid phase. All of the models described in this part are based on the following assumptions (Guiochon, 2002):

1) The packed bed in homogenous and packed with spherical particles of constant diameter.

2) Density and viscosity of fluid phase are constant.

3) Radial distribution is negligible.

4) The process is isothermal.

5) The fluid phase is inert.

6) There is no mass convection inside the particles.

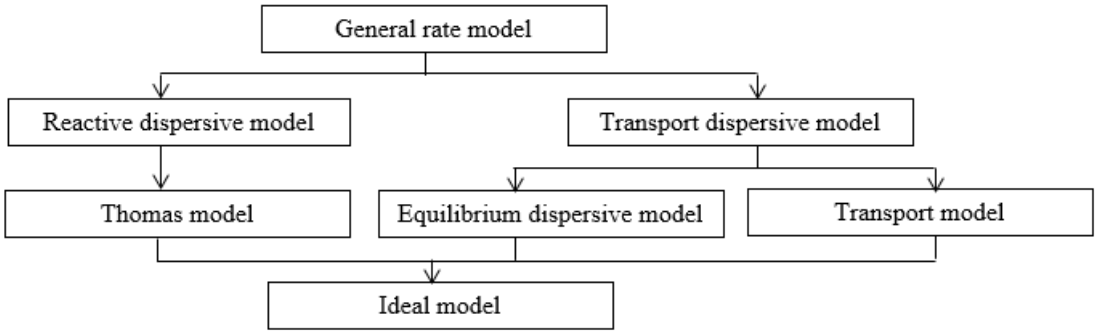

Figure 2. 16 Classification of mathematical model for chromatographic process (Guiochon et al., 1994)

Figure 2.16 shows the classification of mathematical model for chromatographic process (Guiochon et al., 1994). The upper models are more complicated. There are different assumptions added to simplify them to the lower models which are simpler. Therefore, each model has limitation and is suitable for a specific system. It means that a suitable model for a system might not be applicable to describe other systems.

General rate model

General rate model is the most complicated model taking into account all possible factors (i.e., axial dispersion, eddy diffusion, film mass transfer resistance and pore diffusion) which influence the band profile shape. The rate of adsorption-desorption is sometimes included but often neglected. In this model, the mass balance in the liquid phase can be written by equation (2.17) (Guiochon, 2002).

$$\varepsilon_e \frac{\partial C}{\partial t} + u \frac{\partial C}{\partial z} + (1 - \varepsilon_e) k_f a_p \left[C - C_p \left(r = R_p \right) \right] = \varepsilon_e D_L \frac{\partial^2 C}{\partial z^2} \quad (2.17)$$

where C and C_p are the concentration of the component in the mobile phase and in the stagnant fluid phase inside the particle pores, respectively. z and t are the abscissa and time. ε_e is the external porosity. a_p is the external surface area of the adsorbent particles. D_L is the axial dispersion coefficient. k_f are the external mass transfer coefficient. The method for D_L and k_f determination is described in section 2.6.2.

Equation (2.17) describes the following phenomena:

1) Mass accumulation in the mobile phase ($\varepsilon_e \frac{\partial C}{\partial t}$)

2) Mass convection ($u \frac{\partial C}{\partial z}$)

3) Mass transfer through the liquid film outside the particles ($(1 - \varepsilon_e) k_f a_p \left[C - C_p \left(r = R_p \right) \right]$)

4) Axial dispersion ($\varepsilon_e D_L \frac{\partial^2 C}{\partial z^2}$)

The mass balance of the component in the stationary phase is expressed by equation (2.18).

$$\varepsilon_p \frac{\partial C_p}{\partial t} + \left(1 - \varepsilon_p \right) \frac{\partial q}{\partial t} = \varepsilon_p \frac{1}{r^2} \frac{\partial}{\partial r} \left(r^2 D_p \frac{\partial C_p}{\partial r} \right) \quad (2.18)$$

where ε_p is particle porosity. q is the concentration of the component in the adsorbed phase, and D_p is effective diffusivity determined by Stoke-Einstein equation described in section 2.6.2.

Equation (2.18) describes the following phenomena:

1) Mass accumulation in the stationary phase ($\varepsilon_p \frac{\partial C_p}{\partial t}$)

2) Adsorption rate ($\left(1 - \varepsilon_p \right) \frac{\partial q}{\partial t}$)

3) Molecular diffusion in radial direction ($\varepsilon_p \frac{1}{r^2}\frac{\partial}{\partial r}\left(r^2 D_p \frac{\partial C_p}{\partial r}\right)$)

To solve the mass balance equations, proper initial and boundary conditions are required. The initial conditions generally assume the concentrations in the mobile phase, stationary phase and the adsorbed phase are zero all along the column as described by equation (2.19) – (2.21)

$$C(0,z) = 0 \text{ for } 0 < z < L_c \tag{2.19}$$

$$C_p(0,r,z) = 0 \text{ for } 0 < z < L_c;\ 0 < r < R_p \tag{2.20}$$

$$q(0,r,z) = 0 \text{ for } 0 < z < L_c;\ 0 < r < R_p \tag{2.21}$$

Two boundary conditions for the column inlet and outlet are:

For $t > 0$ and $z = 0$

$$uC_f - uC(0,t) = -\varepsilon_e D_L \frac{\partial C}{\partial z} \tag{2.22}$$

$$C_f = \begin{cases} C_0 & 0 < t \le t_{inj} \\ 0 & t > t_{inj} \end{cases} \tag{2.23}$$

where C_f is feed concentration at time t. C_0 is initial feed concentration and t_{inj} is injection time.

For $t > 0$ and $z = L_c$

$$\frac{\partial C}{\partial z} = 0 \tag{2.24}$$

And two boundary conditions inside the stationary phase are:

For $t > 0$ and $r = R_p$

$$D_L \frac{\partial C_p(t,r)}{\partial r} = k_f a_p \left[C - C_p(t,r)\right] \tag{2.25}$$

For $t > 0$ and $r = 0$

$$\frac{\partial C_p}{\partial r} = 0 \tag{2.26}$$

However, the complexity of the model and much longer solution time required for such complicated model would counteract the model precise calculations. Generally, compromise between the model accuracy and the model complexity must general be made with additional assumptions to general rate model. Depending on the simplifications, four alternative models are derived: the transport-dispersive model, the equilibrium-disperisve model, the transport model and the ideal model, each of which is described as follows:

Transport-dispersive model

The transport-dispersive model or the lumped pore model is a simplified form of the general rate model and can be applied when the mass transfer kinetics is moderately fast (Guiochon, 2002). From equation (2.18), the value of q is assumed to be in equilibrium with C_p for all particles. The relationship between q and C_p is described by the adsorption isotherm, which is discussed in section 2.6.3. When the diffusion is not normal diffusion from pore liquid, but it is solid diffusion, pore diffusion, or surface diffusion, the transport-dispersive model is assumed by integrating equation (2.17) and (2.18) and averaging by particle volume (V_p) to give average volume of particle as equation (2.27) (Morbidelli et al., 1982).

$$\frac{1}{V_p}\int f(C_p)dV_p = f(\overline{C_p}) \tag{2.27}$$

where $\overline{C_p}$ is average concentration in the stationary phase.

The Laplacian operation can be applied to the first term of the right side of equation (2.25) and substitute the boundary condition to give

$$k_f a_p\left[C - C_p(t,r)\right] = k_{ov}\left(C - \overline{C_p}\right) \tag{2.28}$$

where k_{ov} is the overall mass transfer coefficient, which is a function of external mass transfer coefficient and effective diffusivity as described in equation (2.29) (Ruthven, 1984).

$$k_{ov} = \left[\frac{d_p}{6k_f a_p} + \frac{d_p^2}{60\varepsilon_p D_p}\right]^{-1} \tag{2.29}$$

Therefore, the mass balance in equation (2.17) and (2.18) can be rearranged to equation (2.30) and (2.31), respectively.

$$\varepsilon_e \frac{\partial C}{\partial t} + u\frac{\partial C}{\partial z} + (1-\varepsilon_e)k_{ov}\left(C - \overline{C_p}\right) = \varepsilon_e D_L \frac{\partial^2 C}{\partial z^2} \tag{2.30}$$

$$\varepsilon_p \frac{\partial C_p}{\partial t} + \left(1-\varepsilon_p\right)\frac{\partial q}{\partial t} = k_{ov}\left(C - \overline{C_p}\right) \tag{2.31}$$

Equilibrium-dispersive model

The equilibrium-dispersive model is derived from transport-dispersive model by assuming the mass transfer between bulk fluid and particle is very fast. Thus, the term $k_{ov}\left(C - \overline{C_p}\right)$ in equation (2.30) and (2.31), representing the rate of mass transfer inside the stationary phase, can be negligible and, then, including similar terms of mass balance equations into one equation to obtain equilibrium-dispersive model as described in equation (2.32).

$$\frac{\partial C}{\partial t} + u\frac{\partial C}{\partial z} + \left(\frac{1-\varepsilon_e}{\varepsilon_e}\right)\frac{\partial q}{\partial t} = D_L \frac{\partial^2 C}{\partial z^2} \tag{2.32}$$

From a comprehensive review, equilibrium-dispersive model is usually applied to model the transfer behavior of small-molecule compounds, such as amino acids, in reverse phase chromatography columns. Kostava and Bart (2007) used the EDM model to preparative chromatographic separation of amino acid racemic mixtures in a reverse phase chromatography column. The results found that EDM model with linear

isotherms could well describe the transfer behavior of the amino acids at low feed concentrations. These results are in good agreement with the study of Chen et al. (2006). However, EDM cannot be applied to describe chromatographic process of large-molecule compounds, such as proteins, because of neglecting the effect of mass transfer kinetic (Gu et al., 2013).

Transport model

The transport model or the lumped kinetic model is derived from transport-dispersive model similar to the equilibrium-dispersive model. The difference between these two models is mass transfer in the transport model is not infinitely fast and the kinetic effect cannot be negligible. However, the mass transfer kinetic of this model, relating to the adsorption rate ($\frac{\partial q}{\partial t}$), is determined by linear driving forces approximation (LDFA) as described in equation (2.33).

$$\frac{\partial q}{\partial t} = k_{ov}(C - C_e) \tag{2.33}$$

where C_e is the stagnant fluid equilibrium concentration, relating to the adsorption isotherm described in section 2.6.3.

Khosravanipour Mostafazadeh et al. (2011) used transport model to study transfer behavior of fructose and glucose from date syrup mixture in a resin chromatography column. The results found that the breakthrough curves predicted by transport model have good agreement with experimental data. Araujo Padilha et al. (2016) used the transport model to describe and optimize the chromatographic purification of Bacillus cereus chitosanase in an expanded bed column. The model could well predict transfer behavior of the compound for all conditions. The deviation,

measured by mean square deviation (MSE), between the model prediction and experimental data was less than 5%. The optimum condition for the process was velocity of 200 cm/h and the column height of 8 cm. At this condition, the process could achieve 26.78% yield.

Ideal model

The ideal model is the simplest mathematical model. It is derived from the equilibrium-dispersive model by assuming that the column has an infinite efficiency. The mass transfer by axial dispersion is also negligible. The band profile arises only from the characteristics of the equilibrium thermodynamics of the compound (Guiochon, 2002). The mass balance equation is simplified to equation (2.34)

$$\frac{\partial C}{\partial t} + u\frac{\partial C}{\partial z} + \left(\frac{1-\varepsilon_e}{\varepsilon_e}\right)\frac{\partial q}{\partial t} = 0 \qquad (2.34)$$

Park et al. (2000) used the ideal model to predict transfer behavior of yew tree taxol in a normal phase chromatography column. The results show that the retention time and peak height of the compound between the model prediction and the experimental data are in good agreement. However, the deviation between the model prediction and the experimental data is rather high, since the model depends only on thermodynamic equilibrium of the compound.

2.6.2 Determination of transport parameters

Prior to chromatographic modelling studies, accurate transport parameters, resulting to precision of the model prediction, must be determined. Since the chromatographic models used in this study were transport model, equilibrium-

dispersive model and ideal model, the transport parameters required to be identified included the axial dispersion and the overall mass transfer coefficients. The correlations used to determine the parameters are described follows:

2.6.2.1 Axial dispersion coefficient

The axial dispersion coefficient, used in transport and equilibrium-dispersive model, was determined from Chung and Wen correlation, equation (2.35) (Welty et al., 2008). This is correlation was derived based on numerous experiments over a broad range of Reynolds number, Re $(10^{-3} \leq Re \leq 10^{3})$. In addition, the equation assumes that the axial dispersion coefficient, relating to Peclect number, of each compound is independent of its molecular weight.

$$Pe = \frac{0.2}{\varepsilon_e} + \frac{0.011}{\varepsilon_e}(\varepsilon_e Re)^{0.48} \qquad (10^{-3} \leq Re \leq 10^{3}) \tag{2.35}$$

where Pe is Peclect number $\left(\frac{ud_p}{D_L}\right)$,$Re$ is Reynolds number $\left(\frac{ud_p\rho}{\mu}\right)$. μ is the mobile phase viscosity and ρ is the mobile phase density.

2.6.2.2 Overall mass transfer coefficient

The overall mass transfer coefficient used in transport model was determined by combining effective diffusivity and external mass transfer coefficient as described in equation (2.29). The effective diffusivity was determined by Stokes-Einstein equation as shown in equation (2.36) (Kim et al., 2006).

$$D_p = \left(\frac{\varepsilon_p}{2-\varepsilon_p}\right)^2 \left(\frac{\kappa T}{6\pi\mu R_m}\right) \tag{2.36}$$

where κ is Boltzmann constant 1.38×10^{-23} J/K. T is temperature and R_m is the radius of compound molecule.

External mass transfer coefficient was calculated from dimensionless correlations relating between Sherwood number, Schmidt number and Reynold number. The correlations present in literature for packed bed column can be arranged in an empirical formula as shown in equation (2.37) and some empirical correlations are summarized in Table 2.4.

$$Sh = ARe^{B}Sc^{C} \tag{2.37}$$

where A, B and C are correlation constants. Sh is Sherwood number $\left(\frac{k_f d_p}{D_m}\right)$. Sc is Schmidt number $\left(\frac{\mu}{\rho D_m}\right)$. D_m is the molecular diffusivity determined by Wilke and Chang correlation given in equation (2.38) (Welty et al., 2008).

$$D_m = \frac{7.4\times10^{-8}(\emptyset M)^{0.5}T}{\mu V^{0.6}} \tag{2.38}$$

where M is the molecular weight of solvent compound, $\emptyset$ is the association parameter (i.e., 1 for non-polar solvents). V is the critical volume of solute compound. Here, it was determined by the group contribution method (shown in Appendix B.3).

Although several correlations for an estimation of the external mass transfer coefficient in several systems have been proposed, they might not be applied in a specific system as can see in several previous works (Lv et. al., 2008, Borba et. al., 2006). The external mass transfer coefficient should be directly measured from the experiments data obtained using a column with similar characteristics with the system. (Richard et al., 2010).

Table 2. 4 Correlations proposed for determination of the external mass transfer coefficient

Authors	Correlation	Domain of validity
Willianson et al. (1963)	$Sh = 2.4\varepsilon_e Re^{0.34} Sc^{0.42}$	$0.08 < Re < 125$ $150 < Sc < 1300$
Wilson and Geankoplis (1966)	$Sh = 1.09\varepsilon_e^{-\frac{2}{3}} Re^{\frac{1}{3}} Sc^{\frac{1}{3}}$	$0.0016 < Re < 55$ $950 < Sc < 70000$ $0.35 < \varepsilon < 0.75$
Kataoka et al. (1972)	$Sh = 1.85\left(\frac{1-\varepsilon_e}{\varepsilon_e}\right)^{\frac{1}{3}} Re^{\frac{1}{3}} Sc^{\frac{1}{3}}$	$Re\left(\frac{\varepsilon}{1-\varepsilon}\right) < 10000$
Kumar et al. (1977)	$Sh = \frac{1.13 Re^{0.21} Sc^{\frac{1}{3}}}{\varepsilon_e}$	$Re < 10$
Dwivedi and Upadhyay (1977)	$Sh = \frac{1.11 Re^{0.28} Sc^{\frac{1}{3}}}{\varepsilon_e}$	$Re < 10$
Ohashi et al. (1981)	$Sh = 2 + 1.58 Re^{0.4} Sc^{\frac{1}{3}}$	$0.001 < Re < 5.8$

2.6.3 Adsorption isotherm

Adsorption is the adhesion of solute molecules on the surface of the adsorbent. In a preparative chromatography column, the stationary phase was filled in column, while mobile phase is a fluid with low viscosity and high solubility of component will percolates and transports the component in the mixture through stationary phase. The concentration of component in stationary phase is always near equilibrium while resident time for contacting or distribution of component through stationary phase

depends on temperature, mobile phase velocity and equilibrium constant in adsorption isotherm (Guiochon et al., 1994).

Adsorption isotherm is the relation of concentration in the stationary phase and the mobile phase at equilibrium, and is related to the adsorption rate in chromatographic process as described in equation (2.33). Consequently, single- and/or multi-component isotherms have to be determined with high accuracy to achieve good agreement between the model prediction and the experimental data. The goal is to obtain the unknown parameters for a selected isotherm equation. The commonly used isotherm models in chromatographic processes are linear, Langmuir and Fruendlich isotherm models. Details of each model are described as followings.

Linear isotherm model

The linear isotherm is the simplest model for describing equilibrium distribution of adsorbed solute on adsorbent surface. When concentration of solute in fluid phase is very low and the equilibrium of solute between fluid phase and adsorbent occurs rapidly, the amount of adsorbed solute varies linearly with the concentration in the fluid phase as described in equation (2.39).

$$q_e = HC_e \tag{2.39}$$

where q_e is equilibrium specific amount adsorbed

H is linear isotherm constant or Henry constant

Langmuir isotherm model

The Langmuir isotherm is developed for describing the saturation site of solid surface for solute molecules. The model assumptions are monolayer adsorption and no interaction between solute molecules (Hines and Maddox, 1985). This model describes equilibrium using chemical equilibrium reaction with two reactions: adsorption and

desorption reactions. The rate of adsorption depends on the concentration of solute in fluid phase and the number free vacant sites on the adsorbent surface while the rate of desorption depends on the amount of adsorbed solute. When the rate of adsorption is equal to the rate of desorption at a given temperature, the equilibrium condition is occurred. The model equation could be expressed by equation (2.40).

$$q_e = \frac{q_0 K_L C_e}{1+K_L C_e} \tag{2.40}$$

where q_0 is maximum specific amount adsorbed

k_L is Langmuir isotherm constant

Freundich isotherm model

The Fruendlich isotherm is a nonlinear correlation that describes the equilibrium of a solute in fluid phase and adsorbed phase. The Freundlich model equation could be described as in equation (2.35).

$$q_e = K_F C_e^{\frac{1}{n_F}} \tag{2.41}$$

where K_f and n_F are Freundlich model constants.

When n_F is closed to 1, the isotherm shape is linear. If n_F is higher than 1, the curve shape is convex and the shape is concave when n is lower than 1. However, this isotherm cannot predict the saturation of solute on adsorbent surface.

In preparative chromatography, the type of adsorption isotherm influence on chromatogram shape as shown in Figure 2.17. The elution profile of an ideal chromatogram depends only on the thermodynamic property of the chromatographic system. On the other hand, in a real chromatogram, additional mass transfer and fluid dynamic factors, i.e, axial dispersion and mass transfer resistance, have to be taken into account.

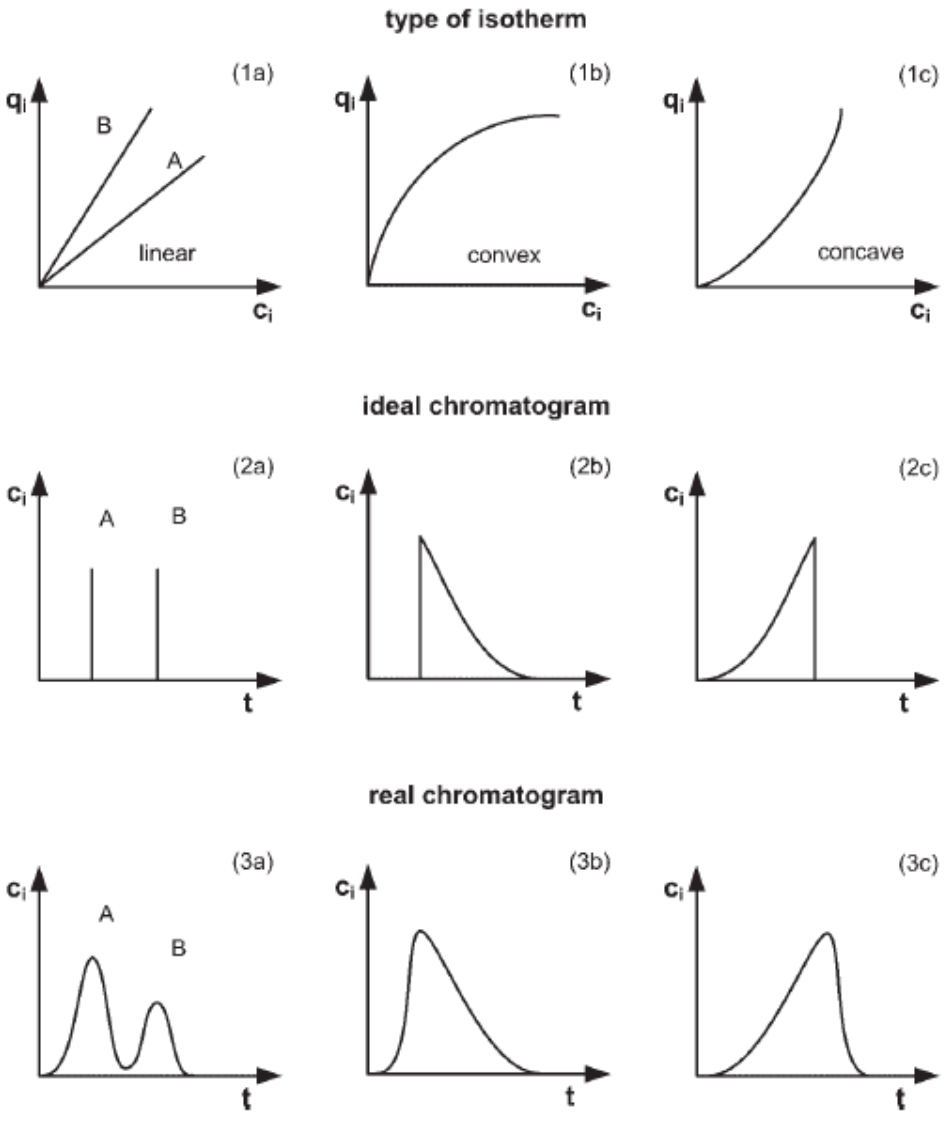

Figure 2. 17 Influence of the type of isotherm on the chromatogram (a) linear isotherm (b) convex isotherm (c) concave isotherm (Schmidt-Traub, 2005)

For linear isotherm (Figure 2.17-1a), the retention time of the compound is independent of the fluid phase concentration. Each injected component then, theoretically, elutes at its retention time as an ideally rectangular pulse (Figure 2.17-2a). The retention time is thus only influenced by the Henry constant. The isotherm of a compound which has higher slope has longer retention time than other compounds. This is because it is better adsorbed on the stationary phase.

For convex isotherms (Figure 2.17-1b), the retention time corresponds to concentration of each compound. During elution of the solute, all concentrations from zero to the maximum elution concentration can be observed. If the maximum elution concentration is over the linear range of the isotherm, the concentration profile of the chromatogram can be determined by convex shape of the isotherm. The slope of a convex isotherm, and thus retention time, decreases with increasing concentration. Regions of lower concentration with longer retention time are caught up with regions of higher concentration and thus shorter retention time. In total, the profile is concentrated and the fronting sharpened. The solute elutes in a compressed front and results in Figure 2.17-2b. The peak maximum is shifted towards the compressive front of the peak while the back of the peak is dispersed. Elution of a substance with a dispersed back of the peak is called tailing. This phenomenon is effect of convex adsorption isotherm (Langmuir type). The opposite behavior is seen with concave isotherms (Figure 2.17-1c). For concave isotherms, lower concentrations move faster and thus back of the late-eluting high concentrations concentrated and sharpened. This results in chromatogram in Figure 2.17-2c. The dispersed shape of the front part of the peak is called fronting (Schmidt-Traub, 2005).

Real chromatograms (Figure 2.17, 3a-3c) take into account the thermodynamic influences as well as the mass transfer kinetics and fluid distribution. A rectangular concentration profile of the solute at the entrance of the column shortly changes into a bell-shape or Gaussian distribution (Figure 2.7(a)), if the isotherm is linear isotherm. For non-linear isotherm, the peaks become asymmetric as shown in Figure 2.7(b). The degree of peak asymmetry can be determined using equation (2.5).

Although a number of studies have been conducted on the determination of adsorption behaviors of natural compounds (Park et al., 2000, Chu et al., 2004, Zhang et al., 2007), only one article (Boonnoun et al., 2012) reported the adsorption behavior of marigold free lutein. The adsorption equilibrium study was carried out in a batchwise system at 30 ^{o}C. Silica gel was used as adsorbent whereas solvent was hexane and ethyl acetate (70:30 v/v). The adsorption was found to reach equilibrium in 5 min and the equilibrium data was found to be more reasonably described by Langmuir isotherm than Frundlich isotherm when the equilibrium concentrations were smaller than 8 µg·ml^{-1}. Nevertheless, the data were available only in a limited range of the concentrations and temperature. Moreover, adsorption isotherm of fatty acids in the system is still not provided. Thus, there is still lack of adequate information for chromatographic separation modelling of free lutein and fatty acids in de-esterified marigold oleoresin.

CHAPTER III
MATERIALS AND METHODS

3.1 Materials

Dried marigold powder was supplied by PPT Global Chemical Public Company Ltd. Hexane (purity >99.5%) was purchased from Sigma-Aldrich, Co. LLC. (St Louis, MO, USA). All chemicals used for de-esterification (i.e., potassium hydroxide and ethanol) were purchased from Merck & Co. Inc. (Wilson, NC, USA). Diethyl ether, ethyl acetate and silica gel (particle size 25-40 μm) were purchased from Merck Ltd. (Bangkok, Thailand). All standard chemicals (analytical grade), free lutein, palmitic acid and stearic acid, were purchased Sigma-Aldrich Pte. Ltd. (Singapore).

3.2 Sample preparation

In this part, the method proposed by Boonnoun et al., (2012) was applied to prepare marigold oleoresin, de-esterified marigold lutein, purified free lutein and purified fatty acids. The detail of each step is described as follows:

3.2.1 Marigold oleoresin

Briefly, in a 1 L beaker placed in a shaking incubator (LSI 1005R Shanking Incubator, Labtech, India), 100 g of dried marigold powder was extracted with 500 ml of hexane at 40 ^{o}C for 4 hr. The mixture was left to stand at room temperature (30 ^{o}C) to allow the residue to settle, and the residue was subsequently separated from the extract by filtration. The supernatant, the carotenoids containing solution, was concentrated by a rotary evaporator at 40 ^{o}C. The extract was then dried in a vacuum oven at 30 ^{o}C for 8 hr. The dried marigold extract, or marigold oleoresin, was then

analyzed by a spectrophotometer to measure the total xanthophyll content and by HPLC to measure the amount of free lutein and fatty acids.

3.2.2 De-esterified marigold lutein

One gram of marigold oleoresin was dissolved in 10 ml of ethanol in a 125 ml Erlenmeyer flask, followed by adding 0.6 g of KOH. The flask was continuously shaken in the shaking incubator at 150 rpm and 50 ^{o}C for 4 hr. After the reaction, the sample was transferred to a 500 ml separation funnel. 50 ml of ethanol, 100 ml of 5% Na_2SO_4 solution (in distilled water) and 80 ml of diethyl ether were then added to the funnel. All components were mixed thoroughly and the mixture was then allowed to separate into 2 phases. The lower phase (water phase), containing all water-soluble impurities, was discarded while the upper phase (ether phase), containing high concentration of free lutein, was collected as de-esterified lutein stock solution. The amount of free lutein and fatty acids in the de-esterified lutein stock solution was measured by HPLC analysis.

3.2.3 Purified free lutein

Firstly, 100 g of silica gel was soaked in a mixture of hexane and ethyl acetate (70:30 v/v) and degassed under sonication for 30 min. The silica gel was then packed into a preparative chromatography column (35×240 mm). A 10-ml de-esterified lutein stock solution was injected into the column at the bottom of the column. The mobile phase, i.e., the mixture of hexane and ethyl acetate, was then pumped into the column at a flow rate of 10 ml/min by a peristaltic pump (Masterflex, model number 7532-60, Cole Parmer, Thailand). The lutein sample was eluted up-flow. Fractions were collected at 5 minutes intervals from the outlet at the top and subsequently analyzed for the amount of free lutein by HPLC. The fractions giving high purity (>95% based on

chromatogram peak area) free lutein was collected and used as a stock solution for the determination of adsorption isotherm, the mathematical modelling of mass transfer behavior in chromatography column, and the determination of the optimum mobile phase velocity studies.

3.2.4 Purified fatty acid

To identify type of fatty acid in de-esterified marigold lutein, the fatty acid must be first separated from the de-esterified sample. The chromatographic apparatus system as shown in Figure 3.1 was used for this purpose. Firstly, 18 g of silica gel was added to 200 ml of a mixture of hexane and ethyl acetate at a ratio of 70:30 v/v. The mixture was degassed under sonication for 30 min and was then packed into the semi-preparative column (17×150 mm). 1 ml of de-esterified lutein stock solution was injected into the column at the top. The hexane-ethyl acetate mixture used as the mobile phase was then pumped into the column at the top by the peristaltic pump at a velocity of 0.19 cm/s. The column temperature was controlled constantly at 30 ^{o}C via circulation of water through the column jacket. The sample was eluted downflow and the outlet fractions were collected at various time intervals: every 1 min in fraction no. 1-4, followed by every 0.5 min in fraction no. 5-14, and every 1 min towards the end of the sample collection. The concentrations of free lutein and fatty acids of each fraction were analyzed by HPLC. The fractions containing high purity fatty acid (>95% based on chromatogram peak area) were combined to one fraction. The solvent in the combined fraction was evaporated under nitrogen gas. The dried sample was then analyzed by C-NMR and FT-IR to confirm the functional group and by MS to identify the type of fatty acids.

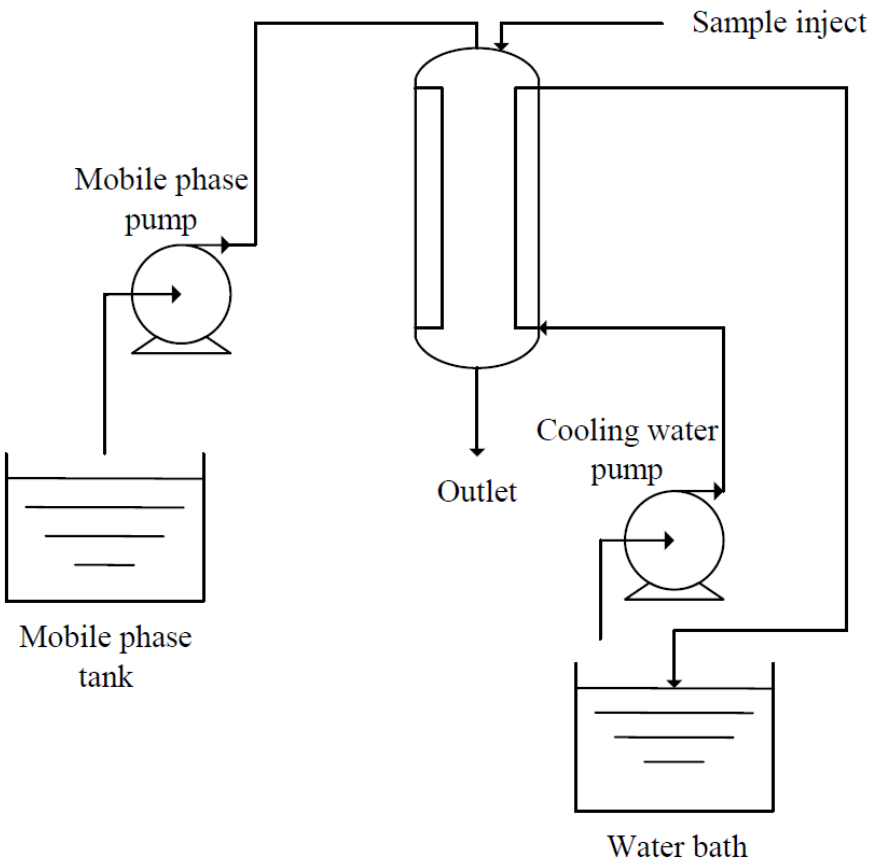

Figure 3. 1 Experimental setup of semi-preparative column

3.3 Chromatographic separation of free lutein and fatty acids

Chromatographic separation of free lutein and fatty acids in de-esterified marigold lutein was carried out using silica gel and mixture of hexane and ethyl acetate as stationary phase and mobile phase, respectively. The optimum mobile phase to giving the highest column efficiency was first determined, using purified free lutein as a test compound. Subsequently, at this velocity, the evaluation of the elution modes, i.e., isocratic and gradient elution modes, on the efficiency of the compounds separation were conducted.

3.3.1 The optimum mobile phase velocity determination

The column for the optimum velocity determination was prepared by the method described in section 3.3.4. 1 ml of purified free lutein stock solution, dissolved in a mixture of hexane-ethyl acetate at 70:30 v/v, having concentration between 20-40 µg/ml, was injected to the column at the top. The mobile phase, i.e., the hexane-ethyl acetate mixture, was then pumped into the column at the top by the peristaltic pump. The mobile phase velocity was varied between 0.12-0.38 cm/s. The outlet fractions were collected by the same manner as described previously. For each fraction, the concentration of free lutein was measured by UV-HPLC. Based on the time profile data of free lutein concentration, the mean and standard deviation of retention time were calculated. The value of the height of equivalent theoretical plate (HETP) of each eluent velocity was calculated based on equation (3.1) and was then plotted against the corresponding velocity in order to evaluate the optimum eluent velocity.

$$HETP = \left(\frac{\sigma_t}{t_R}\right)^2 L_c \tag{3.1}$$

where t_R and σ_t are mean and standard deviation of retention time; L_c is the column length.

3.3.2 Chromatographic separation in a semi-preparative column

The semi-preparative column for chromatographic separation of free lutein and fatty acids was prepared by the same manner as described in section 3.2.4. 1 ml of de-esterified lutein stock solution, containing free lutein and fatty acids about 380 and 150 µg/ml, respectively, was loaded to the column at the top. The mobile phase was then pumped to the top of the column at the optimum velocity determined in the previous section. In the isocratic mode elution, the mobile phase was only a mixture of hexane-ethyl acetate at a ratio of 70:30 v/v. On the other hand, in the gradient mode elution, the mobile phase was a mixture of hexane-ethyl acetate at a ratio of 85:15 v/v in the first

part of the elution with the desired time intervals (12 and 20 min), followed by a ratio of 70:30 v/v until all components were completely eluted. The fraction collection was performed as described previously. The concentrations of free lutein and fatty acid of each fraction were analyzed by HPLC.

3.3.3 Chromatographic separation in a preparative column

The preparative column apparatus was set up similarly to the semi-preparative scale. 100 g of silica gel, soaked by hexane-ethyl acetate mixture (70:30 v/v) and degassed under sonication for 30 min, was packed into the column. 10 ml of the de-esterified lutein stock solution was loaded into the column at the top. The mobile phase was then pumped into the column by mean of the peristaltic pump at the velocity 0.115 cm/s. In the isocratic elution, the experiment was run using only a mixture of hexane and ethyl acetate at a ratio of 70:30 v/v. Conversely, in the gradient elution, the experiment started with a mixture of hexane and ethyl acetate at a ratio of 85:15 v/v and was run for 20 min, before instantly changing to the mixture a ratio of 70:30 until all components were completely eluted. The outlet fractions were collected every 2 min and were analyzed by HPLC to determine free lutein and fatty acid concentrations.

3.4 Adsorption isotherms determination

The single component adsorption isotherms of free lutein and palmitic acid, using as standard fatty acid, were determined using batch adsorption studies. Stock solutions of free lutein and fatty acid were prepared by dissolving known amounts of the compounds in mixtures of hexane and ethyl acetate at ratios of 70:30 v/v and 85:15 v/v. Working solutions were then prepared by diluting different volumes of the stock solutions to achieve several solutions at the desired concentration, 5-300 µg/ml for free

lutein and 100-1000 µg/ml for fatty acid. To obtain the adsorption isotherm data, 0.5 g of silica gel (25-40 µm) was added into each of 125-ml Erlenmeyer flasks containing 10 ml of the working solution at different concentrations. The flasks were continuously shaken in the incubator with a constant speed of 120 rpm at 30 ^{o}C for 2 hours to ensure that the adsorption equilibrium was reached in each flask. After the power for the incubator was shut off, 1 ml of solution from each flask was collected using a filtering syringe and was subsequently analyzed by HPLC. The specific equilibrium amounts adsorbed (q_e) of free lutein and fatty acid of each experiment was calculated based on equation (3.2).

$$q_e = \frac{(C_0 - C_e)V_s}{W} \tag{3.2}$$

where C_0 and C_e are the initial and the equilibrium concentrations, respectively; V_s is the solution volume; and W is the silica gel weight.

3.5 Selection of the most suitable mass transfer model

In general, mathematical modelling for chromatographic process is based on mass, energy and momentum balances of components in a controlled volume of chromatography column as shown in Figure 3.2.

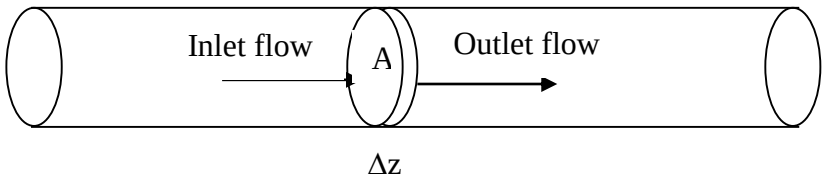

Figure 3. 2 Schematic diagram of chromatography column

The following assumptions were made for the formulation of the mathematical model used in this study:

1. radial dispersion was neglected;
2. the mobile phase properties, i.e., density and viscosity, were constants;
3. the mobile phase was inert;
4. the stationary phase material was a spherical shape and was packed homogeneously in the column;
5. void fraction of the column was constant;
6. the process was isothermal;
7. the fluid velocity was constant;
8. the interaction between the components was negligible;
9. the column pressure was constant.

In this study, 3 mass transfer models: ideal model, equilibrium-dispersive model, and transport model, were developed to model transfer behavior of free lutein in the semi-preparative column. The simplest model is the ideal model. In addition to the previous assumptions, the model assumes infinite column efficiency, infinite rate of mass transfer at the interface of the stationary phase and mobile phase, and no axial dispersion. Accordingly, the band profile arises only from the thermodynamic equilibrium of each compound. The balance equation which is derived from the material balance of each species i in a small controlled volume in the chromatography column is shown in equation (3.3).

Rate of species i in - Rate of species i out = Rate of Accumulation of species i in mobile phase + Rate of Accumulation of species i in stationary phase

$$uc_i\varepsilon_e A|_z - uc_i\varepsilon_e A|_{z+\Delta z} = \frac{\partial}{\partial t}[(\varepsilon_e c_i A\Delta z) + (1-\varepsilon_e)(q_i A\Delta z)] \quad (3.3)$$

Divide equation (3.3) by $\varepsilon_e A \Delta z$ and take limit of $\Delta z \rightarrow 0$, the following equation is resulted.

$$-\frac{\partial}{\partial z}(uc_i) = \frac{\partial}{\partial t}(c_i) + \frac{(1-\varepsilon_e)}{\varepsilon_e}\frac{\partial}{\partial t}(q_i)$$

Since the mobile phase velocity is assumed to be constant, the following equation is obtained.

$$-u\frac{\partial}{\partial z}(c_i) = \frac{\partial}{\partial t}(c_i) + \frac{(1-\varepsilon_e)}{\varepsilon_e}\frac{\partial}{\partial t}(q_i)$$

or $$\frac{\partial}{\partial t}(c_i) + u\frac{\partial}{\partial z}(c_i) + \frac{(1-\varepsilon_e)}{\varepsilon_e}\frac{\partial}{\partial t}(q_i) = 0 \quad (3.4)$$

This equation describes the following phenomena:

- Accumulation rate in the mobile phase $\left(\frac{\partial c_i}{\partial t}\right)$
- Convective transport in the mobile phase $\left(u\frac{\partial c_i}{\partial z}\right)$
- Adsorption rate in the stationary phase $\left(\frac{(1-\varepsilon_e)}{\varepsilon_e}\frac{\partial q_i}{\partial t}\right)$

Equation (3.4) can be converted to dimensionless equation as described by equation (3.5).

$$\frac{\partial}{\partial x}(c) + \frac{\partial}{\partial \tau}(c) + \frac{(1-\varepsilon_e)}{\varepsilon_e}\frac{\partial}{\partial \tau}(n) = 0 \quad (3.5)$$

where $x = \frac{z}{L}$ $\tau = \frac{tu}{L}$ $c = \frac{c_i}{c_{i0}}$ $n = \frac{q_i \rho}{c_{i0}}$

The second model, the equilibrium-dispersive model (EDM), is developed from the ideal model. The model still assumes that the mass transfer between the stationary phase and the mobile phase is infinitely fast. Nevertheless, it differs from the ideal model in that it takes into account the effects of mass transport by axial dispersion. This effect was added on the right side of equation (3.4). The mass balance of the component

i in a chromatography column becomes equation (3.6).

$$u\frac{\partial}{\partial z}(c_i) + \frac{\partial}{\partial t}(c_i) + \frac{(1-\varepsilon_e)}{\varepsilon_e}\frac{\partial}{\partial t}(q_i) = D_L\left(\frac{\partial^2 c_i}{\partial z^2}\right) \tag{3.6}$$

Equation (3.6) can be converted to dimensionless equation as described in equation (3.7).

$$\frac{\partial}{\partial x}(c) + \frac{\partial}{\partial \tau}(c) + \frac{(1-\varepsilon_e)}{\varepsilon_e}\frac{\partial}{\partial \tau}(n) = \frac{1}{Pe}\left(\frac{\partial^2 c}{\partial x^2}\right) \tag{3.7}$$

where $Pe = \frac{uL}{D_L}$

Lastly, the transport model is the model that takes into account both the axial dispersion effect and the effect of mass transfer kinetics between stationary phase and the mobile phase, which is related to the rate of variation of the local concentration on the stationary phase and the equilibrium concentration in the mobile phase. The adsorption rate of the stationary phase can be described by a linear driving force approximation as expressed in equation (2.33)

$$\frac{\partial q_i}{\partial t} = k_{ov}\left(c_i - c_{e,i}\right) \tag{2.27}$$

Equation (2.33) can be converted to dimensionless equation as described in equation (3.8)

$$\frac{\partial}{\partial \tau}(n) = F\left(\frac{c}{\rho} - \frac{n}{H}\right) \tag{3.8}$$

where F is $\frac{k_{ov}L}{u}$ and H is the linear isotherm constant.

To obtain the numerical solution, the model equations were discretized with respect to the dimensionless space coordinate (x), using forward finite difference method for the first order derivative (equation (3.9)) and central finite difference method for the second order derivative (equation (3.10)). It resulted in a system of ordinary differential equations (ODEs) in dimensionless time (τ). The system of ODEs,

with adsorption isotherm, initial and boundaries conditions, was simultaneously solved using equation (3.11) and equation (3.12). The numerical solutions were obtained using MATLAB (MATLAB 8.3, Mathworks Co., Natick, MA). The numerical algorithm is provided in Appendix B.

$$\frac{\partial c(x,\tau)}{\partial x} = \frac{c(x_{m+1},\tau_n)-c(x_m,\tau_n)}{\Delta x} \tag{3.9}$$

$$\frac{\partial^2 c(x,\tau)}{\partial x^2} = \frac{c(x_{m+1},\tau_n)-2c(x_m,\tau_n)+c(x_{m-1},\tau_n)}{\Delta x^2} \tag{3.10}$$

$$\frac{dc(\tau)}{d\tau} = \frac{c(\tau_{n+1})-c(\tau_n)}{\Delta \tau} \tag{3.11}$$

$$\frac{dn(\tau)}{d\tau} = \frac{n(\tau_{n+1})-n(\tau_n)}{\Delta \tau} \tag{3.12}$$

The model predictions were compared with the experimental results. The deviation of the model prediction from the experimental data was measured by the standard error (S.E.) defined by equation (3.13).

$$S.E. = \sqrt{\frac{\Sigma_{i=1}^{n_{exp}}(C_{exp}-C_{mol})^2}{n_{exp}-1}} \tag{3.13}$$

where n_{exp} is the number of data point, C_{exp} and C_{mol} are the concentrations obtained from experiment and model, respectively. The model having the lowest S.E., implying the best fitting of the mass transfer model, was then used to model the separation of free lutein and fatty acids.

3.6 Mass transfer correlation development and validation

A correlation of external mass transfer coefficient was developed in order to increase the precision of mass transfer model prediction. The experiment was performed in the semi-preparative column by similar manner as described in section 4.1, using purified free lutein as a test compound. The value of external mass transfer

coefficient of each velocity (varied between 0.12-0.21 cm/s) was obtained by minimizing the standard error. According to the external mass transfer correlation (equation (2.37)), it can be linearized as described in equation (3.14). The correlation parameters A and B could be evaluated from the y-intercept and the slope of the plot $\ln(Sh)$ vs $\ln(Re)$, respectively.

$$\ln Sh = B \ln Re + \ln A Sc^{\frac{1}{3}} \tag{3.14}$$

The mass transfer model with the new correlated external mass transfer coefficient was then validated with the experimental data in both semi-preparative and preparative columns. The degree of consistency between the experimental results and model prediction was measured by standard error and correlation coefficient (r_{cor}) defined in equation (3.15).

$$r_{cor} = \frac{n\sum_{i=1}^{n} C_{exp}C_{mol} - \sum_{i=1}^{n} C_{exp}C_{mol}}{\sqrt{\left(n\sum_{i=1}^{n} C_{exp}^2 - \left(\sum_{i=1}^{n} C_{exp}\right)^2\right)\left(n\sum_{i=1}^{n} C_{mol}^2 - \left(\sum_{i=1}^{n} C_{mol}\right)^2\right)}} \tag{3.15}$$

3.7 Sample analysis

3.7.1 Total xanthophyll analysis by spectrophotometer

To determine the total amount of xanthophylls in the marigold oleoresin, the marigold oleoresin was dissolved in ethanol. The solution was then measured to identify xanthophyll concentration by a spectrophotometer (G20, Genesys, NY, USA) at a wavelength of 478 nm using free lutein as a standard (Vechpanich, 2008).

3.7.2 Free lutein analysis by UV-HPLC

To analyze the concentration of free lutein by HPLC, the oleoresin, the de-esterified marigold lutein, the purified free lutein and all collected fractions underwent

solvent evaporation under nitrogen gas. The dried samples were then redissolved in ethyl acetate which was the mobile phase in the HPLC analysis.

The free lutein concentration was analyzed by reverse phase HPLC, carried out using Agilant 1100, Licrhocart C-18 column (30 cm in length), a Diode Array Detector Module 335 and an automatic injector. The mobile phase was a gradient solvent system composed of acetonitrile: methanol (9:1 v/v) (solvent A) and ethyl acetate (solvent B). The system was run by linearly increasing of solvent B from 0% to 100% in 30 min at a flow rate of 1 ml/min. The sample injection volume was 50 µl and the UV-detector wavelength was set at 450 nm (Piccaglia et al., 1998).

3.7.3 Fatty acid analysis using ELSD-HPLC

To analyze the concentration of fatty acid in the oleoresin, the de-esterified marigold lutein and all collected fractions by HPLC, the samples must be prepared by evaporating the solvent under nitrogen gas and redissolving in the HPLC mobile phase, i.e., ethyl acetate. The HPLC column was packed by µBondapack C-18, 125 A^{o}, 10 µm, 3.9 mm I.D. × 300 mm and was set at room temperature (25 ^{o}C). The ELSD detector (Alltech ELSD 2000 ES, Artisan Technology Group, IL, USA) was set at tube temperature of 60 ^{o}C, nitrogen gas flow of 1.7 L/min, and with the impactor was turned off. The mobile phase system was an isocratic solvent composed of methanol: isopropanol (3:2 v/v) and the flow rate was controlled at 0.9 ml/min. The sample injection volume was 20 µl (Anjinta, 2013).

3.7.4 Fatty acid analysis by Carbon Nuclear Magnetic Resonance Spectrometry (C-NMR)

Carbon Nuclear Magnetic Resonance analysis was used to confirm the functional group of the fatty acids purified from the de-esterified marigold lutein. The

C-NMR method was acquired on a Varian INOVA model (Fourier 300, Bruker Biospin Co., MS, USA). All spectra were measured in $CDCl_3$ at 25 ^oC with CP/MAS solid probe and Nano probe.

3.7.5 Fatty acid analysis by Fourier transform infrared spectroscopy (FT-IR)

Fourier transform infrared spectroscopy was used to identify the chemical bonds of the purified fatty acids. FT-IR measurement was performed in a KBr disc. (PerkinElmer Spectrum One, PerkinElmer Inc., MA, USA).

3.7.6 Fatty acid analysis by mass spectrometry (MS)

Mass spectrometry was used to identify type of the purified fatty acids. 5 µl of fatty acid sample dissolved in ethanol was directly injected into the MS analyzer (MicrOTOF, Bruker Daltonics Inc., MA USA). MS analysis was carried out in a positive ion measurement mode with a detection voltage of 1.6 kV, an AOCI temperature of 400 ^oC, a curved desolvation lime of 250 ^oC, and a block temperature of 200 ^oC. The flow rate of the nebulizer gas was 2.5 ml/min. Full scan spectra were obtained by scanning masses between m/z 200 and 400.

CHAPTER IV
CHROMATOGRAPHIC SEPARATION OF FREE LUTEIN AND FATTY ACIDS

In this chapter, the quantification of free lutein and fatty acids in marigold oleoresin and de-esterified marigold lutein samples was reported. In addition, types of the fatty acids in the samples were identified. Finally, the optimum condition for chromatographic separation of free lutein and fatty acids was investigated in a semi-preparative column.

4.1 Analysis of marigold oleoresin and de-esterified marigold lutein

Marigold oleoresin was characterized by a spectrophotometer to measure the total amount of xanthophylls and by HPLC to measure amounts of free lutein and fatty acids. Based on 1 g of marigold oleoresin, the total amount of xanthophylls was 256.98 mg (23.64 mg/g dried marigold). These xanthophylls were mostly in the form of xanthophyll esters, namely lutein esters, whose retention time was between 25-28 min as shown Figure 4.1(a) (Piccaglia et al. 1998, Vechpanich and Shotipruk 2011). The amount of free lutein (retention time 9.9 min) was only 0.36 mg (0.03 mg/g dried marigold). These results were in good agreement with the study of Abdel-Aal and Rabalski (2015). By comparing with the retention time of standard reagents, the ELSD-HPLC analysis result (Figure 4.1(b)) shows that the fatty acids in the marigold oleoresin were palmitic acid and stearic acid, whose retention times were 3.43 and 3.97 min, respectively. The total amount of the fatty acids was 2.6 mg (0.23 mg/g dried marigold).

After the de-esterification process, all lutein esters were completely de-esterified to free lutein and fatty acid as can see from Figure 4.2(a). The amount of free lutein increases from 0.36 mg to 129.76 mg. However, the amount of fatty acid, mostly

palmitic acid (Figure 4.2(b)), also increases from 2.6 mg to 49.12 mg, resulting in low purity (74.55%) of lutein product. This purity is still lower than the suitable level for human consumption (<90%). A further purification is therefore required to achieve higher product purity. In addition, during the de-esterification process, some free lutein was oxidized with oxygen and became anhydrolutein whose retention time was 10.9 min as shown in Figure 4.2(a). (Craft and Soares, 1992, Boonnoun et al., 2012) The amount of anhydrolutein was 14.12 mg. However, anhydrolutein has also been reported to be an antioxidant and anticancer compound (Molnar et al., 2004, Dorjgochoo et al., 2009). Thus, it might not need to be separated.

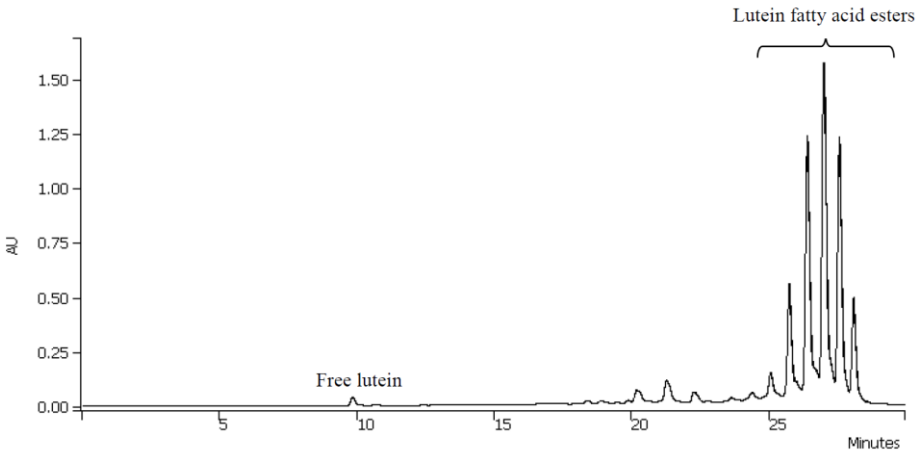

(a)

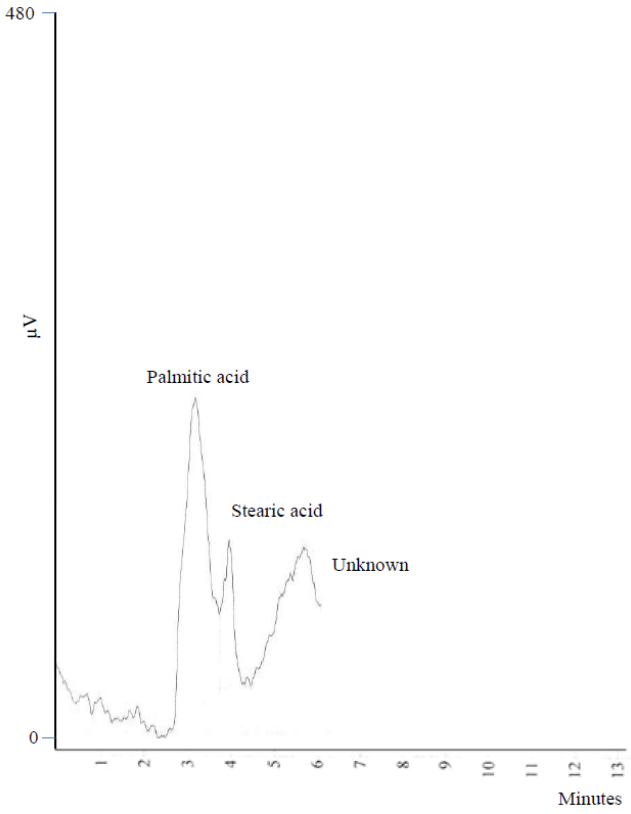

(b)

Figure 4. 1 Characterization of marigold oleoresin by HPLC (a) UV-HPLC (b) ELSD-HPLC

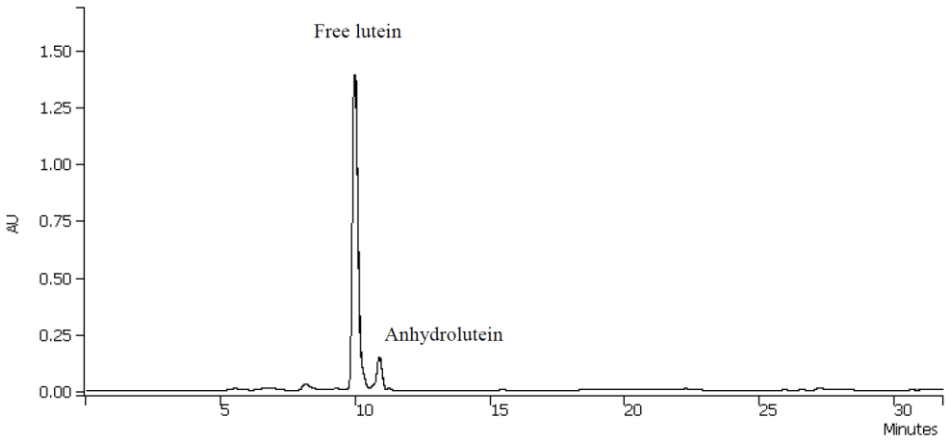

(a)

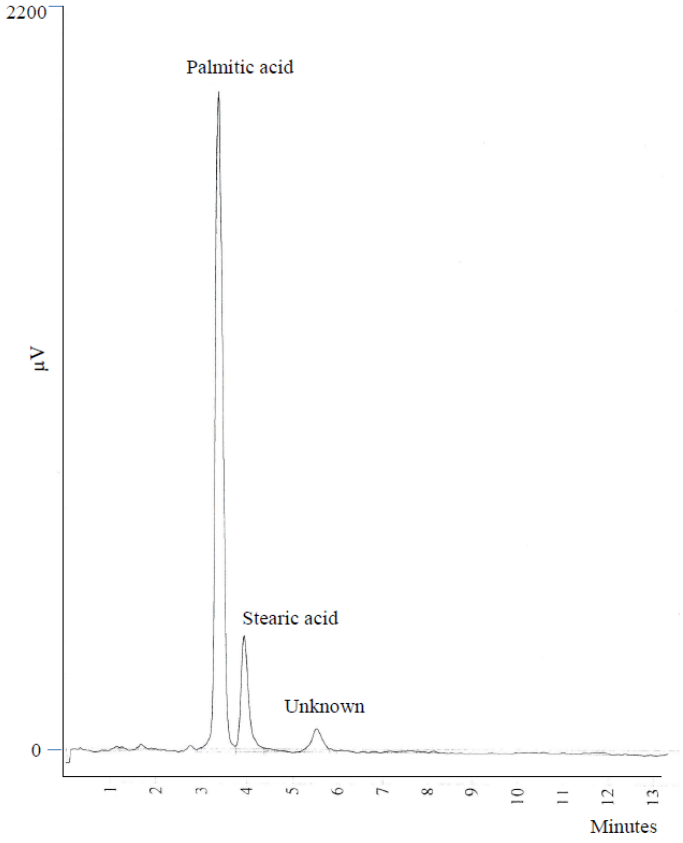

(b)

Figure 4. 2 Characterization of de-esterified marigold lutein by HPLC (a) UV-HPLC (b) ELSD-HPLC

4.2 Identifying type of fatty acid in de-esterified marigold lutein

To identify the type of fatty acids, the de-esterified marigold lutein was loaded to a chromatography column to separate the fatty acids. The elution profiles of free lutein and fatty acid, eluted at the mobile phase velocity of 0.19 cm/s, are shown in Figure 4.3. From the figure, the elution of components in the column occurs in the order of increasing polarity; therefore, free lutein is eluted from the column before fatty acid due to relatively lower polarity. At this condition, however, the separation of the compounds is incomplete because of overlapping of the peaks. The fractions having fatty acid purity >95% could be therefore collected after 32-min retention time. They were then analyzed by NMR and FT-IR to confirm the functional group and by MS to identify type of the fatty acids. The chemical shift of the compound in NMR results (Figure 4.4) correspond to the NMR pattern of standard palmitic acid, particularly the chemical shift at 178 ppm in C-NMR pattern which represents the functional group of carboxyl group (Pretsch. et al., 2009). The FT-IR spectrum bands of the fatty acid sample (Figure 4.5) display at the wavenumbers 3424 cm^{-1} (-OH) and 1702 cm^{-1} (C=O), which are assigned to the functional group of a carboxylic compound (Gumel et al. 2014). The MS result in Figure 4.6 shows that there are 3 major components in the fatty acid sample. The molecular weights of 279.22 and 307.26 correspond to palmitic acid and stearic acid in the form of $[M+Na]^+$, respectively. This result agrees with the ELSD-HPLC analysis as shown in Figure 4.1(b) and 4.2(b). However, the molecular weight of 325.22 is still unknown but it may correspond to the peak at the retention time of 5.5 min in the ELSD-HPLC chromatograms. Further characterization is required.

Based on the above results, it could be concluded that the total amount of fatty acid was 49.12 mg/g oleoresin, and of this, the major fatty acid in de-esterified marigold lutein was palmitic acid.

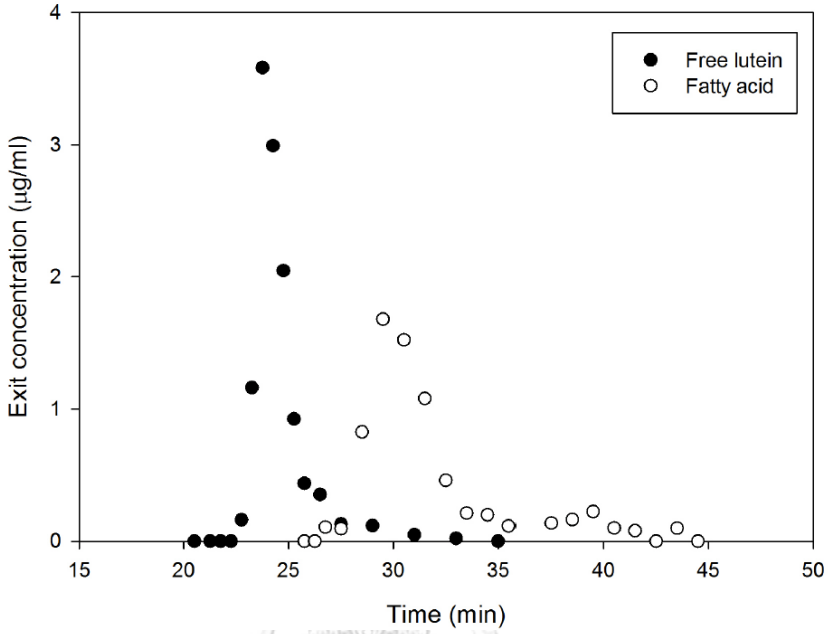

Figure 4. 3 Elution profile of free lutein and fatty acid at mobile phase velocity 0.19 cm/s

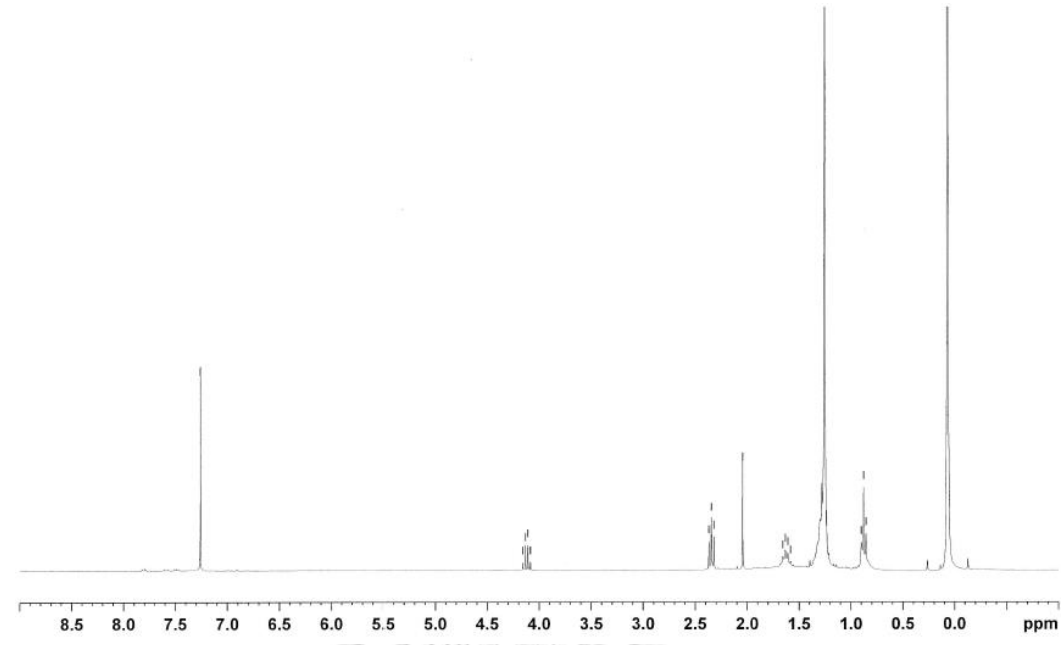

(a)

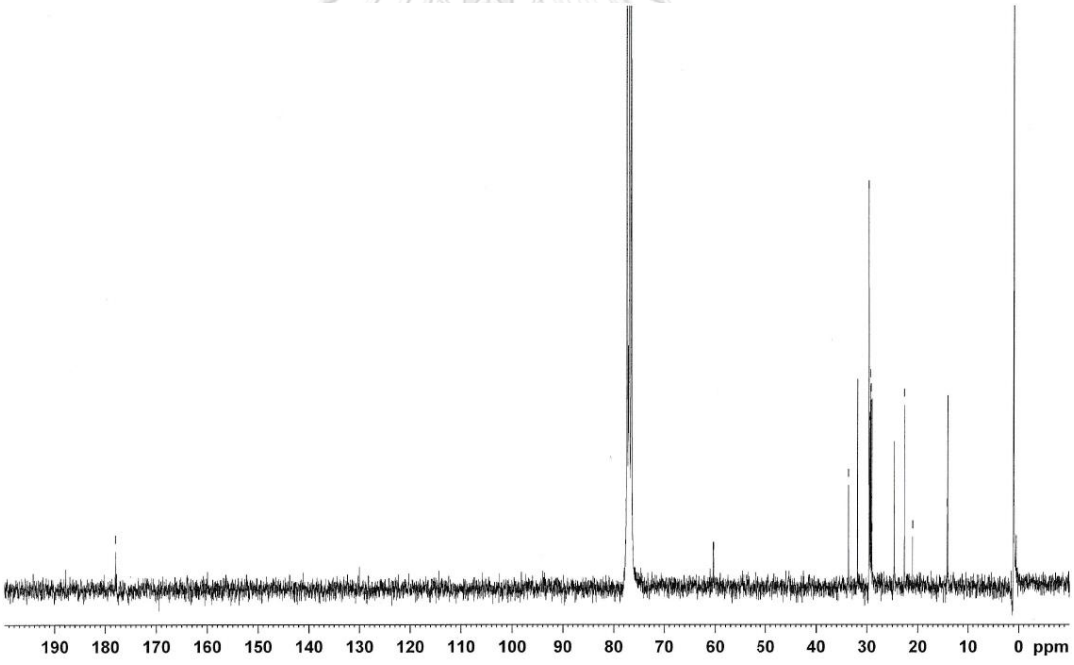

(b)

Figure 4. 4 NMR pattern of fatty acid sample (a) H-NMR (b) C-NMR

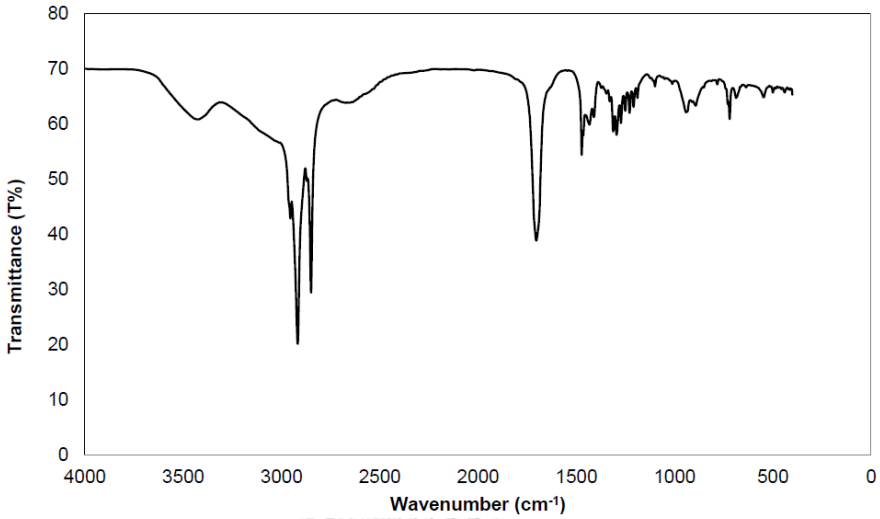

Figure 4. 5 FT-IR characterization of fatty acid sample

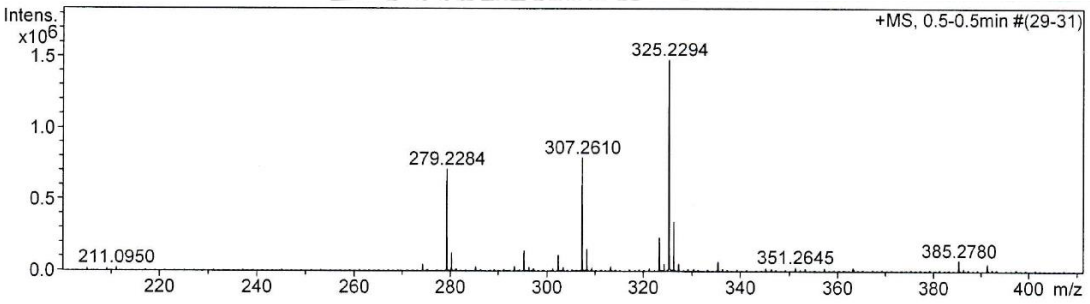

Figure 4. 6 MS characterization of fatty acid sample

4.3 Chromatographic separation of free lutein and fatty acid

4.3.1 Determination of the optimum eluent velocity

The optimum mobile phase velocity, which achieves the highest column efficiency, was determined, using purified free lutein as a test compound. The chromatographic experiments were carried out in a semi-preparative column using silica gel as stationary phase and mixture of hexane-ethyl acetate (70:30 v/v) as mobile phase. The HETP of each mobile phase velocity determined from equation (3.1) was plotted against the corresponding velocity. The result is shown in Figure 4.7. From the

figure, the optimum velocity is 0.16 cm/s corresponding to the HETP of 0.0158 cm. The eluent velocity less than or above 0.16 cm/s results in greater HETP and, hence, lower column's performance. When the velocity is smaller than 0.16 cm/s, the axial diffusion is dominant over the mass transfer resistance effect. Thus, the band-broadening in this velocity range is mainly contributed by the axial diffusion since free lutein has long retention time in the column. On the other hand, at the velocity range more than 0.16 cm/s, mass transfer resistance effect is dominant over the axial diffusion effect. The band-broadening in this velocity range is resulted from free lutein in the mobile phase which was eluted and moved ahead of free lutein adsorbed in the stationary phase. Therefore, the eluent velocity of 0.16 cm/s will be used in further analysis of free lutein and fatty acid separation.

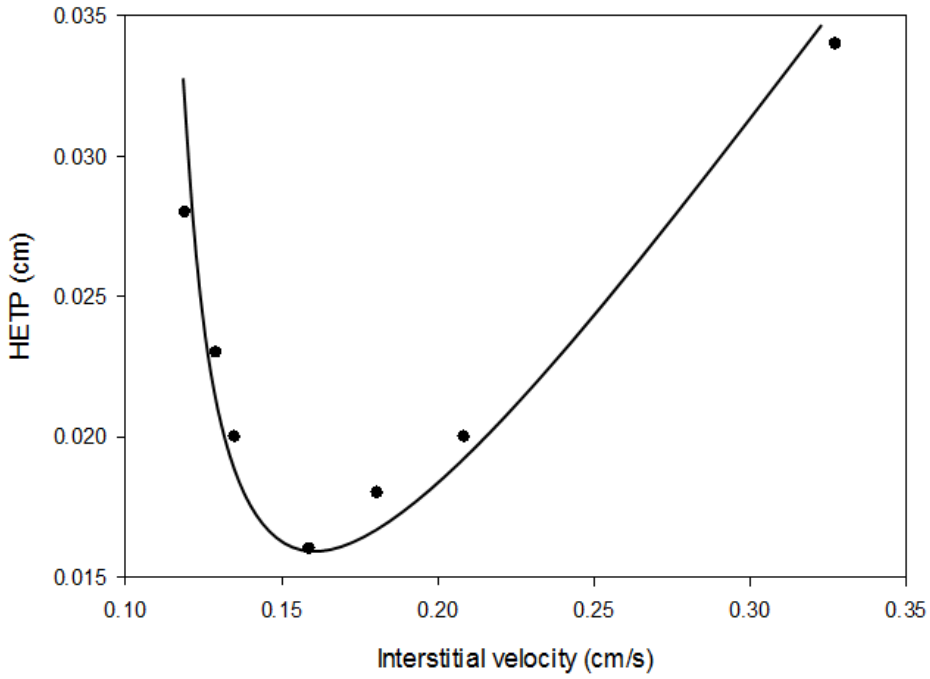

Figure 4. 7 Relationship between HETP and mobile phase velocity

4.3.2 Effect of elution mode on chromatographic separation

The chromatographic separation of free lutein and fatty acid in the de-esterified marigold lutein was investigated using two different elution modes, i.e., isocratic and gradient modes. The quality of the separation was evaluated by the resolution, R_s, as described in equation (2.9). The result of isocratic mode elution, using 70:30 v/v hexane-ethyl acetate mixture as mobile phase, is shown in Figure 4.8 (a). From the chromatogram, the free lutein and fatty acid peaks overlapped, which implies that they could not be well separated using this elution method. Furthermore, the resolution was found to be only 1.13 which is much samller than the baseline resolution. Consequently, further modification is needed to achieve a higher resolution.

Gradient elution mode was employed to improve the resolution. In this study, mixtures of hexane ethyl acetate in 2 different ratios, which were selected based on the TLC studies of Boonnoun et al. (2012) and Anjinta (2013), were used. From the TLC studies, an increase in hexane ratio in the mobile phase could extend the elution time of free lutein and fatty acids in the chromatography column, resulting in better separation. This is because the compounds could less dissolve in the mobile phase and were better adsorbed because of increased interaction force between the compounds and silica gel (Ralston and Hoerr 1942, Craft and Soares 1992, Schmidt et al. 2006). At very high ratio of hexane to ethyl acetate (>90:10 v/v) however, strong interaction of free lutein and fatty acids with the stationary phase became larger making them more difficult to elute, thus resulting in longer retention time. Two ratios of hexane and ethyl acetate mixtures, i.e., 85:15 v/v and 70:30 v/v, were therefore selected for the study on the effect of a step-gradient elution mode. The experiments of the step-gradient elution

were carried out by employing the mixture ratio of 85:15 v/v in the first part of the elution, followed by the ratio of 70:30 v/v until all components were completely eluted.

Compared to isocratic elution, a step-gradient elution using the hexane and ethyl acetate mixture at the ratio of 85:15 v/v in the first part of the elution can increase the resolution as shown in Figure 4.8 (b-c). The baseline resolution could be achieved by employing the process with the mixture at the ratio of 85:15 v/v in the first 12 min (Figure 4.8(b)). At this condition, the purity and recovery of free lutein were improved to 99.2% and 95.2%, respectively. In addition, this condition was more reasonably economical than using the 85:15 v/v mixture for 20 min (Figure 4.8(c)) because it consumed less process time. However, an extended process (longer time) with the mixture ratio of 85:15 v/v may be required when a large amount of sample is loaded to the chromatography column due to broaden compound peaks.

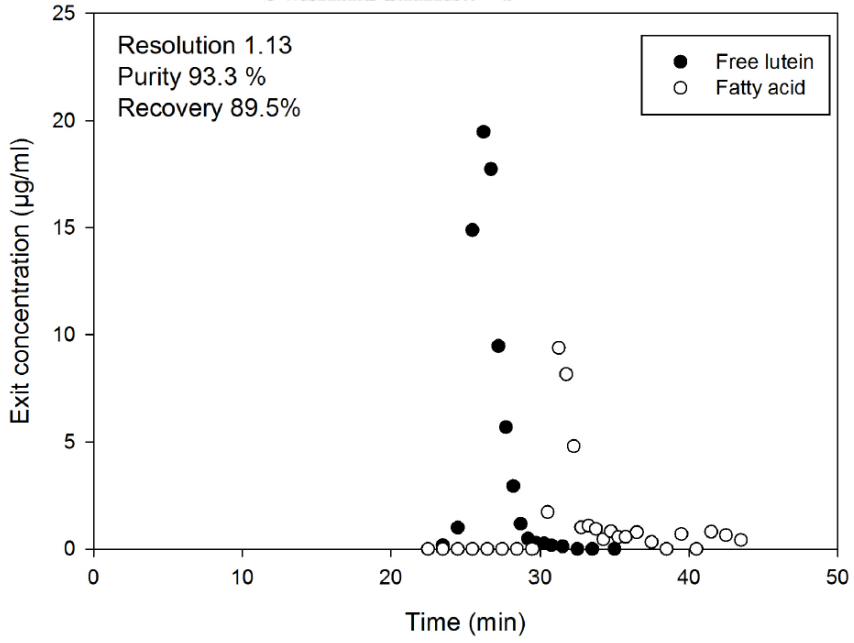

(a)

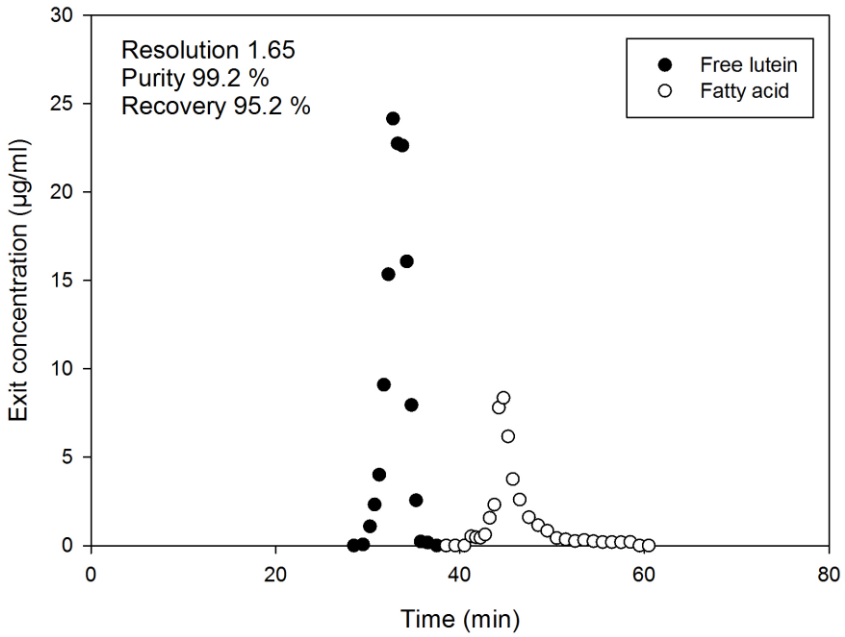

(b)

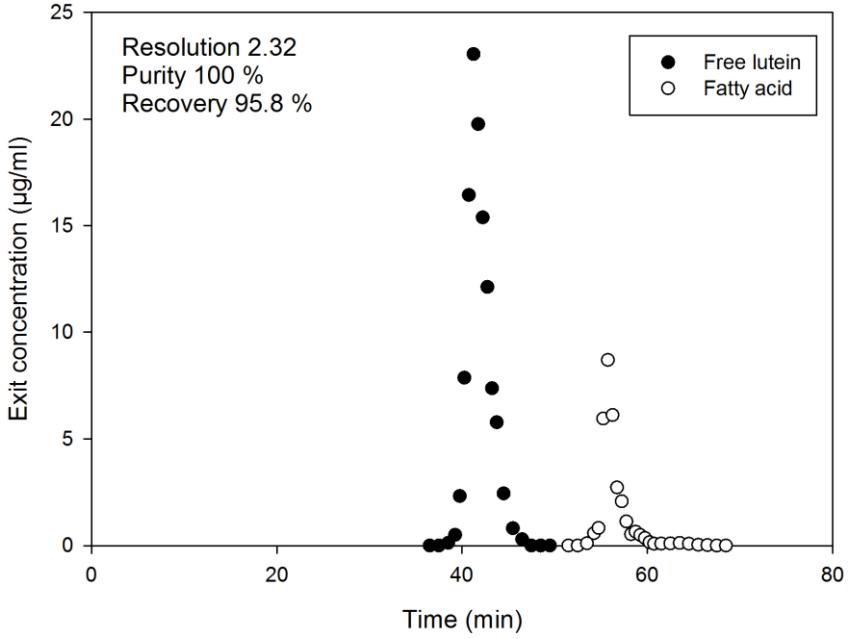

(c)

Figure 4. 8 Elution profile in semi-preparative column at the velocity 0.16 cm/s of (a) isocratic mode (b) gradient elution using hexane-ethyl acetate 85:15 v/v in the first 12 min (c) gradient elution using hexane-ethyl acetate 85:15 v/v in the first 20 min

CHAPTER V
MATHEMATICAL MODEL FOR CHROMATOGRAPHIC SEPARATION OF FREE LTUEIN AND FATTY ACIDS

In the previous chapter, the optimum condition for chromatographic separation of free lutein and fatty acids was determined on a small semi-preparative column. As a first step to further up-scaling the process, in this chapter, possible mathematical models describing the transport behavior of the compounds in chromatographic column were evaluated. In so doing, adsorption isotherms of free lutein and fatty acids were first determined. Then, three different mass transfer models: ideal model, equilibrium-dispersive model, and transport model, were applied to determine to the most suitable model for the chromatographic process. Finally, the comparison between the experimental results and the model prediction was performed to evaluate the model prediction of the experimental transfer behavior of the compounds.

5.1 Adsorption isotherm determination

The results of single adsorption isotherms of free lutein and fatty acid carried out using batch adsorption are shown in Figure 5.1. From the figure, the specific amounts adsorbed of free lutein and fatty acid are linearly proportional to the equilibrium concentration within the concentration range of 1-100 μm/ml. The Henry's constant for free lutein in a mixture of hexane and ethyl acetate at a ratio 70:30 v/v of this study was found to be 9.40 ml/g, which was consistent with that reported by Boonnoun et al. (2014), in which the value of 9.06 ml/g was reported. Nevertheless, the value obtained in this study was valid over a wider range of concentrations. On the other hand, the Henry's constant for fatty acids determined in this study was

approximately 3 folds higher than the value reported by Ozgul-Yucal and Turkay (2003). This was possibly because the experiments were carried out in different solvent system (hexane-ethyl acetate vs iso-octane).

From Figure 5.1, the adsorption isotherm constants increase as the ratio of hexane in the mobile phase is increased. This was because the compounds could less dissolve in the mobile phase (Ralston and Hoerr, 1942, Craft and Soares, 1992) and were better adsorbed on the adsorbent surface as mentioned in the previous chapter. In addition, from these results, it can be implied that free lutein was eluted out of a chromatography column before fatty acid because of the lower isotherm constants. This result was in agreement with the elution profiles of the compounds in the previous chapter.

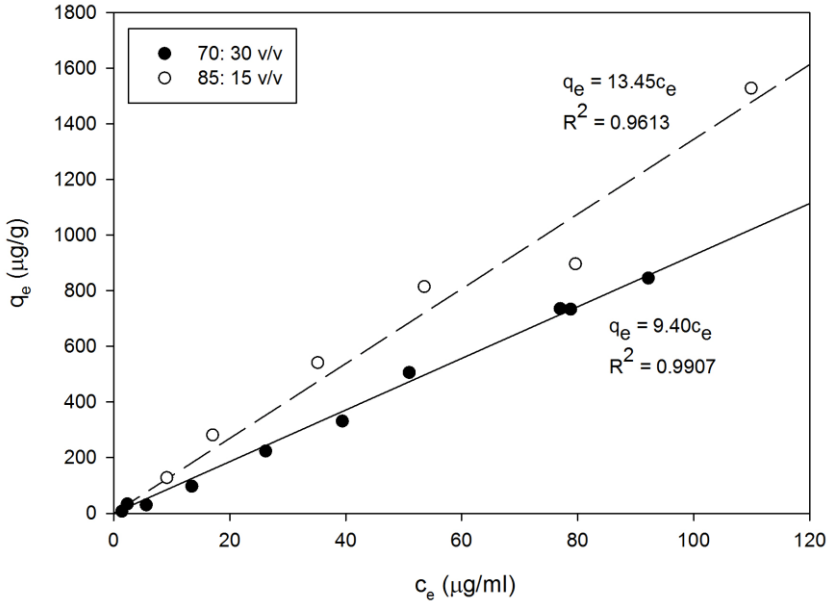

(a)

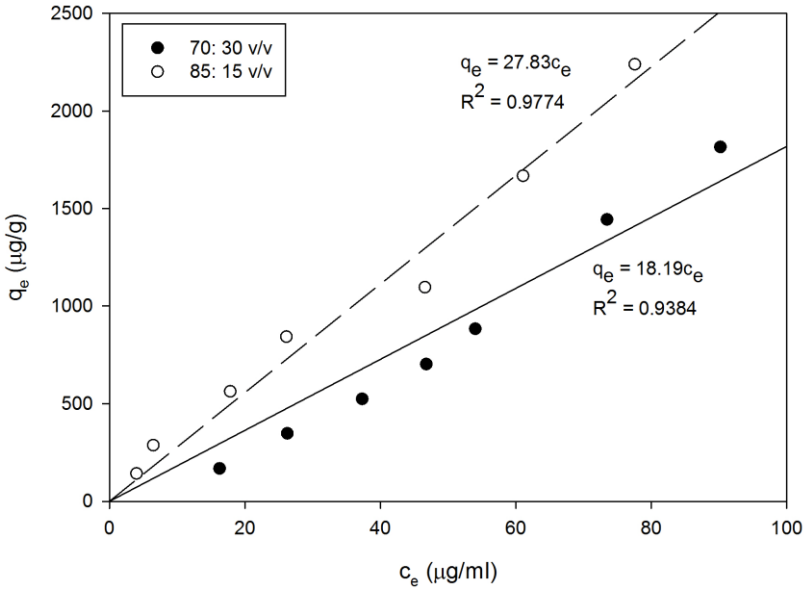

(b)

Figure 5. 1 Adsorption isotherm on silica gel at 30 ^{o}C of (a) free lutein (b) fatty acid

5.2 Determination of most suitable mass transfer model

In this part, the most suitable mass transfer model for chromatographic separation of free lutein and fatty acid was determined. The validity of mass transfer model predictions was checked by comparing the model results with chromatographic

experimental data. The experiment was performed by isocratic elution mode in the semi-preparative column using free lutein as a test compound.

Based on the model parameters in Table 5.1, the chromatograms of free lutein predicted by the mass transfer models (ideal model, EDM and transport model) along with the experimental data at various mobile phase velocities are shown in Figure 5.2 (a-c). The standard errors of the model predictions compared with the experimental data are summarized in Table 5.2. From Figure 5.2, the peak widths predicted by the ideal model are narrower than that of the experimental data and the peak heights of the model are higher than that of the experimental data. This was because the model did not take into account the axial dispersion effect. However, the model can reasonably predict the transport behavior of free lutein at high velocity region as shown in Figure 5.2(c). The results agree with the model assumption that the dispersion effect could be neglected at high velocities since the molecules take less time in the chromatography column.

The prediction of EDM model, developed from the ideal model by including the axial dispersion effect, was found to be more reasonable than the ideal model prediction at the same velocities as implied by the lower standard error in Table 5.2. However, the EDM model predicted greater total peak area, which represents the total amount of free lutein eluted from the column, than that of the experimental data. This might be because the mass transfer resistance between the stationary phase and the mobile phase which is a main band-broadening effect for compounds of large molecular size was neglected in the EDM model. In addition, the EDM model predicted broader peak width than that of the experimental data, particularly at higher velocities (Figure 5.2(b-c)). This might be explained by systems' Biot number (Bi), which reflects the influence of the external mass transfer coefficient and the effective molecular diffusivity as described in equation

(5.1). Large Biot numbers (≥ 10) mean intraparticle diffusion is the rate-controlling step. On the other hand, the mass transfer process is limited by external mass transfer when the value of Biot number is smaller than 1 (Li et al., 1998, Richard et al., 2010).

$$Bi = \frac{k_f d_p}{2\varepsilon_p D_L} \quad (5.1)$$

The values of Biot number for all volumetric flow rates in this study were in the range of 18-22. This implies that the intraparticle diffusion was the rate-controlling mechanism. Moreover, at higher flow rates the effects of axial dispersion and external mass transfer resistance would be diminished, while the influence of intraparticle diffusion would be increased. As a result, the EDM model, which neglects the mass transfer resistance, resulted in greater deviation from the experimental data at higher velocities. However, the effect of mass transfer resistance may be neglected for small-molecule compounds (e.g., amino acids) in a high-efficiency chromatography column because of the rapid mass transfer inside the stationary phase and at the mobile phase and stationary phase interface (Bellot and Condoret, 1991, Guiochon, 2002). This suggests that EDM model may be reasonable for chromatographic process of small-molecule compounds.

The prediction by the transport model (Figure 5.2 (a-c)) indicates that the model seems to be the most suitable for describing the chromatographic process of free lutein compared with the ideal and EDM models. This is also implied by the lowest standard error in Table 5.2. This is because the transport model takes into account both axial dispersion effect and the effect of mass transfer kinetics between the stationary phase and the mobile phase. Generally, transport model can describe the chromatographic processes of both small and large-molecule compounds. However, for small-molecule compounds, a simpler model such as EDM model might be applied. On the other hand,

the transport model may be required for chromatographic process of large-molecule compounds, such as free lutein and proteins, because the mass transfer kinetics is the rate-controlling step (Gu et al. 2013). For these reasons, the most suitable mass transfer model for describing the transport behavior of free lutein. In addition, this model is assumed to applicably describe transport behavior of fatty acids.

Table 5. 1 Parameters for modelling mass transfer model of free lutein in chromatography column

Parameter	**Velocity (cm/s)**		
	0.12	**0.18**	**0.23**
Initial concentration (µg/ml)	32.46	37.68	36.12
Reynolds number (-)	0.0882	0.1130	0.1554
Axial dispersion coefficient (10^8 m^2/s)*	5.45	7.26	9.96
Overall mass transfer coefficient (10^5 m/s)**	3.09	3.23	3.39

*Calculated by equation (2.29)

**Estimated by Wilson and Geanpoklis correlation shown in Table 2.4

Table 5. 2 Standard error of ideal model, EDM and transport model comparing to the experimental data at various mobile phase velocities

Velocity (cm/s)	**Ideal model**	**EDM**	**Transport model**
0.12	0.82	0.38	0.31
0.18	0.46	0.39	0.28
0.23	0.37	0.33	0.15

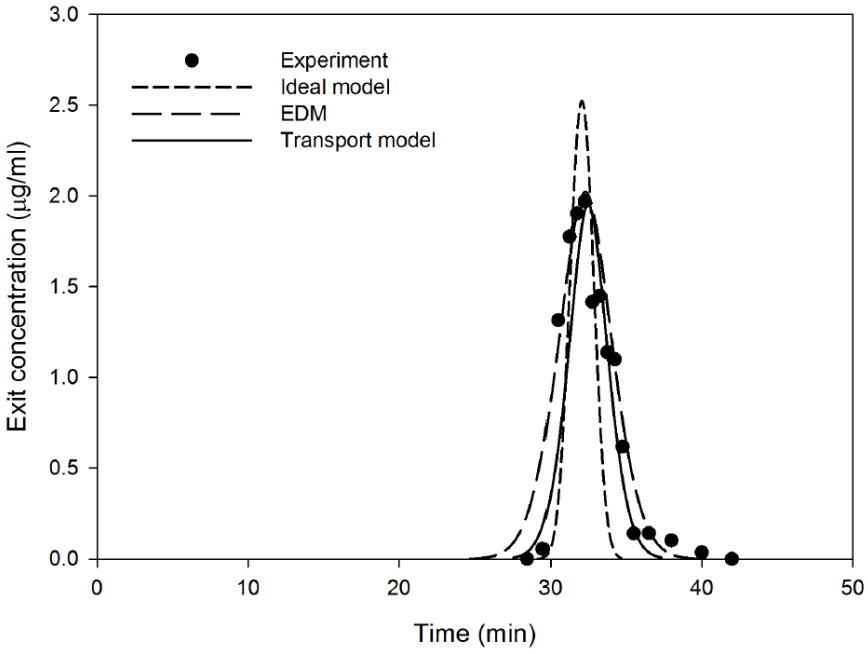
Experiment
Ideal model
EDM
Transport model
Exit concentration (µg/ml)
Time (min)
0.0
0.5
1.0
1.5
2.0
2.5
3.0
0
10
20
30
40
50

(a)

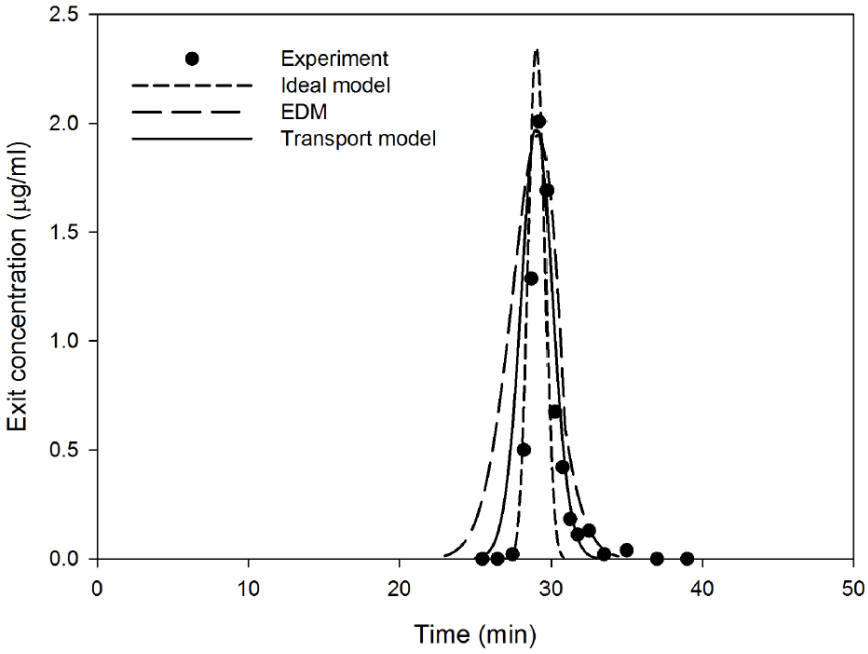
Experiment
Ideal model
EDM
Transport model
Exit concentration (µg/ml)
Time (min)
0.0
0.5
1.0
1.5
2.0
2.5
0
10
20
30
40
50

(b)

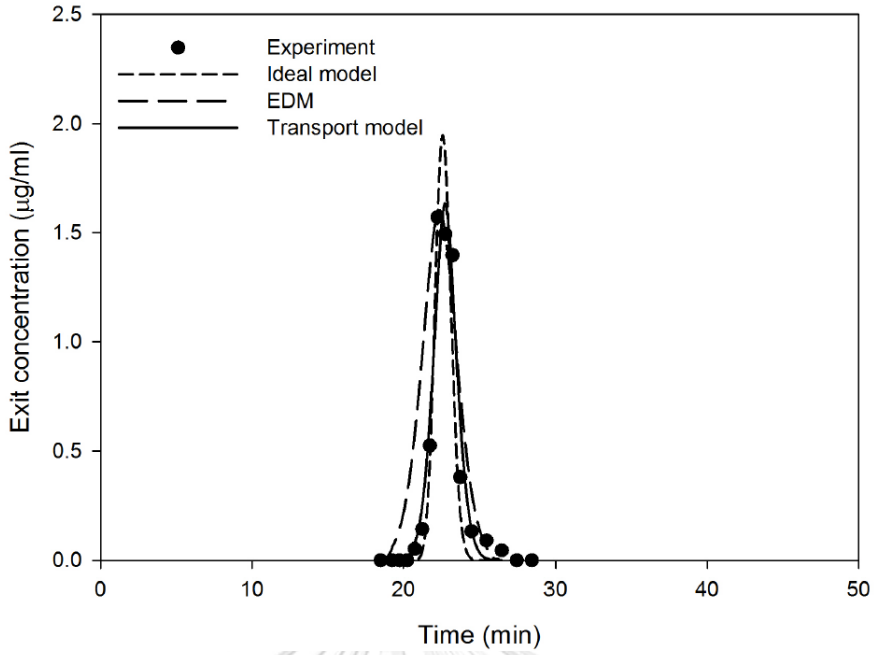

(c)

Figure 5. 2 Experimental results compared with the predicted results from ideal model, EDM and transport model at various mobile phase velocities (a) 0.12 cm/s (b) 0.18 cm/s (c) 0.23 cm/s

5.3 Development of interface mass transfer correlation

In the previous part, the most suitable mass transfer model for chromatographic separation of free lutein and fatty acids was found to be the transport model. The key factor in this model is the overall mass transfer coefficient, which is generally calculated by combining external mass transfer coefficient and intraparticle diffusion coefficient, described in equation (2.29). The intraparticle diffusion coefficient is independent of the mobile phase velocity and can be determined using Stokes-Einstein equation (equation (2.36)). On the other hand, the external mass transfer coefficient depends on the mobile phase velocity and can be determined using dimensionless correlations described in equation (2.37). From the results of previous studies (Schmidt-

Traub, 2005, Richard et al., 2010), it could be suggested that external mass transfer correlation should be directly measured in a column with similar characteristics.

In this study, experiments for developing external mass transfer correlation were carried out in a semi-preparative column packed with silica gel, using free lutein as a test compound. The value of external mass transfer coefficient for each mobile phase velocity could be obtained by minimizing the S.E value. The correlation constants were then determined from the plot between $\ln(\mathrm{Sh})$ and $\ln(\mathrm{Re})$ as described in equation (3.14). Derived from experiments with free lutein standards, dimensionless correlation obtained was presumably be applied to estimate the external mass transfer coefficient of fatty acid by changing the value of molecular diffusivity in the correlation.

A linear plot of $\ln(\mathrm{Sh})$ versus $\ln(\mathrm{Re})$, together with trendline equation and correlation coefficient (R^2), is presented in Figure 5.3. The parameters of mass transfer correlation, A and B, were determined from the y-interception and the slope of the plot, respectively. The mass transfer correlation could be expressed as shown in equation (5.2).

$$\mathrm{Sh} = 3.51\mathrm{Re}^{0.34}\mathrm{Sc}^{0.33} \quad (5.2)$$

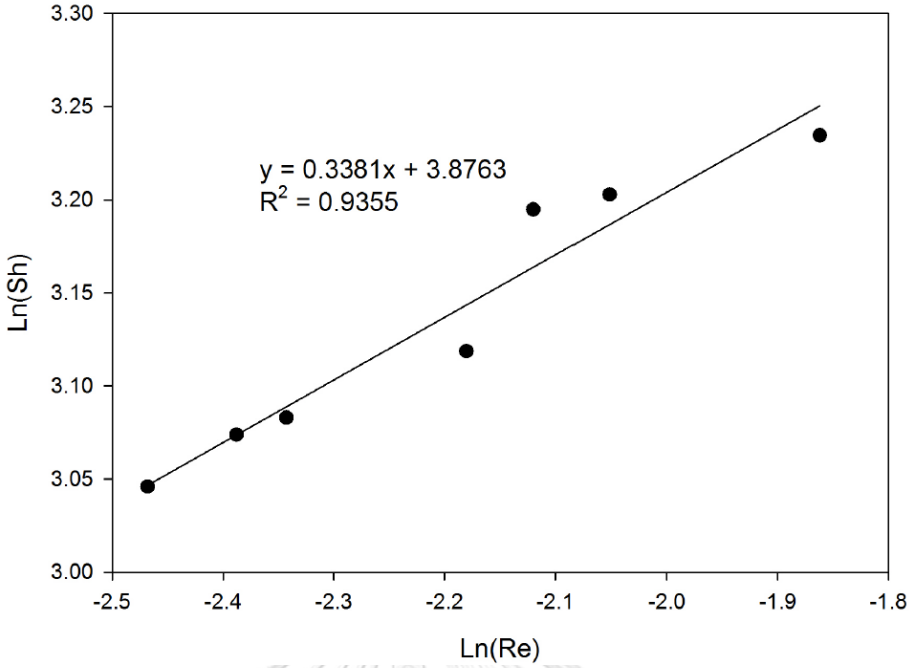

Figure 5. 3 Correlation of $ln(Sh)$ vs $ln(Re)$ at various mobile phase velocities

Comparison of external mass transfer coefficient predicted by the developed mass transfer correlation in equation (5.2) and Wilson and Geankoplis correlation is summarized in Table 5.3. From the table, the external mass transfer coefficient might not be critical as implied by the insignificant difference of the value of S.E. This is because the process was dominated by intraparticle diffusion inside the stationary phase as mentioned previously.

Table 5. 3 Standard error of experimental data compared with mass transfer prediction modeled by new correlated k_f of equation (21) and Wilson and Geankoplis correlation

Mobile phase velocity (cm/s)	**New correlated k_f**		**Wilson and Geankoplis correlation**	
	$k_f\ (m/s)$	S.E.	$k_f\ (m/s)$	S.E.
0.13	1.11×10^{-4}	0.37	6.56×10^{-5}	0.44
0.16	1.19×10^{-4}	0.36	7.06×10^{-5}	0.39
0.19	1.28×10^{-4}	0.48	7.58×10^{-5}	0.49

5.4 Mass transfer model verification

The model used in this study was developed based on the following assumptions: 1) no radial dispersion, 2) density and viscosity of mobile phase were constant, 3) stationary phase were spherical shape and were packed in the column homogeneously, 4) isothermal process, 5) mobile phase velocity was constant, 6) all transport parameters were independent of concentration. In addition, in a multicomponent system such as this, interactions between different compounds may exist and can definitely affect the transfer behavior of the components in the mixture. In this study however, such interaction was neglected and the adsorption rate of each component was therefore considered to be independent of other components. These assumptions are usually valid in the low concentration range. (Jiang et al., 2014, Junghuttakarnsatit, 2002, Khosravanipour-Mostafazandeh et al., 2011, Yoon et al., 2012)

The model with new correlated mass transfer coefficient was experimentally verified with isocratic and gradient elution modes in both semi-preparative and preparative columns. In the semi-preparative column, the mobile phase velocity was set at 0.16 cm/s which was the optimum mobile phase velocity, determined in the previous chapter. Experimental data and model predictions for elution profiles of free lutein and fatty acids are illustrated in Figure 5.4. in which isocratic and gradient elution modes are presented in Figure 5.4 (a) and 5.4 (b), respectively. The model was based on the model parameters in Table 5.4. The figure shows that the model can well predict the experimental data. In addition, the value of S.E. is lower than 3.25 and the value of r is higher than 0.80, indicating that the model prediction and the experimental data in the semi-preparative column are highly consistent (Montgomery and Runger, 2011). However, a little discrepancy between the model prediction and the experimental data was found in the prediction of fatty acid. From the figure, the fatty acid amount in the experimental data is slightly lower than the model prediction. This is possibly because some fatty acid was adsorbed in the column due to strong interaction between the compound and the stationary phase (Anjinta, 2013); this was neglected in the simulation.

For the preparative scale used in this work, due to the limitation of the equipment, the mobile phase velocity was set at 0.115 cm/s, which was lower than the optimum velocity previously determined. The comparison between model prediction and experimental result is presented in Figure 5.5. From the figure, the experimental elution profile of fatty acid is a relatively Gaussian peak which is similar shape to model predictions. However, the experimentally generated free lutein peaks exhibit tailing behavior. In general, tailing behavior is resulted from the fact that a large amount of

compound was injected into the column. The equilibrium concentration might therefore exceed the linear range and must be described by a non-linear isotherm, typically a convex-shape Langmuir isotherm (Schmidt-Traub, 2005). At low concentration region, components are well adsorbed on the surface of stationary phase. As the concentration continues to increase however, the adsorption ability starts to plateau. Most of the component amount would relatively quickly be eluted out of the column. Hence, the peak maximum would be shifted towards the compressive front of the peak. On the other hand, the back of the peak or the peak tailing would result from the component which is adsorbed in the stationary phase and eluted from the column more slowly. Essentially, the experimental profile of free lutein could be fitted to the linear isotherm mass transfer model at only the first part of elution. Although the values of S.E. increase as the chromatography scale is increased, based on the value of r (i.e., >0.70), the results are highly consistent (Montgomery and Runger, 2011).

Table 5. 4 Model parameters for chromatographic mass transfer model

Parameters	**Semi-preparative column**	**Preparative column**
Axial dispersion coefficient (m^2/s)		
(a) hexane-ethyl acetate at ratio 70:30 v/v	6.53×10^{-8}	4.70×10^{-8}
(b) hexane-ethyl acetate at ratio 85:15 v/v	6.54×10^{-8}	4.71×10^{-8}
Overall mass transfer coefficient of free lutein (m^2/s)		
(a) hexane-ethyl acetate at ratio 70:30 v/v	3.86×10^{-5}	3.72×10^{-5}
(b) hexane-ethyl acetate at ratio 85:15 v/v	3.31×10^{-5}	3.20×10^{-5}
Overall mass transfer coefficient of fatty acid (m^2/s)		
(a) hexane-ethyl acetate at ratio 70:30 v/v	5.81×10^{-5}	5.57×10^{-5}
(b) hexane-ethyl acetate at ratio 85:15 v/v	5.02×10^{-5}	4.80×10^{-5}

Table 5. 5 Standard error and correlation factor of mass transfer model comparing to the experimental data at various conditions

Column	**Elution mode**	**Free lutein**		**Fatty acids**	
		S.E.	r_{cor}	S.E.	r_{cor}
Semi-preparative	Isocratic	1.05	0.97	1.22	0.89
	Gradient	3.17	0.88	2.21	0.85
Preparative	Isocratic	12.70	0.86	3.61	0.89
	Gradient	14.30	0.81	7.18	0.77

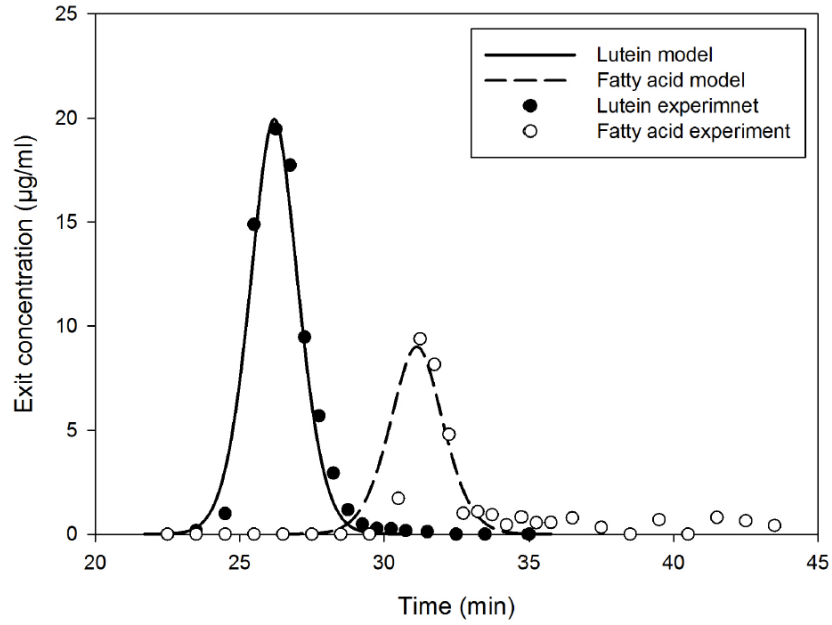

(a)

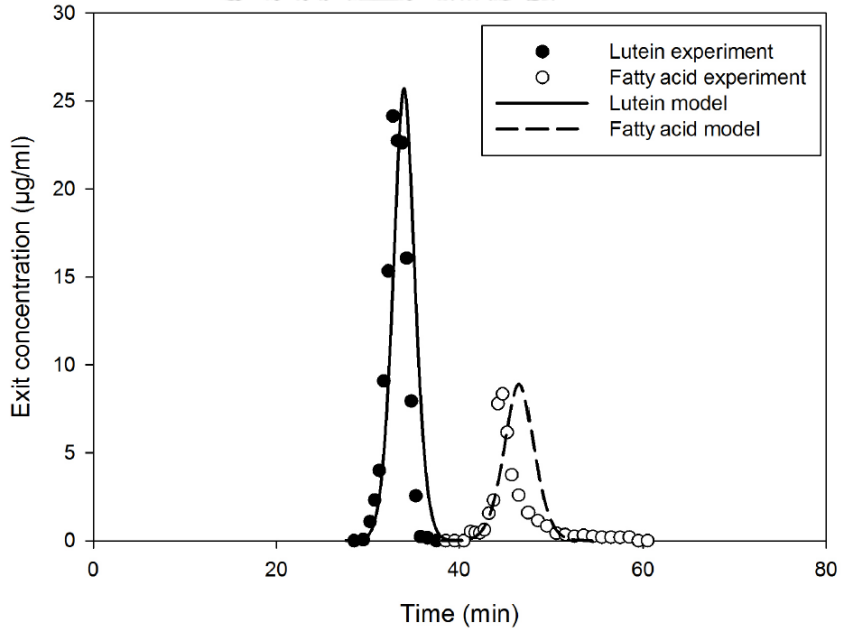

(b)

Figure 5. 4 Experimental results in semi-preparative scale compared with the predicted results from the mass transfer model (a) isocratic elution (b) gradient elution

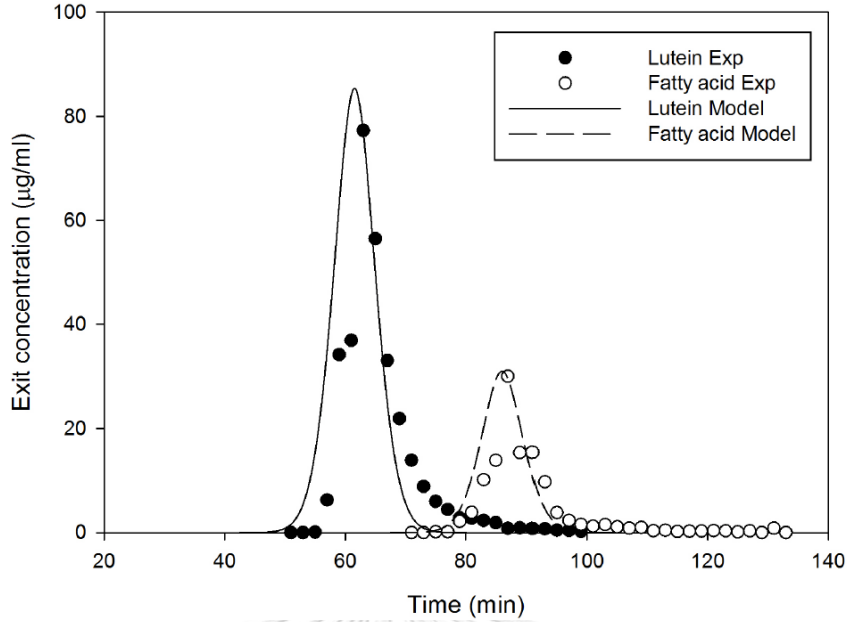

(a)

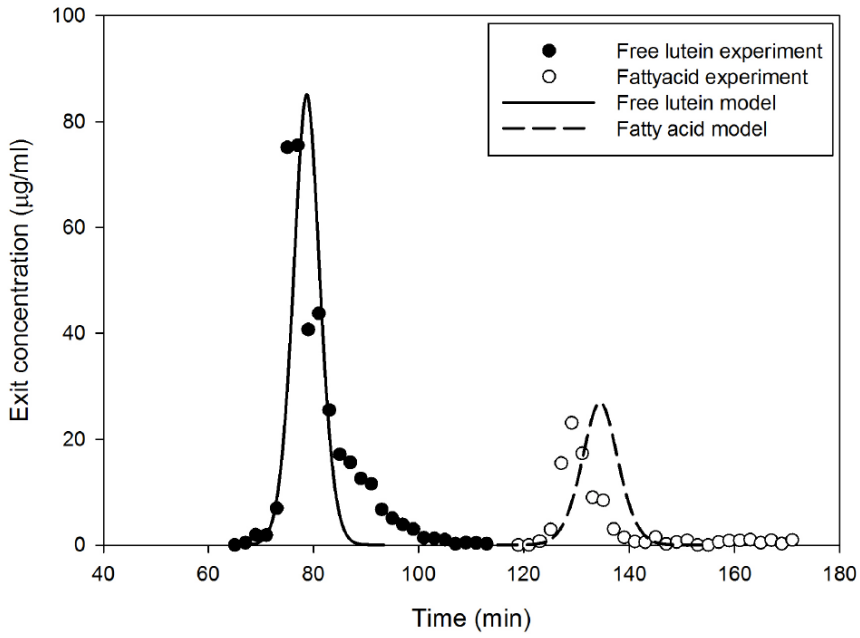

(b)

Figure 5. 5 Experimental results in preparative scale compared with the predicted results from the mass transfer model (a) isocratic elution (b) gradient elution

CHAPTER VI
CONCLUSIONS AND RECOMMENDATIONS

6.1 Conclusions

The objectives of this study are 1) to identify and quantify fatty acids in de-esterified marigold oleoresin and find a suitable chromatographic condition to separate free lutein and the fatty acids, and 2) to develop the most suitable mass transfer model for describing transfer behavior of free lutein and fatty acids in both semi-preparative and preparative chromatography columns.

The amount of total xanthophyll in marigold oleoresin was 256.98 mg/g oleoresin (23.64 mg/g dried marigold), which are mostly in the form of lutein esters, while the amount of free lutein was only 0.36 mg/g oleoresin (0.03 mg/g dried marigold). The fatty acids presented in the oleoresin were palmitic acid and stearic acid and their total amount was 0.26 mg/g oleoresin (0.23 mg/g marigold). After the de-esterification, all lutein esters were converted to free lutein and fatty acids. The amounts of free lutein and fatty acids rose to 129.76 and 49.12 mg/g oleoresin, respectively. At the most optimum mobile phase velocity (0.16 cm/s), as evaluated from the plot HETP against mobile phase velocity, the chromatographic separation of free lutein and fatty acids could be accomplished using a step-gradient elution. The processes were run by employing 85:15 v/v hexane-ethyl acetate mixture during the first elution step, followed by change of the mixture composition to that of 70:30 v/v ratio. The purity and recovery of free lutein were 99.2% and 95.2%, respectively, for the semi-preparative column, and, were 100% and 71.2%, respectively, for in the preparative column.

The required model parameters: adsorption isotherm, the overall mass transfer and axial dispersion coefficients, were determined. Batch adsorptions of free lutein and palmitic acid, used as standard fatty acid, were conducted to determine adsorption isotherm constants in the linear range. On the other hand, the axial dispersion coefficients were determined from Chung and Wen correlation and the overall mass transfer coefficient was determined from the correlation developed experimentally in this study. The model parameters were then applied to the ideal model, equilibrium-dispersive model and transport model to select the most suitable model. The experimental mass transfer behavior of free lutein and fatty acid in the chromatography columns was found to be reasonably described by the transport model taking into account both axial dispersion effect and effect of mass transfer kinetics. The model was then applied to predict the mass transfer behavior of free lutein and fatty acids, which were then compated with the experimental results in both semi-preparative and preparative columns. The results found that the correlation factor between the model prediction and the experimental results was higher than 0.70, indicating that the numerical and experimental results are highly consistent.

6.2 Recommendations

Recommendations for further study are separated into 2 parts: recommendation for developing mathematical model and for developing isolation process.

6.2.1 Recommendations for developing mathematical model

1. In this study, mass transfer model was developed based on the assumption that interaction force between the components can be negligible and the adsorption isotherms followed single linear isotherm model. These assumptions are valid only for

low concentration system (Jiang et. al., 2014, Junghuttakarnsatit, 2002). In an indsutrail scale, the solution concentration is usually over the linear range. In addition, the molecular interation between the molecules being separated cannot be neglected. The use of non-linear adsorption isotherm will be necessary for developing mathematical mode for a large scale chromatographic process. Lesko et. al., (2015) investigated the effect of adsorption isotherm type on chromatographic separation modelling of cyclohexanone and cycloheptanone. The adsorption experiments were conducted using a dynamic method. A mixture of the compounds dissolved in methanol, with initial concentration 0.1 – 0.4 M, was injected into a C18-bonded porous silica column with sample volume 5 µL. The outlet concentration was plotted and compared with the model results predicted by 4 isotherm models (Langmuir, bi-Langmuir, competitive bi-Langmuir and Toth isotherms). From the comparision, competitive bi-Langmuir isotherm, taking into account interaction between components, was the most suitable isotherm for describing the process. The isotherm parameters could be determined by minimizing the difference between the experimental data and the model prediction. To further improve the accuaracy of model prediction, the same method can possibly be applied to determine multicomponent isotherms of free lutein and fatty acids in de-esterified marigold lutein in the future study.

2. All transport parameters used in this study were estimated from empirical correlation from literature or from correlations developed experimentally based on the assumption that they were independent of concentration, which is again valid for low concentration systems. However, in an indsuctrail scale, the concentration is rather high. The effect of concentration on transport parameters must be taken into account. Nesmelova et. al., (2001) studied effect of concentration on the molecular diffusivity

of several proteins (i.e., myoglobin, BSA, barstar and lysozyme). The molecular diffusivity of the proteins was measured using NMR pulsed-gradient spin-echo technique at several concentrations. A correlation of molecular diffusivity as a function of concentration was then developed. The results found that the molecular diffusivities of proteins were found to be independent of concentration when the concentrations were lower than 60%. Above this concentration, the molecular diffusivity tends to decrease as the concentration increased. However, the decreasing rate of molecular diffusivity was found to be depedent on the characteristics of molecules, solvent system, pH, etc. The concept of this work might be applied to the present study to further determine the effect of concentration on other transport paramters.

6.2.2 Recommendations for developing isolation process

1. Although activity of free lutein has been reported, it should be tested to determine the ability for use in pharmaceutical applications. This is because the activity of free lutein varies depending on species of marigold flowers and method of extraction. Li et al. (2007) studied the effect of type of solvents used in marigold extraction. They found that using ethanol as a solvent gave higher activity than using ethyl acetate and n-hexane. Gong et al. (2012) studied effect of extraction parameters: ethanol concentration, temperature, and time, on activity of free lutein. They found that the most suitable condition was 79.7% ethanol concentration at 74.2 ^{o}C for 8.1 hours. At this condition, the activity of free lutein could achieve 2.42 mmol of Troxol/g of extract. In addition, Ingkasupart et al. (2015) used ATBS method to test activity of free lutein, extracted from 11 species of marigold flowers grown in Thailand. They found that the activity of free lutein varied depending on marigold flower species and agricultural

method. Redeo Gold specie was found to give the highest activity which was 0.92 mmol of Trolox/g of extract.

2. Free lutein is easily susceptible to UV-light, high temperature, pH, reductant and oxidant. Because of these disadvantages, it is necessary to find a method to improve its stability. Wang et al. (2012) proposed a spray-drying method to encapsulate free lutein. They found that microencapsulated free lutein prepared by the method could be protected against heat, UV-light, oxygen and pH change. The retention rate was greatly improved by about 15-50% of that of free lutein. In addition, the water solubility of the microencapsulated free lutein was also improved. These results might be useful in pharmaceutical applications.

3. After extraction process of lutein esters, marigold flower residues are generally discarded or used as manure. However, the economic value of the residue could possibly be enhanced by recovering other antioxidant compounds, e.g., phenolic compounds and flavonoids. Gong et al. (2012) studied the extraction of flavonoids and phenolic compounds from defatted marigold using ethanol. The total contents of phenolic compounds and flavonoids of 70.01 and 109.38 mg/g of defatted marigold, respectively, could be obtained. The yields were indeed comparable to those extracted from fresh marigold flowers (Li et al., 2007).

4. In general, because of the different objectives, the most suitable condition for a laboratory scale chromatography can be rather different from that of the industrial scales. After the process is up-scaled, some conditions, e.g., stationary phase particle size, need to be re-evaluated. For example, Figure 6.1 shows recommended stationary phase size for each column size. For small columns used in a laboratory scale as an analysis unit, stationary phase of small size is required to make the compounds separate.

Applying small particle size in large chromatography columns leads to high column pressure, which in turn leads to high equipment costs as the systems needs to be resistant to the pressure.

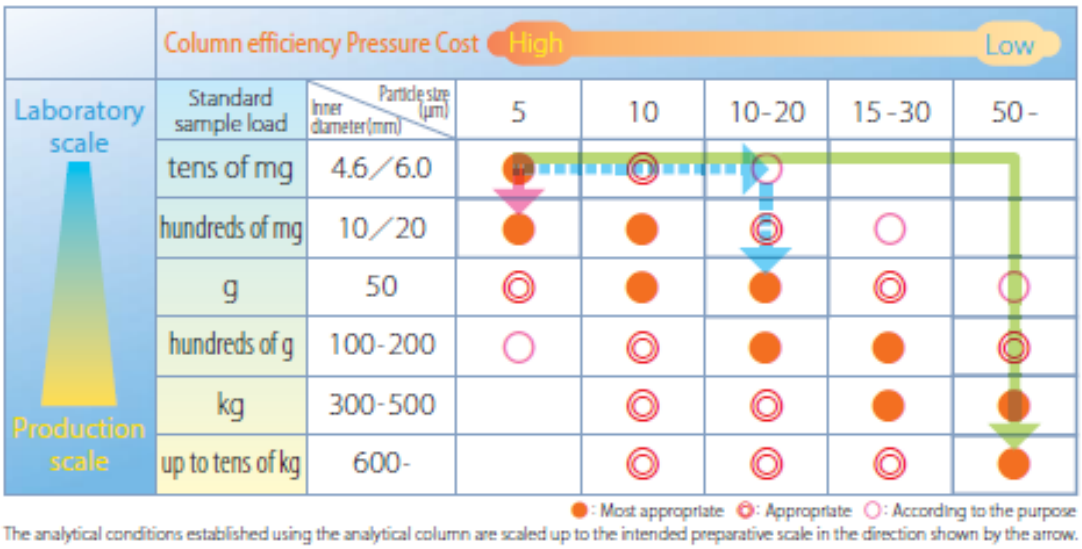

Figure 6. 1 Recommended particle size for different column sizes (YCP Co., LTD, 2016)

REFERENCES

Abdel-Aal, E. S. M. and I. Rabalski (2015). "Composition of lutein ester regioisomers in marigold flower, dietary supplement, and herbal tea." Journal of agricultural and food chemistry **63**: 9740-9746.

Alves-Rodrigues, A. and A. Shao (2004). "The science behind lutein." Toxicology Letters **150**: 57-83.

Anjinta, A. (2013). Chromatographic purification of gamma oryzanol from by-products of rice bran oil refinery Master, Chulalongkorn University.

Araujo Padilha, C. E., N. K. Araujo, D. F. Santana Souza, J. A. Oliveira, G. R. Macedo and E. S. Santos (2016). "Modeling and simulation of Bacillus cereus chitosanase activity during purification using expanded bed chromatography." Korean. J. Chem. Eng. **33**(9): 2650-2658.

Ausich, R. L. and D. J. Sanders (1997). Process for the formation, isolation, and purification of comestible xanthophyll crystals from plants. United States Patent Application Publication, 5648564.

Bellot, J. C. and J. S. Condoret (1991). "Liquid Chromatography Modelling: A Review." Process Biochemistry **26**: 363-376.

Boonnoun, P., T. Opaskonkun, P. Prasitchoke, M. Goto and A. Shotipruk (2012). "Purification of free lutein from marigold flowers by liquid chromatography." Engineering Journal **16**: 145-155.

Borba, C.E., R. Guirardello, E.A., Silva, M.T., Veit, C.R.G., Tavares (2006). "Removal of nickel (II) ions from aqueous solution by biosorption in a fixed bed column: Experimental and theorectical breakthrough curves." Biochemical Engineering Journal **30**: 184-191

Breithaupt, D. E., A. Bamedi and U. Wirt (2002). "Carotenoid fatty acid esters: Easy substrates for digestive enzymes?" Comparative Biochemistry and Physiology Part B: Biochemistry and Molecular Biology **132**: 721-728.

Chen, Y., W. Dai, Y. Cheng and H. Qu (2006). "Kinetic modeling for chromatographic separation of cytosine monophosphate and uracil monophophate." Korean Journal of Chemical Engineering **23**: 784-788.

Choopakdee, W. (2012). Computational fluid dynamics modeling of free lutein purification in a preparative chromatography column. Master, Chulalongkorn Univeristy.

Chu, B. S., B. S. Baharin, Y. B. Che Man and S. Y. Quek (2004). "Separation of vitamin E from palm fatty acid distillate using silica: I Equilibrium of batch adsorption." Journal of Food Engineering **62**: 97-103.

Craft, N. E. and J. E. Soares (1992). "Relative solubility stability and absorptivity of lutein and b-carotene in organic solvents." Journal of Agricultural and Food Chemistry **40**: 431-434.

Crittenden, J. C., N. J. Hutzler, D. G. Geyer and J. L. Oravitz (1986). "Model development and parameter sensivity." Water Resources Research **22**: 271-284.

Dorjgochoo, T., Y. T. Gao, W. H. Chow, X. O. Shu, H. Li, G. Yang, Q. Cai, N. Rothman, H. Cai, A. A. Franke, W. Zheng and Q. Dai (2009). "Plasma carotenoids, tocopherols, retinol and breast cancer risk: results from the Shanghai Women Health Study (SWHS)." Breast Cancer Research and Treatment **117**: 381-389.

Dwivedi, P. N. and S. N. Upadhyay (1977). "Particle-fluid mass transfer in fixed and fluidized beds." Industrial & Engineering Chemistry Process Design and Development **16**: 157-165.

Gong, Y., Z. Hou, Y. Gao, Y. Xue, X. Liu and G. Liu (2012). "Optimization of extraction parameters of bioactive components from defatted marigold (Tagetes erecta L.) residue using response surface methodology." Food and Bioproducts Processing **90**: 9-16.

Granado, F., B. Olmedilla and I. Blanco (2002). "Serum depletion and bioavailability of lutein in type I diabetic petients." European Journal of Nutrition **41**: 47-53.

Gu, T., G. Iyer and K. C. Cheng (2013). "Parameter estimation and rate model simulation of partial breakthrough of bovine serum albumin on a column packed with large Q Sepharose anion-exchange particles." Separation and Purification Technology **116**: 319-326.

Guiochon, G. (2002). "Preparative liquid chromatography." Journal of Chromatography A **965**: 129-161.

Guiochon, G., S. Golshan-Shirazi and A. M. Katti (1994). Fundamental of preparative and nonlinear chromatography. Boston, MA, Academic Press.

Gumel, A. M., M. S. M. Annuar and T. Heidelberg (2014). "Growth kinetics, effect of carbon substrate in biosynthesis of mcl-PHA by Pseudomonas putida Bet001." Brazilian Journal of Microbiology **45**: 427-438.

Hines, A. L. and R. N. Maddox (1985). Mass Transfer: Fundamentals and Applications, Prentice Hall.

Ingkasupart, P., B. Manochai, W. T. Song and J. H. Hong (2015). "Antioxidant activities and lutein content of 11 marigold cultivars (Tagetes spp.) grown in Thailand." Food Science and Technology (Campinas) **35**: 380-385.

Jiang, X., L. Chen and C. Zhou (2005). "Lutein and lutein esters in marigold flowers by high performance chromatography." Journal of Central South University of Technology **12**: 306-308.

Junghattakarnsatit, N. (2002). Separation of isoflavones from soybean flake extracts by high performance liquid chromatography. Master, Chulalongkorn University.

Kataoka, T., H. Yoshida and K. Ueyama (1972). "Mass transfer in lamina region between liquid and packing material surface in the packed bed." Journal of Chemical Engineering Japan **5**: 132-136.

Khachik, F. (1995). Process for isolation, purification, and recrystallization of lutein from saponified marigold oleoresin and uses thereof. United States Patent Application Publication, 5382714.

Khachik, F. (2001). Process of extraction, purification of lutein, zeaxanthin and rare carotenoids from marigold flowers and plants. United States Patent Application Publication, 6262284.

Khosravanipour Mostafazadeh, A., M. Sarshar, S. Javadian, M. R. Zarefard and Z. Amirifard Haghighi (2011). "Separation of fructose and glucose from date syrup using resin chromatographic method: Experimental data and mathematical modeling." Separation and Purification Technology **79**: 72-78.

Kim, H., K. Kaczmarski and G. Guiochon (2006). "Intraparticle mass transfer kinetics on molecularly imprinted polymers of structural analogues of a template." Chemical Engineering Science **61**: 1122-1137.

Kostava, A. and H. Bart (2007). "Preparative chromatographic separation of amino acid racemic mixtures: II. Modelling of the separation process." Separation Purification and Technology **54**: 315-321.

Kumar, S., S. N. Upadhyay and V. K. Mathur (1977). "Low Reynolds number mass transfer in packed beds of cylindrical particles." Industrial & Engineering Chemistry Process Design and Development **16**: 1-8.

Landrum, J. T. and R. A. Bone (2001). "Lutein, zeaxanthin and macular pigment." Archives of Biochemistry and Biophysics **385**: 28-40.

Lesko, M., D., Asberg, M., Enmark, J., Samuelesson, T., Fornstedt and K., Kaczmarski (2015). "Choice of model for estimation of adsorption isotherm parameters in gradient elution preparative liquid chromatography." Chromatographia **78**: 1293-1297.

Li, W., Y. Gao, J. Zhao and Q. Wang (2007). "Phenolic, flavonoid, and lutein ester content and antioxidant activity of 11 cultivars of Chinese marigold." Journal of agricultural and food chemistry **55**: 8478-8484.

Li, Z., Y. Gu and T. Gu (1998). "Mathematical modeling and scale-up of size-exclusion chromatography." Biochemical Engineering Journal **2**: 145-155.

Lin, J. H., D. J. Lee and J. S. Chang (2015). "Lutein production from biomass: Marigold flowers versus microalgae." Bioresource Technology **184**: 421-428.

Lv, L., Y. Zhang, K.Wang, A.K. Ray, X.S. Zhao (2008). "Modeling of the adsorption breakthrough behaviors of Pb^{2+} in a fixed bed of ETS-10 adsorbent." Journal of Colloid and Interface Science **325**: 57-63

Madhavi, D. L. and D. I. Kagan (2002). Process for the isolation of mixed carotenoids from plants. United States Patent Application Publication, 6380442.

May, P. and K. W. Quirin (2014). "Supercritical marigold flower CO_2-extract-evergreen in evidence based cosmetic application." Cosmetic Science Technology: 18-25.

Meyer, V. R. (2004). Practical high-performance liquid chromatography, John Wiley & Sons, Ltd.

Meyer, V. R. (2010). Practical high-performance liquid chromatography, John Wiley & Sons, Ltd.

Molnar, P., Z. Szado, E. Osz, P. Olah, G. Toth and J. Deli (2004). "Separation and identification of lutein derivatives in processed food." Chromatographia **60**: S101-S105.

Montgomery, D. C. and G. C. Runger (2011). Applied statistics and probability for engineers. USA, John Wiley and Sons, Ltd.

Morbidelli, M., A. Servida, G. Storti and S. Carra (1982). "Simulation of multicomponent adsorption beds. Model analysis and numerical solution." Industrial & Engineering Chemistry Fundamentals **21**: 123-131.

Muley, B. P., S. S. Khadabadi and N. B. Banarase (2009). "Phytochemical constituents and pharmacological activities of *Calendula officinalis Linn* (*Asteraceae*): A Review." Tropical Journal of Pharmaceutical Research **8**(5): 455-465.

Nesmelova, I., V.D. Skirda, and V.D. Fedotov (2002). "Generalized concentration dependence of globular protein self-diffusion coefficients in aqueous solutions." Biopolymers **63**: 132-140

Ohashi, H., T. Sugavara, K. I. Kihushi and H. Konno (1981). "Correlation of liquid-side mass transfer coefficient for single particles and fixed beds." Journal of Chemical Engineering Japan **14**: 433-438.

Ozhul-Yucel, S. and S., Turkay (2003). "Purification of FAME by rice hull ash adsorption." Journal of American Oil Society **80**: 373-376.

Park, Y. K., K. H. Row and S. T. Chung (2000). "Adsorption characteristics and separation of taxol from yew tree by NP-HPLC." Separation and Purification Technology **12**: 27-37.

Pena, G. R. (2009). Process for purification of free xanthophylls. United States Patent Application Publication, 7629007.

Philip, T. (1977). Purification of lutein-fatty acid esters from plant materials. United States Patent Application Publication, 4048203.

Piccaglia, R., M. Marotti and S. Grandi (1998). "Lutein and lutein ester content in different types of Tagetes patula and T. erecta." Industrial Crops and Products **8**: 45-51.

Pretsch. E., Buhlmann. P. and Badertscher. M. (2009). Structure Determination of Organic Compounds, Berlin, Springer.

Ralston, A. W. and C. W. Hoerr (1942). "The solubilities of the normal saturated fatty acids." Journal of Organic Chemistry **7**: 549-555.

Richard, D., M. Nunez and D. Schwiech (2010). "Adsorption of complex phenolic compounds on active charcoal; Breakthrough curves." Chemical Engineering Journal **158**: 213-219.

Ruthven, D. M. (1984). Principles of adsorption and adsorption processes. United States of America, John Wiley & Sons., Ltd.

Sarkar, C. R., B. Bhagawati, L. Das and B. C. Goswami (2012). "An efficient condition of saponification of lutein ester from marigold flower." Annals of Biological Research **3**: 1461-1466.

Schmidt, W. F., J. R. Barone, B. Franics and J. B. Reeves III (2006). "Stearic acid solubility and cubic phase volume." Chemistry and Physics of Lipids **142**: 23-32.

Schmidt-Traub, H. (2005). Preparative Chromatography of Fine Chemicals and Pharmaceutical Agents. Wiley-VCH Verlag GmbH & Co. KGaA.

Schulte, M. and A. Epping (2005). Fundamentals and General Terminology In Preparative Chromatography Wiley-VCH Verlag GmbH & Co. KGaA.

Shibata, S., C. Ishihara and C. Matsumoto (2004). "Improved separation method for highly purified lutein from Chlorella powder using jet mill and flash column chromatography on silica gel." Journal of Agricultural and Food Chemistry **52**: 6286.

Siriamornpun, S., O. Kaisoon and N. Meeso (2012). "Changes in colour, antioxidant activities and carotenoids (lycopene, β-carotene, lutein) of marigold flower (Tagetes erecta L.) resulting from different drying processes." Journal of Functional Food **4**: 757-766.

Skoog, D. A. and J. J. Leary (1992). Principle of Instrumental Analysis. London, Saunders College Publishing.

Sowbhagya, H. B., S. R. Sampathu and N. Krishnamurthy (2004). "Natural colorant from marigold-chemistry and technology." Food Reviews International **20**: 33-50.

Tsao, R. and R. Yang (2011). "Lutein in selected Canadian crops and agri-food processing by-products and purification by high-speed counter current chromatography." Journal of Chromatography A **1112**: 202-208.

Tsao, R., R. Yang, J. C. Young, H. Zhu and T. Manolis (2004). "Separation of geometric isomers of native luein diesters in marigold (Tagetes erecta L.) by high-performance liquid chromatography-mass spectrometry." Journal of Chromatograhy A **1045**: 65-70.

Vasudevan, P., S. Kashyap and S. Sharma (1997). "Tagetes: a multipurpose plant." Bioresource Technology **62**: 29-35.

Vechpanich, J. (2008). Extraction and purification of lutein fatty acid esters from marigold flower. Master, Chulalongkorn University.

Vechpanich, J. and A. Shotipruk (2011). "Recovery of free lutein from Tagetes erecta: Determination of suitable saponification and crystallization conditions." Separation Science and Technology **46**: 265-271.

Wang, Y., H. Ye, C. Zhou, F. Lv, X. Bie and Z. Lu (2012). "Study on the spray-drying encapsulation of lutein in the porous starch and gelatin mixture." European Food Research and Technology **234**: 157-163.

Welty, J. R., C. E. Wicks, R. E. Wilson and G. L. Rorrer (2008). Fundamentals of Momentum, Heat, and Mass Transfer. USA, John Wiley & Sons., Ltd.

Willianson, J. E., K. E. Bazarie and C. J. Geankoplis (1963). "Liquid-phase mass transfer at low Reynold numbers." Industrial & Engineering Chemistry Fundamentals. **2**: 126-129.

Wilson, E. J. and C. J. Geankoplis (1966). "Liquid mass transfer at very low Reynold numbers in packed beds." Industrial & Engineering Chemistry Fundamentals **5**: 9-14.

Xu, X., B. Shao, D. Zhou, S. Ye, Wang. Y. and Chen. B. (2007). Process for isolation and purification of xanthophyll crystal from plant oleoresin. United States Patent Application Publication, 7271298.

YCP Co., Ltd, (2016) "Preparative chromatography production lineup" YMC Co., Ltd, Japan.

Yingyeun, P. (2013). Effect of various factors on pufication of marigold derived lutein by chromatography. Master, Chulalongkorn University.

Yoon, C. H., T. Zhu and K. H. Row (2012). "Competitive adsorption of protocatechuic acid and caffeic acid on C18 particles." Korean Journal of Chemical Engineering **29**: 135-138.

Zhang, Y., S. Li, X. Wu and X. Zhao (2007). "Macroporous resin adsorption for purification of flavonoids in Houttuyniacordata Thunb." Chinese Journal of Chemical Engineering **15**: 872-876.

Zorn, H., D. E. Breithaupt, M. Takenberg, W. Schwack and R. G. Berger (2003). "Enzymatic hydrolysis of carotenoid esters of marigold flowers (Tagetes erecta L.) and red paprika (Capsicum annuum L.) by commercial lipases and Pleurotus sapidus extracellular lipase." Enzyme and Microbial Technology **32**: 623-628.

APPENDICES

APPENDIX A
EXPERIMENTAL DATA FOR ANALYSIS

A-1 Standard calibration curve of xanthophylls from spectrophotometer analysis

Table A-1 Standard calibration curve data of xanthophylls from spectrophotometer analysis

Concentration of xanthophylls (µg/ml)	Absorbance at 478 nm
0	0
1	0.186
2	0.336
3	0.534
4	0.622
5	0.932
6	1.061
7	1.262

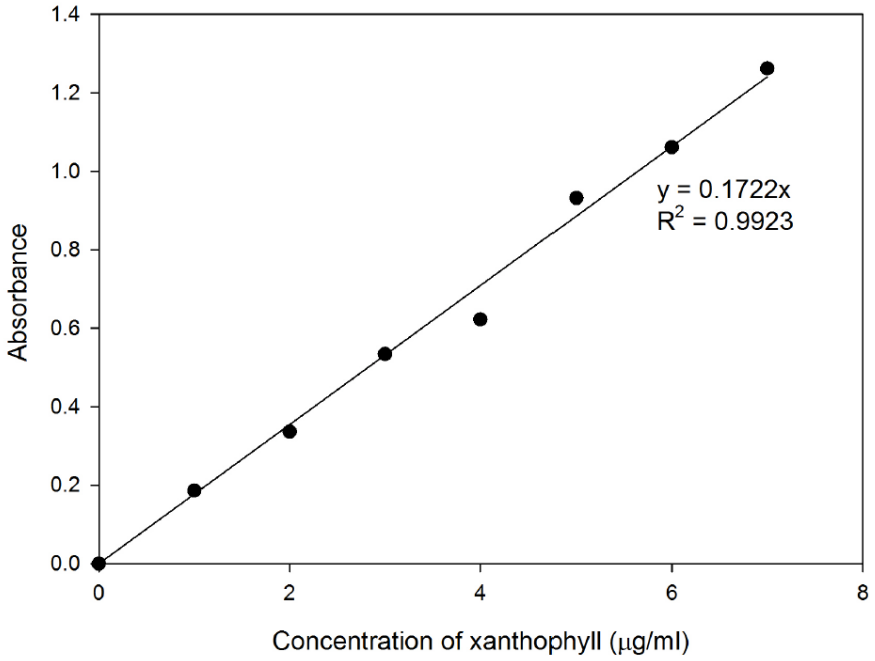

Figure A-1 Standard calibration curve data of xanthphylls from spectrophotometer analysis

A-2 Standard calibration curve of free lutein from HPLC analysis

Table A-2 Standard calibration curve data of free lutein from HLPC analysis

Concentration of free lutein (μg/ml)	Peak area
10	53846969
20	99836648
30	145272960
40	201325380
50	260840352
100	531458128

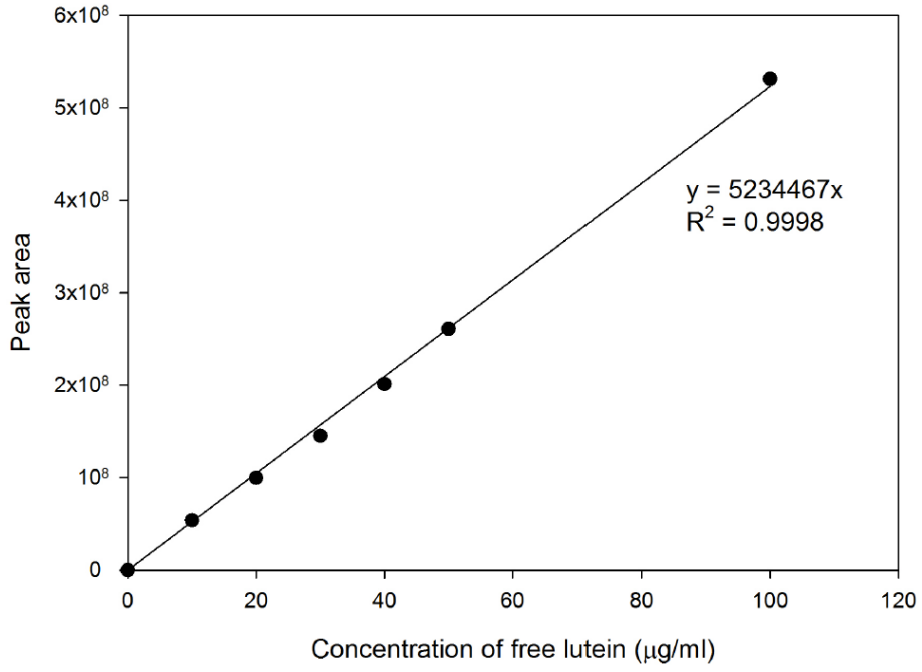

Figure A-2.1 Standard calibration curve data of free lutein from HPLC analysis

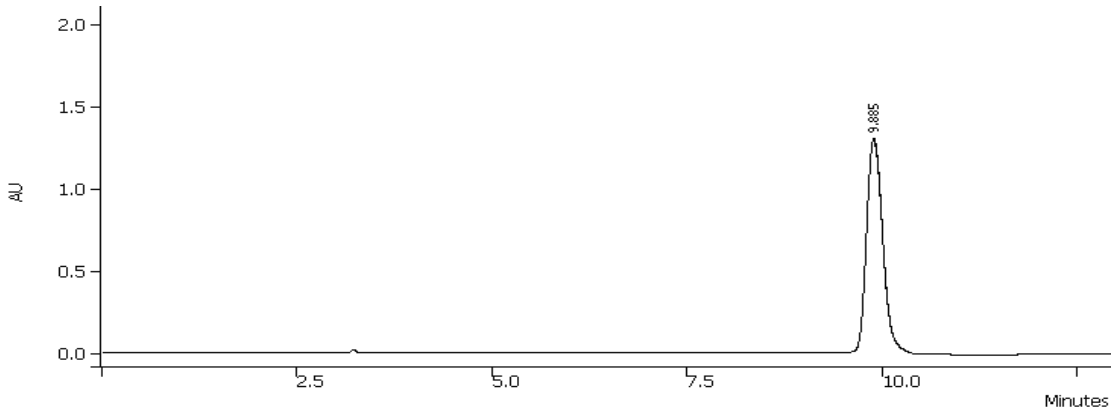

Figure A-2.2 Chromatogram of free lutein standard

A-3 Standard calibration curve of fatty acid HPLC analysis

Table A-3.2 Standard calibration curve data of fatty acid (Palmitic acid) from HLPC analysis

Concentration of fatty acid (µg/ml)	Peak area
100	4915.12
200	11727.23
300	21136.96
400	29608.15
500	31196.08
1000	51217.14

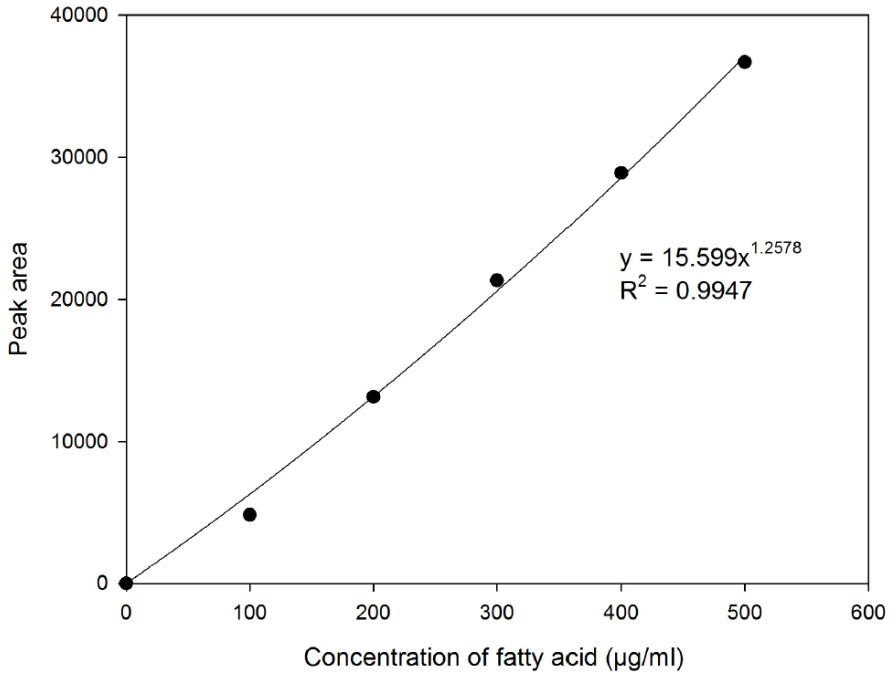

Figure A-3.1 Standard calibration curve data of fatty acid from HPLC analysis

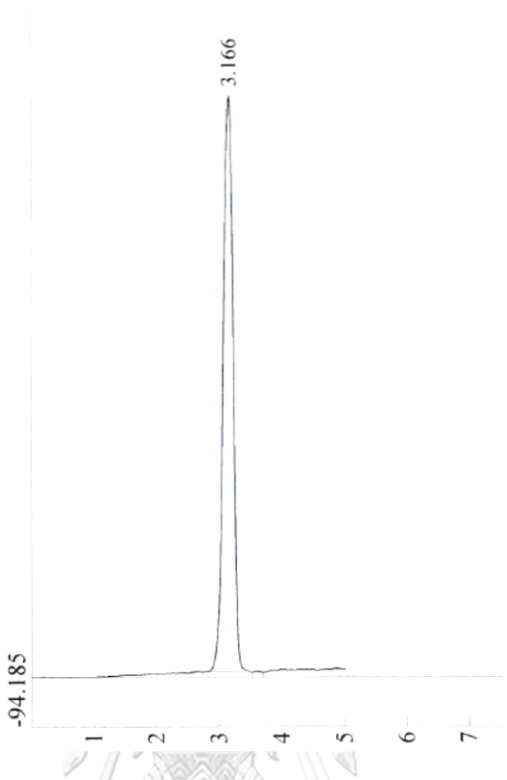

Figure A-3.2 Chromatogram of fatty acid standard

APPENDIX B
EXPERIMENTAL DATA AND CALCULATION

B.1 Determination of HETP at several mobile phase velocities

The experimental data of free lutein concentration for HETP determination at several mobile phase velocities are summarized in Table B.1-1 – B.1-7

Table B.1-1 Experimental data of free lutein eluted at mobile phase velocity 0.1191 cm/s

Time (min)	Concentration (µg/ml)
28.5	0
29.5	0.0549
30.5	1.3141
31.25	1.7762
31.75	1.9046
32.25	1.9706
32.75	1.4158
33.25	1.4495
33.75	1.1386
34.25	1.0987
34.75	0.6182
35.5	0.1398
36.5	0.1407
38	0.1015
40	0.0353
42	0

Table B.1-2 Experimental data of free lutein eluted at mobile phase velocity 0.1291 cm/s

Time (min)	Concentration (µg/ml)
26.5	0
27.5	0
28.5	0
29.5	0.1384
30.25	1.1645
30.75	1.7633
31.25	1.9170
31.75	1.3879
32.25	0.5549
33	0.1932
34	0.1005
35	0.0289
36	0.0162
37.5	0
39.5	0
41.5	0

Table B.1-3 Experimental data of free lutein eluted at mobile phase velocity 0.1350 cm/s

Time (min)	Concentration (µg/ml)
28.5	0
29.5	0
30.25	0.3353
30.75	0.6956
31.25	1.0320
31.75	1.7531
32.25	2.9025
32.75	2.4007
33.5	1.5537
34.5	0.5126
36	0.2894
38	0.1565
40	0
42	0
44	0
48	0

Table B.1-4 Experimental data of free lutein eluted at mobile phase velocity 0.1589 cm/s

Time (min)	Concentration (µg/ml)
25.5	0
26.5	0
27.5	0.0209
28.25	0.4997
28.75	1.2878
29.25	2.0076
29.75	1.6918
30.25	0.6758
30.75	0.4212
31.25	0.1823
31.75	0.1110
32.5	0.1286
33.5	0.0205
35	0.0388
37	0
39	0

Table B.1-5 Experimental data of free lutein eluted at mobile phase velocity 0.1807 cm/s

Time (min)	Concentration (µg/ml)
22.5	0
23.5	0.0054
24.25	0.0144
24.75	0.0493
25.25	0.7255
25.75	1.3266
26.25	1.8146
26.75	1.5966
27.25	1.0483
27.75	0.3688
28.25	0.0299
28.75	0.0215
29.5	0.0201
30.5	0.0223
32	0.0240
34	0.0279

Table B.1-6 Experimental data of free lutein eluted at mobile phase velocity 0.2087 cm/s

Time (min)	Concentration (µg/ml)
18.5	0
19.25	0
19.75	0
20.25	0
20.75	0.0518
21.25	0.1432
21.75	0.5247
22.25	1.5707
22.75	1.4944
23.25	1.3972
23.75	0.3798
24.5	0.1326
25.5	0.0897
26.5	0.0451
27.5	0
28.5	0

Table B.1-7 Experimental data of free lutein eluted at mobile phase velocity 0.3274 cm/s

Time (min)	Concentration (µg/ml)
9.75	0
10.25	0.0182
10.75	0.0710
11.165	0.3370
11.5	1.5557
11.835	3.1971
12.165	6.0041
12.5	6.9715
12.835	4.5885
13.165	3.8917
13.5	1.3103
13.835	0.7801
14.25	0.1127
14.75	0
15.25	0
15.75	0

Before calculation of mean and standard deviation of retention time, the type of peak must be identified. There are two types of peak: symmetric and asymmetric peaks. Types of peak are determined using Figure B-1.1 and equation B.1-1.

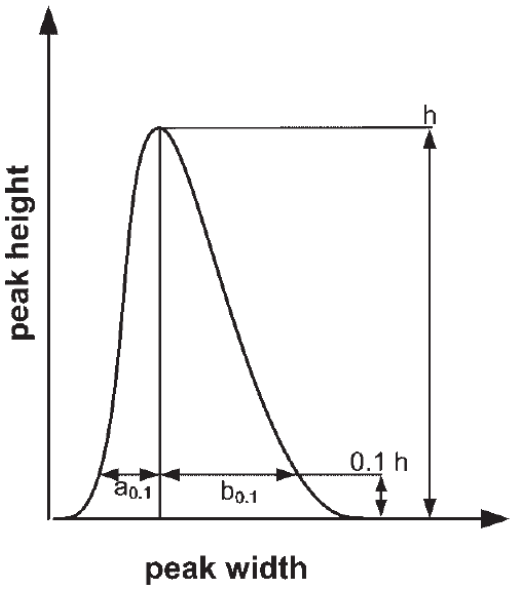

Figure B-1.1 asymmetric peak

$$T_p = \frac{b_{0.1}}{a_{0.1}} \quad \text{(B-1.1)}$$

where T_p is the degree of peak asymmetric

If T is in the range of 0.9-1.1, the peak is symmetric peak, otherwise asymmetric peak. An example of peak asymmetry calculation is shown as following.

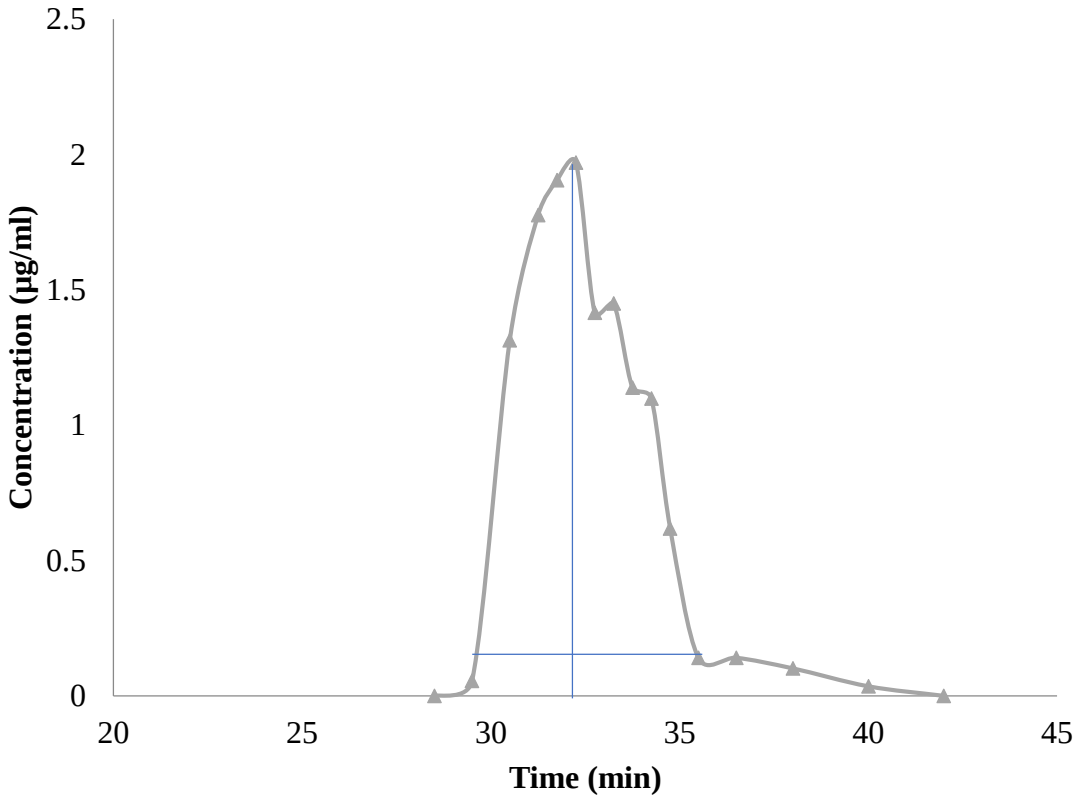

Figure B.1-2 The peak chromatogram of free lutein at mobile phase velocity of 0.1191 cm/s

From the Figure B.1-2

h_{lutein} = 1.9706 µg/ml

$0.1\ h_{lutein}$ = 0.19706 µg/ml

$a_{0.1,\ lutein}$ = 32.25 – 30 = 2.25 min

$b_{0.1,\ lutein}$ = 35.25 – 32.25 = 3 min

T_{lutein} = $\frac{2.25}{3}$ = 0.75

Thus, the peak is an asymmetric peak.

For asymmetric peaks, the mean retention time of chromatogram is calculated by the first absolute moment which shows in equation B-1.2

$$\mu_t = \frac{\int_0^\infty tc(t)dt}{\int_0^\infty c(t)dt} \approx \frac{\sum_{i=1}^\infty t_i c_i \Delta t}{\sum_{i=1}^\infty c_i \Delta t} \quad \text{(B-1.2)}$$

The variance, σ_t^2 is calculated from the second absolute moment which is represented in equation B.1-3

$$\sigma_t^2 = \frac{\int_0^\infty (t-\mu)^2 c(t)dt}{\int_0^\infty c(t)dt} \approx \frac{\sum_{i=1}^\infty (t_i-\mu)^2 c_i \Delta t}{\sum_{i=1}^\infty c_i \Delta t} \quad \text{(B-1.3)}$$

An example of mean and standard deviation of retention time calculation is shown in Table B.1-8.

Table B.1-8 Experimental results of free lutein at mobile phase velocity 0.1191 cm/s

i	Time (t_i, min)	Concentration of lutein (C_i, µg/ml)	$C_i*\Delta t$	$t_i*C_i*\Delta t$	$(t_i-\mu)^2*C_i*\Delta t$
1	28.5	0	0.0000	0.0000	0.0000
2	29.5	0.0549	4.7462	0.0259	1.1802
3	30.5	1.3141	21.1919	0.4828	2.0278
4	31.25	1.7762	45.1454	1.5653	1.3269
5	31.75	1.9046	60.0571	1.7890	0.3974
6	32.25	1.9706	63.0841	1.9132	0.0034
7	32.75	1.4158	51.5527	1.2389	0.4618
8	33.25	1.4495	34.8049	0.5479	1.1357
9	33.75	1.1386	20.0932	0.1772	1.4149
10	34.25	1.0987	10.1170	0.0436	1.2312
11	34.75	0.6182	4.4987	0.0084	0.8363
12	35.5	0.1398	0.0000	0.0000	0.0000
13	36.5	0.1407	0.0000	0.0000	0.0000
14	38	0.1015	0.0000	0.0000	0.0000
15	40	0.0353	0.0000	0.0000	0.0000
16	42	0	0.0000	0.0000	0.0000
			$\sum_{i=1}^{25} C_i\Delta t =$ 315.29	$\sum_{i=1}^{25} t_iC_i\Delta t =$ 8.79	$\sum_{i=1}^{25}(t_i - \mu)^2C_i\Delta t =$ 10.02
				$\mu_t = 32.57$ min	$\sigma_t^2 = 1.44$ min^2

The HETP of the column was determined by equation B-1.4.

$$HETP = \left(\frac{\sigma_t}{t_R}\right)^2 L_c \quad \text{(B-1.4)}$$

where t_R is retention time component i (min)

L_c is column length (cm) which is 15 cm in the experiments

Thus, the HETP value at mobile phase velocity 0.1191 cm/s is

$$HETP = \frac{(1.44)}{32.57^2}(15) = 0.028\ cm$$

The HETP value for other mobile phase velocities are summarized in Table B.1-9

Table B.1-9 Mean and standard deviation of retention time, and HETP of free lutein at several mobile phase velocities

Interstitial velocity (cm/s)	Mean retention time (min)	Standard deviation (min)	HETP (cm)
0.1268	32.57	1.44	0.028
0.1374	34.40	1.35	0.023
0.1437	34.48	1.26	0.020
0.1691	29.58	0.96	0.016
0.1924	26.45	0.92	0.018
0.2325	22.77	0.82	0.020
0.3804	12.51	0.58	0.034

B.2 Resolution calculation

The exit concentrations of free lutein and fatty acids in the semi-preparative column at the optimum mobile phase velocity are summarized in Table B.2-1 – B.2-6.

Table B.2-1 Experimental data of free lutein eluted by isocratic elution at the optimum velocity.

Time (min)	Free lutein concentration (µg/ml)
22.50	0.0000
23.50	0.1738
24.50	0.9912
25.50	14.8952
26.25	19.4716
26.75	17.7371
27.25	9.4753
27.75	5.6942
28.25	2.9434
28.75	1.1761
29.25	0.4780
29.75	0.2730
30.25	0.2566
30.75	0.1663
31.50	0.1179
32.50	0.0000
33.50	0.0000
35.00	0.0000

Table B.2-2 Experimental data of fatty acids eluted by isocratic elution at the optimum velocity.

Time (min)	Fatty acid concentration (µg/ml)
22.5	0.0000
23.5	0.0000
24.5	0.0000
25.5	0.0000
26.5	0.0000
27.5	0.0000
28.5	0.0000
29.5	0.0000
30.5	1.7266
31.25	9.3858
31.75	8.1573
32.25	4.8006
32.75	1.0065
33.25	1.0810
33.75	0.9365
34.25	0.4467
34.75	0.8214
35.25	0.5464
35.75	0.5632
36.5	0.7766
37.5	0.3231
38.5	0.0000
39.5	0.6947
40.5	0.0000
41.5	0.8034
42.5	0.6361
43.5	0.4115

Table B.2-3 Experimental data of free lutein eluted by gradient elution with hexane and ethyl acetate mixture at ratio 85:15 v/v in the first 12 min at the optimum velocity.

Time (min)	Free lutein concentration (µg/ml)
28.5	0
29.5	0.0567
30.25	1.0780
30.75	2.3141
31.25	3.9980
31.75	9.0918
32.25	15.3476
32.75	24.1496
33.25	22.7510
33.75	22.6255
34.25	16.0734
34.75	7.9447
35.25	2.5518
35.75	0.2247
36.5	0.1647
37.5	0

Table B.2-4 Experimental data of fatty acids eluted by gradient elution with hexane and ethyl acetate mixture at ratio 85:15 v/v in the first 12 min at the optimum velocity.

Time (min)	Fatty acid concentration (µg/ml)
38.5	0
39.5	0
40.5	0
41.25	0.5233
41.75	0.4611
42.25	0.4333
42.75	0.6232
43.25	1.5648
43.75	2.3044
44.25	7.7963
44.75	8.3561
45.25	6.1703
45.75	3.7530
46.5	2.5940
47.5	1.5947
48.5	1.1458
49.5	0.8318
50.5	0.4164
51.5	0.3437
52.5	0.2505
53.5	0.3118
54.5	0.2455
55.5	0.1943
56.5	0.1888
57.5	0.1843
58.5	0.1976
59.5	0
60.5	0

Table B.2-5 Experimental data of free lutein eluted by gradient elution with hexane and ethyl acetate mixture at ratio 85:15 v/v in the first 20 min at the optimum velocity.

Time (min)	Free lutein concentration (µg/ml)
36.5	0
37.5	0
38.5	0.1020
39.25	0.4140
39.75	1.9293
40.25	6.5527
40.75	13.6981
41.25	19.2010
41.75	16.4693
42.25	12.8223
42.75	10.1056
43.25	6.1404
43.75	4.8143
44.5	2.0337
45.5	0.6761
46.5	0.2421
47.5	0
48.5	0
49.5	0

Table B.2-6 Experimental data of fatty acids eluted by gradient elution with hexane and ethyl acetate mixture at ratio 85:15 v/v in the first 20 min at the optimum velocity.

Time (min)	Fatty acid concentration (µg/ml)
51.5	0
52.5	0
53.5	0.1056
54.25	0.5718
54.75	0.8242
55.25	5.9553
55.75	8.6993
56.25	6.1124
56.75	2.7178
57.25	2.0690
57.75	1.1254
58.25	0.5289
58.75	0.6477
59.25	0.4903
59.75	0.3497
60.25	0.1514
60.75	0.0780
61.5	0.0869
62.5	0.0974
63.5	0.1145
64.5	0.0831
65.5	0.0341
66.5	0.0189
67.5	0
68.5	0
69.5	0
70.5	0
71.5	0

The chromatographic resolution, R_s, the parameter which can measure how well two adjacent peak profiles of similar area separated, is calculated by equation B.2-1.

$$R_s = \frac{2(t_{R,j} - t_{R,i})}{w_j + w_i} \quad \text{(B-2.1)}$$

where $t_{R,i}$ and $t_{R,j}$ are the mean retention time of component i and j, respectively, of which component i eluted first ($t_{R,j} > t_{R,i}$). w_i and w_j are the peak width of component i and j, respectively. The peak width of each compound can be estimated by equation B.2-2.

$$w_i = 4\sigma \quad \text{(B-2.2)}$$

where σ is standard deviation of retention time of the component i

Based on the data in Table B.2-1 to B.2-6, the resolution of free lutein and fatty acid can be summarized as in Table B.2-7

Table B.2-7 Resolution of free lutein and fatty acids in several conditions

Elution mode	Component	Mean retention time (min)	Base peak width (min)	Resolution
Isocratic	Free lutein	26.49	4.06	1.13
	Fatty acids	32.29	6.64	
Gradient (12 min)	Free lutein	33.07	4.12	1.65
	Fatty acids	46.15	11.96	
Gradient (20 min)	Free lutein	41.87	4.84	2.32
	Fatty acids	56.37	7.68	

B.3 Calculation of critical volume of lutein and fatty acid from grouped contribution

The critical volume is one parameter used to estimate mass diffusivity of a compound. One choice which is successful to estimate is group contribution method. It uses basic structural information of a chemical molecule like a list of simple functional groups, adds parameters to these functional groups, and then calculates thermophysical and transport properties as a function of the sum of group parameters.

For the critical volume of a compound, it can be estimated by equation B-3.1.

$$V_c = 40 + \sum N\Delta V \qquad \text{(B-3.1)}$$

where V_c = critical volume of free lutein $\left(\frac{cm^3}{mol}\right)$

N = number of group

ΔV = individual of critical volume in each group $\left(\frac{cm^3}{mol}\right)$

Figure B-3.1 and Figure B-3.2 represent structures of lutein and palmitic acid, using standard fatty acid. The sum up structural contributions of the individual property increment of the compounds are shown in Table B-3.1 and Table B-3.2. The calculations can be set out in the following arrays, in which N stands for the number of groups.

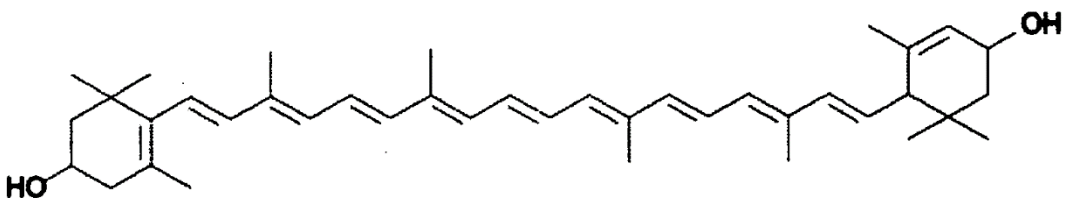

Figure B.3-1 Free lutein structure

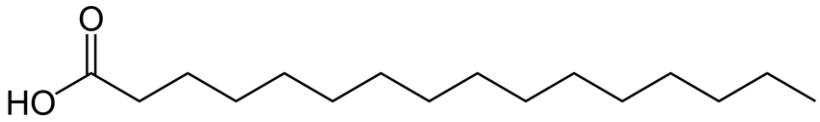

Figure B.3-2 Palmitic acid structure

Table B-3.1 Numbers of group contribution in free lutein

Group type		N	ΔV	NΔV
—C— (ring)		2	31	62
—CH_2—	(ring)	4	44.5	178
—CH	(ring)	6	46	276
—OH	(alcohol)	2	18	36
—CH_3	(non-ring)	10	55	550
=C=	(non-ring)	4	36	144
=CH	(non-ring)	14	45	630
Total				1876

Table B-3.2 Numbers of group contribution in palmitic acid

Group type		N	ΔV	NΔV
—CH_2—	(non-ring)	14	55	770
—CH_3	(non-ring)	1	55	55
—COOH	(non-ring)	1	80	80
Total				905

Thus, the critical volume of free lutein is

$$V_c = 40 + 1876 = 1916 \left(\frac{cm^3}{mol}\right)$$

The critical volume of fatty acid is

$$V_c = 40 + 905 = 945 \left(\frac{cm^3}{mol}\right)$$

B.4 Mass diffusivity calculation

Mass diffusivity of a compound in liquid phase is generally determined Wilke and Chang equation which is represented in equation B-4.1.

$$\frac{D_m \mu_B}{T} = \frac{7.4\times10^{-8}(\emptyset_B M_B)^{0.5}}{V_A^{0.6}} \quad \text{(B-4.1)}$$

where μ is the viscosity of solution B

$\emptyset$ is the associated parameter

M_B is the molecular weight of solution B

T is temperature

V_A is the critical volume of species A

The solution used in the experiments was mixture of hexane and ethyl-acetate ratios of 70:30 and 85:15 v/v. The physical properties of the solvent at 303 K are summarized in Table B.4-1.

Table B.4-1 Physical properties of hexane and ethyl acetate mixture at ratios of 70:30 and 85:15 v/v

Property	Hexane to ethyl acetate ratio (v/v)	
	70:30	85:15
Viscosity (kg/m·s)	0.00026	0.00032
Density (kg/m^3)	739.4	775.2
Associated parameter (-)	1	1
Solvent molecular weight (g/mol)	86.86	86.47

Based on the parameters in Table B.4-1 and the critical volumes in section B.3, the mass diffusivity of free lutein and fatty acids can be summarized in Table B.4-2

Table B.4-2 Mass diffusivity of free lutein and fatty acid in hexane and ethyl acetate mixture

Component	Hexane to ethyl acetate ratio (v/v)	
	70:30	85:15
Free lutein	1.26×10^{-6} cm^2/s	1.94×10^{-6} cm^2/s
Fatty acid	1.02×10^{-6} cm^2/s	1.58×10^{-6} cm^2/s

B.5 Effective diffusivity calculation

The effective diffusivity of free lutein and fatty acid is determined from Stokes-Einstein equation as shown in equation B.5-1.

$$D_p = \left(\frac{\varepsilon_p}{2-\varepsilon_p}\right)^2 \left(\frac{\kappa T}{6\pi\mu R_m}\right) \quad \text{(B.5-1)}$$

where ε_p is particle porosity which is 0.28

κ is Boltzmann constant which is 1.38×10^{-23} J/K

T is temperature

μ is the solvent viscosity

R_m is the molecular radius of compound which is 16.05 nm for free lutein and 10.09 nm for fatty acid.

Based on the data, the effective diffusivity of free lutein and fatty acid can be summarized in Table B.5-1.

Table B.5.1 Mass diffusivity of free lutein and fatty acid in hexane and ethyl acetate mixture

Component	Hexane to ethyl acetate ratio (v/v)	
	70:30	85:15
Free lutein	5.97×10^{-5} m/s	4.85×10^{-5} m/s
Fatty acid	9.76×10^{-5} m/s	7.93×10^{-5} m/s

B.6 Axial dispersion coefficient calculation

Axial dispersion coefficient is generally determined by Chung and Wen correlation as described in equation B.6-1.

$$Pe = \frac{0.2}{\varepsilon} + \frac{0.011}{\varepsilon}(\varepsilon Re)^{0.48} \quad \text{(B-5.1)}$$

where ε is the column porosity which is 0.3

The axial dispersion coefficients of free lutein and fatty acid in the semi-preparative column at several mobile phase velocities are summarized in Table B.6-1.

Table B-6.1 Axial dispersion coefficients of free lutein and fatty acid in the semi-preparative column at various velocities

velocity (cm/s)	Reynold No	Pelect No	Axial dispersion coefficient $(10^8\ m^2/s)$
0.1268	0.0885	0.6515	4.87
0.1331	0.0929	0.6516	5.11
0.1374	0.0959	0.6517	5.27
0.1437	0.1003	0.6519	5.51
0.1670	0.1165	0.6524	6.40
0.1691	0.1180	0.6524	6.47
0.1797	0.1254	0.6526	6.88
0.1923	0.1342	0.6529	7.37
0.2325	0.1622	0.6536	8.89

B.7 External mass transfer coefficient calculation

In the determination of the most suitable mass transfer model, the external mass transfer coefficient of free lutein was determined Wilke and Chang correlation, equation B.7-1.

$$Sh = 1.09\varepsilon^{-\frac{2}{3}}Re^{\frac{1}{3}}Sc^{\frac{1}{3}} \quad \text{(B.7-1)}$$

where Sc is Schmidt number

The external mass transfer coefficient of free lutein at several mobile phase velocities is summarized in Table B.7-1

Table B-7.1 External mass transfer coefficient of free lutein in the semi-preparative column at various velocities

velocity (cm/s)	Reynold No	Sherwood No	External mass transfer coefficient $(10^5\ m/s)$
0.1268	0.0885	8.9018	1.15
0.1374	0.0959	9.1400	1.18
0.1437	0.1003	9.2772	1.20
0.1691	0.1180	9.7883	1.27
0.1797	0.1254	9.9861	1.29
0.1923	0.1342	10.2134	1.32
0.2325	0.1622	10.7073	1.39

B.8 Numerical algorithm

Numerical algorithm of ideal model

```
%Ideal model code
%Ideal model with mobile phase velocity 0.16 cm/s
%Input characteristic column
ep =0.30; %particle porosity
ee =0.37; %external porosity
Len =15; %column length (cm)

%Input condition of experiment
t1  =3600; %run time (s)
tp  =1; %time for injection (s)
vel =0.16; %interstitial velocity (cm/s)
tal1 =t1*vel/Len; %dimensionless of time t1
talp =tp*vel/Len; %dimensionless of time tp
yf =45; %concnetration at the inlet of column
y0 =0; %initial concentration

%Input condition for numerical
dt =0.0005; %time step size (s)
dz =0.001; %distance step size (cm)
i =t1/dt;%no.of interval of time
j =Len/dz;%no.of interval in column

%Input transfer parameters
Iso =9.52; %isotherm constant

%matrix for concentration profile
ci =zeros(i+1,j+1); %column dimensionless
cid =zeros(i+1,j+1); %column with dimension
for p=1:j+1
    ci(p,1)=0;
end

%Input initial condition
for n=2:tp/dt
    ci(n,1)=1;%concentration injected into column (microgram/gram)
end

%Calculation of constant
S =1+((Iso*(1-ee)/ee));

%loop calculation
 for n=2:i+1
  for m=2:j+1
        ci(n,m)=((S*ci(n-1,m)/dt)+(vel*ci(n,m-1)/dz))/((S/dt)+(vel/dz));
```

```
    cid(n,m)=ci(n,m)*yf;
 end
end
```

Numerical algorithm of equilibrium-dispersive model

```
%Equilibrium-dispersive model code
%Equilibrium-dispersive model model with mobile phase velocity 0.16
cm/s
%Input characteristic column
ep =0.30; %particle porosity
ee =0.37; %external porosity
Len =15; %column length (cm)

%Input condition of experiment
t1  =3600; %run time (s)
tp  =1; %time for injection (s)
vel =0.16; %interstitial velocity (cm/s)
tal1 =t1*vel/Len; %dimensionless of time t1
talp =tp*vel/Len; %dimensionless of time tp
yf =45; %concnetration at the inlet of column
y0 =0; %initial concentration

%Input condition for numerical
dt =0.0005; %time step size (s)
dz =0.001; %distance step size (cm)
i =t1/dt;%no.of interval of time
j =Len/dz;%no.of interval in column

%Input transfer parameters
Iso =9.52; %isotherm constant
Axi =6.48*10^-8; %axail dispersion (m^2/s)

%matrix for concentration profile
ci =zeros(i+1,j+1); %column dimensionless
dci =zeros(i+1,j+1); %concentration gradient in time
cid =zeros(i+1,j+1); %column with dimension
for p=1:j+1
    ci(p,1)=0;
    cid(p,1)=0;
end

%Input initial condition
for n=2:tp/dt
    ci(n,1)=1;%concentration injected into column (microgram/gram)
end
```

```
%Calculation of constant
Pe =vel*Len/Axi; %dimensionless number of axial dispersion coefficient
H =Iso/rho; %dimensionless number of isotherm

%loop calculation
for m=1:i
 for n=2:j
        dci(m,n)=((ee/Pe)*(ci(m,n+1)-2*ci(m,n)+ci(m,n-1))/(dz^2))-((2*dz))*(ci(m,n+1)-
ci(m,n-1));
        ci(m+1,n)=(ee+(1-ee)*H)*(dci(m,n)*dt)+ci(m,n);
        cid(n,m)=ci(n,m)*yf;
 end
end
```

Numerical algorithm of transport model

```
%Equilibrium-dispersive model code
%Equilibrium-dispersive model with mobile phase velocity 0.16 cm/s
%Input characteristic column
ep =0.30; %particle porosity
ee =0.37; %external porosity
Len =15; %column length (cm)

%Input condition of experiment
t1  =3600; %run time (s)
tp  =1; %time for injection (s)
vel =0.16; %interstitial velocity (cm/s)
tal1 =t1*vel/Len; %dimensionless of time t1
talp =tp*vel/Len; %dimensionless of time tp
yf =45; %concnetration at the inlet of column
y0 =0; %initial concentration
rho =2.2; %particle density (kg/m^3)

%Input condition for numerical
dt =0.0005; %time step size (s)
dz =0.001; %distance step size (cm)
i =t1/dt;%no.of interval of time
j =Len/dz;%no.of interval in column

%Input transfer parameters
Iso =9.52; %isotherm constant
Axi =6.11*10^-4; %axail dispersion (cm^2/s)
Mas =2.7*10^-4; %mass transfer coefficient

%matrix for concentration profile
ci =zeros(i,j); %concentration in mobile phase (microgram/gram)
qi =zeros(i,j); %concentration in adsorbed phase
dc =zeros(i,j); %concentration gradient in mobile phase
dq =zeros(i,j); %concentration gradient in adsorbed phase
```

```
Dc =zeros(i,j); %total gradient
cid =zeros(i+1,j+1); %column with dimension

for p=1:j+1
    ci(p,1)=0;
    qi(p,1)=0;
end

%Input initial condition
for n=2:tp/dt
    ci(n,1)=1;% concentration injected into column (microgram/gram)
end

%Calculation of constant and dimensionless number
K =Mas*Len/vel; %dimensionless number of mass transfer coefficient
Pe =vel*Len/Axi; %dimensionless number of axial dispersion coefficient
H =Iso/rho; %dimensionless number of isotherm

%loop calculation
for n=2:i+1
 for m=2:j+1
        dq(t,z)=(K*(ci(t,z)-(qi(t,z)/H)))/(1-ee); %discrete mass transfer
resistance
        Dc(t,z)=ee*((ci(t,z-1)-2*ci(t,z)+ci(t,z+1))/Pe)/(dz^2)-(ci(t,z+1)-ci(t,z-
1))/(2*dz); %discrete mass balance
        dc(t,z)=(1/ep)*(Dc(t,z)-dq(t,z)); %concentration gradient in mobile
phase
        qi(t+1,z)=qi(t,z)+dt*dq(t,z);
        ci(t+1,z)=ci(t,z)+dt*dc(t,z);
        cid(n,m)=ci(n,m)*yf;
 end
end
```

VITA

Mr. Weerawat Clowutimon was born in Bangkok, on January 9, 1987. He finished high school from Samsenwittayalai School, Bangkok in 2005. He received his Bachelor's Degree in Chemical Engineering from King Mongkut's Institute of Technology Landkrabang in 2009. He continued studying Master's Degree in Chemical Engineering Chulalongkorn University in 2010 and graduated in 2011. During studying Master's Degree, he received grant fund from Department of Chemical Engineering Chulalongkorn University. He subsequently continued studying Doctoral degree of Chemical Engineering, Chulalongkorn University since October 2011 and received grant fund from Thailand Research Fund (TRF) through the Royal Golden Jubilee Ph.D. Program (RGJ-TRF).